

**Engineering *Pseudomonas putida* KT2440
for Efficient Bioelectrochemical Production of Glycolipids**

Von der Fakultät für Mathematik, Informatik und Naturwissenschaften der RWTH

Aachen

University zur Erlangung des akademischen Grades eines
Doktors der Naturwissenschaften genehmigte Dissertation
vorgelegt von

M. Biotech

Theresia Desy Askitosari

aus

Surakarta, Indonesien

Berichter: Univ.-Prof. Dr.-rer. nat. Miriam Agler-Rosenbaum
Univ.-Prof. Dr.-Ing. Lars M. Blank

Tag der mündlichen Prüfung: 09.07.2019

Diese Dissertation ist auf den Internetseiten der Universitätsbibliothek verfügbar

Eidesstattliche Erklärung

Theresia Desy Askitosari

erklärt hiermit, dass diese Dissertation und die darin dargelegten Inhalte die eigenen sind und selbstständig, als Ergebnis der eigenen originären Forschung, generiert wurden. Hiermit erkläre ich an Eides statt

1. Diese Arbeit wurde vollständig oder größtenteils in der Phase als Doktorand dieser Fakultät und Universität angefertigt
2. Sofern irgendein Bestandteil dieser Dissertation zuvor für einen akademischen Abschluss oder eine andere Qualifikation an dieser oder einer anderen Institution verwendet wurde, wurde dies klar angezeigt
3. Wenn immer andere eigene -oder Veröffentlichungen Dritter herangezogen wurden, wurden diese klar benannt
4. Wenn aus anderen eigenen -oder Veröffentlichungen Dritter zitiert wurde, wurde stets die Quelle hierfür angegeben. Diese Dissertation ist vollständig meine eigene Arbeit, mit der Ausnahme solcher Zitate
5. Alle wesentlichen Quellen von Unterstützung wurden benannt
6. Wenn immer ein Teil dieser Dissertation auf der Zusammenarbeit mit anderen basiert, wurde von mir klar gekennzeichnet, was von anderen und was von mir selbst erarbeitet wurde
7. Ein Teil oder Teile dieser Arbeit wurden zuvor veröffentlicht und zwar in

Theresia D. Askitosari, Santiago T. Boto, Lars M. Blank, Miriam A. Rosenbaum. Boosting heterologous phenazine production in *Pseudomonas putida* KT2440 through the exploration of the natural sequence space. *Frontiers in Microbiology*.

Aachen, 25.07.2019

Theresia Desy Askitosari

„Ich bin etwa nicht damit einverstanden, daß es ausnahmslos für jeden von mir hier etwas gegeben hat, aufgrund dessen er sich gesagt hat: „Ich fange an?“ Irgendetwas...und daher habe ich angefangen, obwohl ich den Weg nicht weiß und diese Sache nicht kenne. Und auch weiß, wie ich zugeben muß, das ein allgemeines Prinzip ist: Bevor man etwas kennenlernen kann, um etwas kennenzulernen, muß man damit anfangen“

Luigi Giussani - Kann Man so Leben

Acknowledgments

My cordial gratitude goes to my supervisor Univ.-Prof. Dr.-rer. nat. Miriam Agler-Rosenbaum for allowing me to work in this project. Thank you for your patient, kindness, support, and providing time to train me scientifically and personally. I am so grateful to have such a great experience to work with you. I am also thankful to my second supervisor Univ.-Prof. Dr.-Ing. Lars Mathias Blank for your support, guidance, and the inspiring discussions. It is a wonderful experience to be part of the Institute of Applied Microbiology (iAMB). I thank *Kementerian Riset, Teknologi, dan Pendidikan Tinggi* (RISTEK-DIKTI) Indonesia for the doctoral research scholarship.

Special thanks to Carola, it is such a long road to get through, but you are there and make me feel I am not alone. I also would like to thank the Rosenbaum lab members: Ivan, Ronny, Erick, Liesa (my super colleague), Simone, Manja, Tatiana, Thomas, Kristina, Annika, Sarah, Judith, Christian, Juan, Valeria, Praveen, Phillip C., Lisa K., also the colleagues and friend from Hans-Knöll-Institut (HKI) Jena: Ronja (immensely), Santiago, Anna, Lisa, Marcus. I would also thank the iAMB colleagues: Martin, Birgitta, Nick, Ulrike, Hendrik, Gisela, Isabel, Brehmi, Annette, Mariam, Carl, Elena, Bernd, Isabel B., Sebastian K., Sandra Schulte, Andrea, Andi, Till, Wing-Jin, Christoph L. (my good gene cloning teacher), Henrik, Vanessa, Birthe, Hao, Conrad, Nugroho, Kerstin, Eik, Dieter, Mathias, Benedikt, Thiemo, Christoph H., Johanna, Maike, Hamed, Nisha, Deiziane, Vaishnavi, Sandra H., Tobias, An, Salome, Dario, Suresh, Ahmed, Philipp D., Kristina K., Melani, Kristina B., Sebastian Kruth, Andreas Wittgens. Thank you all for the sincere working relationship, scientific discussions, and individual assistance supporting this work.

My cordial appreciation goes to my family: Papa, Mama, mas Anton, mbak Bintari, mbak Candria, Endra. Thank you for support, love, and prayers that encourage me to finish this work. I would like to appreciate the spiritual support from Peter, Vr. Jean-Marie, Leopold, David, Antonius, Phillip S., Maximillian, Victor, Paul, Marvin, Irene, Marystella, Martina. Thank you for making my life so colorful. And of course, I thank God for giving me the strength to keep going.

Funding



The here presented research was part of the DFG funded project entitled “Mechanistic investigations of the syntrophy between *Pseudomonas aeruginosa* and 2,3-butanediol fermenters within the context of the optimized phenazine-based current generation in bioelectrochemical systems” (grant no AG156/1-1) Germany



This work was also funded by the *Beasiswa Pendidikan Pascasarjana Luar Negeri (BPP-LN) Scholarship, Kementerian Riset, Teknologi, dan Pendidikan Tinggi (RISTEK DIKTI) Indonesia*

Table of Contents

Summary	IV
Zusammenfassung.....	VI
List of abbreviations	VIII
List of figures	IX
List of tables	XII
Chapter 1 General Introduction	1
1.1 Valuable microbial glycolipids as sustainable surfactant compound	2
1.2 Rhamnolipids as a valuable glycolipid surfactant	3
1.3 <i>Pseudomonas putida</i> KT2440 as multifaceted biocatalyst	5
1.4 Bioelectrochemical systems as means of converting and conserving resources	6
1.5 Phenazines as electron shuttle compound in BES	9
1.6 Scope and outline of the thesis.....	12
Chapter 2 Materials and Methods	14
2.1 Strain engineering.....	15
2.1.1 Bacterial strains, media preparation, and strain cultivation	15
2.1.2 Genetic engineering of <i>P. putida</i> for phenazine synthesis	15
2.1.3 Tailoring heterologous rhamnolipid-producing <i>P. putida</i> with phenazine production	19
2.1.4 Plasmid sustainability experiments to determine the strain stability.....	21
2.1.5 Aerobic strain characterization and evaluation.....	22
2.1.6 Anaerobic strain characterization and evaluation.....	22

2.2	Bielectrochemical experiments.....	23
2.2.1	Oxygen-limited bioelectrochemical system experiments	23
2.2.2	Bioelectrochemical production of rhamnolipids under oxygen-limited condition ..	24
2.3	Analytical methods.....	24
2.3.1	Bioinformatics analysis	24
2.3.2	Analysis of sugar metabolites	25
2.3.3	Phenazine analysis	25
2.3.4	Rhamnolipid detection using thin layer chromatography (TLC).....	26
Chapter 3 Results and Discussions		25
3.1	Boosting heterologous phenazine production in <i>Pseudomonas putida</i> KT2440 through the exploration of the natural sequence space	28
3.1.1	Summary	28
3.1.2	Introduction	29
3.1.3	Results and discussions.....	31
3.1.4	Conclusions	46
3.2	Coupling the electroactive <i>P. putida</i> KT2440 with bioelectrochemical foam-free rhamnolipids production.....	48
3.2.1	Summary	48
3.2.2	Introduction	49
3.2.3	Results and Discussions.....	51
3.2.4	Conclusions	64
Chapter 4 General Discussion		65
4.1	State-of-the-art in rhamnolipid production for bio-detergents industry.....	66
4.2	Evaluation of the productivity of the recombinant rhamnolipid strain	68
4.3	Bioelectrochemical production optimization	71

4.4	Expanding the concept to the heterologous production of other types of glycolipid surfactants.....	73
Chapter 5 Concluding remarks and Outlook.....		74
5.1	Concluding remarks	75
5.2	Outlook.....	76
5.2.1	Rhamnolipid recombinant host improvement	76
5.2.2	BES reactor operation	76
5.2.3	Integrated redox and flux balance analysis	77
References.....		78
Appendix.....		A1
A.1 Supplementary information Chapter 3.1		A1
A	Constructed Plasmids expressing phenazine genes used in Chapter 3.1	A1
B	<i>In silico</i> phenazine gene origin analysis	A1
C	Structural analysis of phenazine synthesis proteins:.....	A8
A.2 Supplementary information Chapter 3.2		A10
A	Constructed Plasmids expressing phenazine and rhamnolipid genes used in Chapter 3.2.....	A10
B	BES experiments	A11
Curriculum vitae		A14

Summary

Sustainability of energy generation and careful use of environmental resources are two of our biggest challenges in the world today. Ecological and energy crises in every country enforce the need for development and exploration of sustainable bioenergy resources. One novel biotechnological approach to implement the means of converting and conserving resources are bioelectrochemical systems or BES. The main advantage of BES application is the generation of electric power or biochemical products from renewable materials and carbon-neutral waste materials. The recent exploration and study of natural microbial electron discharge to extracellular anodes might offer significant improvements strategies in bioelectrochemical processes for the production of many valuable products, such as bio detergents. However, the natural activity of biocatalysts on electrodes is limited, and molecular engineering approaches are required to tailor new bioelectrochemical active production hosts. Schmitz et al has just reported a successful initial proof-of-principle study. propose a new concept of using an engineered strain of *Pseudomonas putida* to enable the utilization of an anode for electron discharge during oxygen-limited growth (Schmitz et al., 2015). Biotechnologically, this organism is already tailored to produce bio-detergents like rhamnolipids, one type of glycolipid surfactants, under aerobic conditions. But costly aeration and subsequent problems with vigorous reactor foaming, which is technically hard to handle with conventional antifoam technologies, are current drawbacks. This challenge might be overcome if the detergent production is combined with oxygen-limited growth in bioelectrochemical systems.

In this study, following the work from Schmitz *et al.*, we successfully expressed the other three phenazine synthesis gene originating from the phenazine synthesis operon two of *P. aeruginosa* PAO1 (PA1899-PA1905), operon one of *P. aeruginosa* PA14 (PA14_09410-PA14_09480), and operon two of *P. aeruginosa* PA14 (PA14_39880-PA14_39970). Notably, the phenazine-1-carboxylic acid (PCA) synthesis operon two from *P. aeruginosa* PA14 was found to be most active in the heterologous phenazine production within *P. putida*. This gene origin was chosen to be tailored further with rhamnolipid production. Hereinafter, the heterologous mono-rhamnolipid production in *P. putida* has been successfully coupled with phenazine production to generate the strains *P. putida rhl-pca* (produces PCA and mono-rhamnolipids) and *P. putida rhl-*

pyo (produces PCA, pyocyanin (PYO), and mono-rhamnolipids). Based on the maximum titer of mono-rhamnolipids produced in aerobic shake flasks, *P. putida* rhl-pca was chosen for bioelectrochemical production experiments in BES.

Oxygen-limited cultivations with redox balancing at an anode via phenazines can be coupled to rhamnolipid biosynthesis by employing plasmid-based genetic engineered *P. putida*. The result of our study showed that passive headspace aeration of BES was suitable to be applied for the bioelectrochemical production of foam-free rhamnolipids with *P. putida* rhl-pca. The increased carbon yield obtained by *P. putida* rhl-pca in passively aerated BES showed a potential economic advantage for glycolipid surfactant bioproduction. Overall, this work is an initial study showing that the bioelectrochemical production of foam-free glycolipid surfactants by utilizing phenazines as electron shuttles is possible.

Zusammenfassung

Nachhaltigkeit bei der Energieerzeugung und bei der Nutzung von Umweltressourcen sind heutzutage zwei unserer größten Herausforderungen auf der Welt. Umwelt- und Energiekrisen in allen Ländern erfordern die Entwicklung und Erforschung nachhaltiger Bioenergieressourcen. Ein neuartiger biotechnologischer Ansatz zur Umwandlung und Schonung von natürlichen Ressourcen sind bioelektrochemische Systeme oder BES. Hauptvorteil der BES ist die Erzeugung von elektrischem Strom oder biochemischen Produkten aus nachwachsenden Rohstoffen und klimaneutralen Abfällen. Die jüngste Erforschung der natürlichen mikrobiellen Elektronübertragung auf extrazelluläre Anoden könnte signifikante Verbesserungen in der Anwendung bioelektrochemischen Prozessen zur Herstellung vieler wertvoller Produkte wie Biodetergenzien nach sich ziehen. Die natürliche Aktivität von Biokatalysatoren an Elektroden ist jedoch begrenzt, und molekulartechnische Ansätze sind erforderlich, um neue bioelektrochemisch aktive Produktionswirte maßzuschneidern. Eine erfolgreiche erste Proof-of-Principle-Studie wurde kürzlich von Schmitz *et al.* veröffentlicht. Hierbei wurde ein genetisch veränderter Stamm von *Pseudomonas putida* genutzt, welcher eine BES Anode zur Elektronenentladung während sauerstoffbegrenzten Wachstums nutzen kann (Schmitz et al., 2015). Biotechnologisch wird *P. putida* bereits genutzt um unter aeroben Bedingungen Biowaschmittel wie Rhamnolipide, eine Art von Glykolipid-Tensiden, herzustellen. Aber teure Belüftung und anschließende Probleme mit starker, technisch nur schwer zu kontrollierender Schaumbildung, limitieren den Prozess. Diese Herausforderung könnte überwunden werden, wenn die Waschmittelproduktion mit einem sauerstoffbegrenzten Wachstum in bioelektrochemischen Systemen einhergeht.

In der hier vorliegenden Disserationsarbeit wurde die Arbeit von Schmitz *et al.* fortgesetzt und die anderen drei Phenazinsynthese-Operone erfolgreich exprimiert: Hierbei handelt es sich um das Phenazinsyntheseoperon 2 aus *P. aeruginosa* PAO1 (PA1899-PA1905), das Operon 1 aus *P. aeruginosa* PA14 (PA14_09410-PA14_09480) und das Operon 2 aus *P. aeruginosa* PA14 (PA14_39880-PA14_39970). Bemerkenswerterweise erwies sich das Phenazin-1-carbonsäure (PCA) Syntheseoperon 2 aus *P. aeruginosa* PA14 als am aktivsten bei der heterologen Phenazinproduktion in *P. putida*. Dieses Operon wurde daher ausgewählt, um mit der

Rhamnolipid-Produktion integriert zu werden. Hierbei konnte die heterologe Mono-rhamnolipid-Produktion in *P. putida* erfolgreich mit der Phenazinproduktion gekoppelt werden. Dabei wurden die Stämme *P. putida* rhl-pca (produziert PCA und Mono-rhamnolipide) und *P. putida* rhl-pyo (produziert PCA, Pyocyanin (PYO) und Mono-rhamnolipide) generiert. Basierend auf dem maximalen Titer an Mono-rhamnolipiden, welche in aeroben Schüttelkolben produziert wurden, wurde *P. putida* rhl-pca für bioelektrochemische Produktionsexperimente in BES ausgewählt.

Ich konnte zeigen, dass sauerstoffbegrenzte Kultivierungen von gentechnisch veränderten *P. putida* unter Redoxausgleich an einer Anode mit Hilfe von Phenazinen möglich sind. Hierbei kann der Stamm so verändert werden, dass gleichzeitig eine Rhamnolipid-Biosynthese stattfinden kann. Das Ergebnis unserer Studie zeigt, dass die passive Luftraumbegasung in BES für die bioelektrochemische Herstellung von schaumfreien Rhamnolipiden mit *P. putida* rhl-pca geeignet ist. Die erhöhte Kohlenstoffausbeute mit *P. putida* rhl-pca in passiv belüfteten BES ist ein potentieller wirtschaftlicher Vorteil bei der Glykolipid-Tensid Bioproduktion. Insgesamt ist diese Arbeit eine erste Studie, die zeigt, dass die bioelektrochemische Herstellung von schaumfreien Glykolipid-Tensiden unter Verwendung von Phenazinen als Elektronen-Shuttle möglich ist.

List of abbreviations

AA	active aeration	R	resistor
AA+	active aeration continuously	r	reactor
ATP	adenosine-tri-phosphate	RBS	ribosome binding sites
BES	bioelectrochemical systems	rDNA	ribosomal DNA
CAD	Corona-charged aerosol detector	RE	reference electrode
CAI	codon adaptation index	redox	oxidation and reduction
CE	counter electrode	RI	refractive index
CFU	colony forming unit	RMSD	root-mean-square deviation of atomic positions
CIGC	chromosomal integration of gene(s) with multiple copies	RP-HPLC	reversed-phase high-performance liquid chromatography
DET	direct electron transfer	rpm	revolutions per minute
DNA	deoxyribonucleic acid	SHE	standard hydrogen electrode
DSMZ	German Collection of Microorganisms and Cell Cultures	sp.	species (sg.)
dTDP-L-rhamnose	2'-deoxy-thymidine- β -L-rhamnose	TFA	trifluoroacetic acid
<i>E.</i>	<i>Escherichia</i>	TLC	thin-layer chromatography
G	gentamycin	UV	ultraviolet
GRAS	Generally Recognized As Safe	v/v	volume per volume
HAAs	3-(3-hydroxyalkanoyloxy) alkanolic acids	WE	working electrode
HPLC	high-performance liquid chromatography		
K	Kanamycin		
LB	Luria-Bertani		
MET	indirect (mediated) electron transfer		
MFC	microbial fuel cell		
m-rhl	mono-rhamnolipid		
MS	mineral salts		
NAD	nicotinamide-adenine-dinucleotide		
NADPH	nicotinamide-adenine-dinucleotide-phosphate		
NEB	New England BioLabs GmbH		
OD	optical density		
phz op 1	phenazine operon 1		
phz op 2	phenazine operon 2		
ORI	Origin of replication		
<i>P.</i>	<i>Pseudomonas</i>		
PA	passive aeration		
PCA	phenazine-1-carboxylic acid		
PCR	polymerase chain reaction		
pH	the negative logarithm of the concentration of hydronium ions		
PHAs	poly-hydroxy-alkanoates		
Phz	phenazines		

List of figures

Figure 1: Examples of valuable glycolipid surfactants.	3
Figure 2: Rhamnolipid biosynthesis by <i>Pseudomonas</i>	5
Figure 3: The general set up of a potentiostatically controlled BES and MFC.	7
Figure 4: A scheme of extracellular electron transfer via redox shuttling compound	9
Figure 5: Phenazine biosynthesis pathways in <i>P. aeruginosa</i>	10
Figure 6: Gene map of phenazine operon 1 and 2 in <i>P. aeruginosa</i> PAO1 and PA14.	11
Figure 7: Research workflow in this study	12
Figure 8: Image of bioelectrochemical reactors used in this study.	23
Figure 9: Growth curve (a) vs PCA production (b) of eight individual clones of <i>P. putida</i> O1.phz1, O1.phz2, 14.phz1, and 14.phz2 in the micro cultivation experiment.	32
Figure 10: Growth curve (a) vs. PCA & PYO production (b) of eight clones of <i>P. putida</i> O1.phz1+, O1.phz2+, 14.phz1+, and 14.phz2+ in the micro cultivation experiment.	33
Figure 11: Growth curve (a) vs PCA production (b) of the selected <i>P. putida</i> O1.phz1, O1.phz2 14.phz1, and 14.phz2.	34
Figure 12: Growth curve (a) vs PCA & PYO production (b) of the selected <i>P. putida</i> O1.phz1+, O1.phz2+, 14.phz1+, and 14.phz2+.	35
Figure 13: Heterologous expression of <i>phz</i> genes in <i>P. putida</i> KT2440.	36
Figure 14: Heterologous phenazine production with <i>P. putida</i> under oxygen-limited conditions in a BES.	38
Figure 15: BES cultivation of <i>P. putida</i> KT2440 (wildtype) under passive aeration conditions.	39
Figure 16: Nucleotide-based analysis of the phenazine operons.	45
Figure 17: Structural analysis of PhzE.	46
Figure 18: Characterization of rhamnolipid producing <i>P. putida</i>	52
Figure 19: Growth curve (a) vs mono-rhamnolipid production (b) of eight clones of the <i>P. putida</i> rhl strain in the micro cultivation experiment in Delft media with 10 g/l glucose.	53
Figure 20: Growth curve (a) vs mono-rhamnolipid production (b) of eight clones of <i>P. putida</i> rhl-MS strain in the micro cultivation experiment in Delft media with 10 g/L glucose.	53
Figure 21: Growth curve vs mono-rhamnolipid & PCA production	53

Figure 22: Growth curve vs mono-rhamnolipid, PCA & PYO production.	54
Figure 23: Fully aerobic flasks cultivation for mono-rhamnolipid (m-rhl) and phenazine production (PCA and PYO).	56
Figure 24: Fully aerobic flasks cultivation for growth observation (OD ₆₀₀).	56
Figure 25: Anaerobic flasks experiment (triplicate) of <i>P. putida</i> SK1 with synthetic PCA and PYO added.....	57
Figure 26: BES performance of <i>P. putida</i> rhl-pca at an applied potential of 0.2 V vs. RE. (Active aeration)	59
Figure 27: Thin-layer chromatography (TLC) analysis of the samples were taken from the second experiment BES reactors of <i>P. putida</i> rhl-pca strain under PA condition.	61
Figure 28: BES performance of <i>P. putida</i> rhl-pca at an applied potential of 0.2 V vs. RE. (Passive aeration).	62
Figure 29: Plasmid sustainability evaluation of <i>P. putida</i> rhl-pca strain BES reactors.....	62
Figure 30: Scheme of bioelectrochemical production of mono-rhamnolipid <i>P. putida</i> rhl-pca....	67
Figure 31: Bubble formation in the passively aerated BES.	68
Figure 32: Comparison of BES performance of <i>P. putida</i> rhl-pca at an applied potential of 0.2 V vs. RE using carbon comb and carbon cloth as WE.	71
Figure S1: Vectors expressing phenazine genes used in chapter 3.1	A1
Figure S2: Structural alignment PhzS.	A7
Figure S3: Phylogenetic tree and genomic plot of the phenazine production clusters.	A7
Figure S4: Structural alignment PhzA.	A8
Figure S5: Structural alignment PhzB.	A8
Figure S6: Structural alignment PhzC.	A9
Figure S7: Structural alignment PhzD.	A9
Figure S8: Structural alignment PhzG.	A10
Figure S9: Vectors expressing mono-rhamnolipid and phenazine genes used in chapter 3.2 ...	A10
Figure S10: Bioreactor performance of <i>P. putida</i> rhl strain without electrode.	A11
Figure S11: BES performance of <i>P. putida</i> rhl at an applied potential of 0.2 V vs. RE.	A11
Figure S12: Bioreactor performance of <i>P. putida</i> rhl-pca strain without electrode.	A11

Figure S13: BES performance of *P. putida rhl-pca* (plasmid sustainability test) at an applied potential of 0.2 V vs. RE..... A12

Figure S14: Second BES performance of *P. putida rhl-pca* at an applied potential of 0.2 V vs. RE.
..... A13

List of tables

Table 1: Bacterial strains and plasmids used for genetic engineering of <i>P. putida</i> for phenazine synthesis	16
Table 2: Primers used for genetic engineering of <i>P. putida</i> for phenazine synthesis.....	18
Table 3: Bacterial strains and plasmids used for tailoring heterologous rhamnolipid-producing <i>P. putida</i> with phenazine production	20
Table 4: Primers used for tailoring heterologous rhamnolipid-producing <i>P. putida</i> with phenazine production	21
Table 5: Bioelectrochemical production of rhamnolipid set-ups.....	24
Table 6: Summary of glucose and metabolite evaluation of oxygen-limited BES experiments	42
Table 7: Recombinant rhamnolipid producer strains in this study compared to other strains	70
Table S1: Codon Adaptation Index data.....	A7

Chapter 1

General Introduction

1.1 Valuable microbial glycolipids as sustainable surfactant compound

Glycolipids are a group of compounds, which consist of a mono- or oligosaccharide bound to a lipid molecule by a glycosidic linkage (Lopez & Schnaar, 2006). Based on their hydrophobic moieties, glycolipids can be divided into glyco-glycerolipids and glycosphingolipids. Due to the presence of both hydrophobic and hydrophilic moieties, the amphiphilic glycolipids show surface activity. They can, therefore, be used as an eco-friendly alternative to commonly used surfactants, which classically are non-biodegradable and contain highly toxic compounds, such as ethylene oxide (Faivre & Rosilio, 2010). Siebenhaller *et al.* described that the majority of surfactants used today, are produced from petroleum-based material and contain aryl or alkyl units as the hydrophobic moiety, as well as sulfonates, alkylammonium salts, amines and carboxylates as the hydrophilic moiety (Siebenhaller *et al.*, 2018). However, in more recent times, surfactants are starting to be produced from renewable resources, and are therefore called “biosurfactants” (Lourith & Kanlayavattanakul, 2009; Santos *et al.*, 2016; Siebenhaller *et al.*, 2018). Glycolipid surfactants are one specific group of these “biosurfactants” (Figure 1). They can contain anionic- and/or cationic charged groups. Hence, they can be grouped into nonionic, anionic, cationic, and amphoteric surfactants. These group of compounds is very useful as an additive agent in food processing, cosmetic, agrochemical, cleaning agents/detergents, and pharmaceutical applications, like the production of foam, emulsions, and dispersions (Sivapathasekaran & Ramkrishna, 2017).

One group of glycolipid surfactants is microbial glycolipids, which are non-toxic to the environment and biodegradable. Microbial glycolipids can be produced under aerobic or anaerobic conditions, depending on the specific compound (Reis *et al.*, 2011). Several examples of microbial glycolipids are shown in Figure 1. Mannosylerythritol lipids (Figure 1a) are naturally produced by *Pseudozyma* sp. and are industrially attractive glycolipids due to their manifold potential applications in pharmaceuticals, bioremediation of petroleum hydrocarbons, and as a chemical agent in protein purification (Rau *et al.*, 2005). Another group of glycolipid surfactants is sophorolipids (Figure 1c), which are mainly produced by *Candida bombicola* in nature (Kulakovskaya & Kulakovskaya, 2014). This group of glycolipid surfactant is regarded as a

promising candidate of biomedical compounds, as they are an effective and safe antimicrobial agent (Diaz De Rienzo et al., 2015). Therefore, this type of glycolipids presents a promising alternative to synthetic medicines (Joshi-Navare & Prabhune, 2013). Furthermore, a short review of rhamnolipids (Figure 1b) is given in section 1.2 of this chapter.

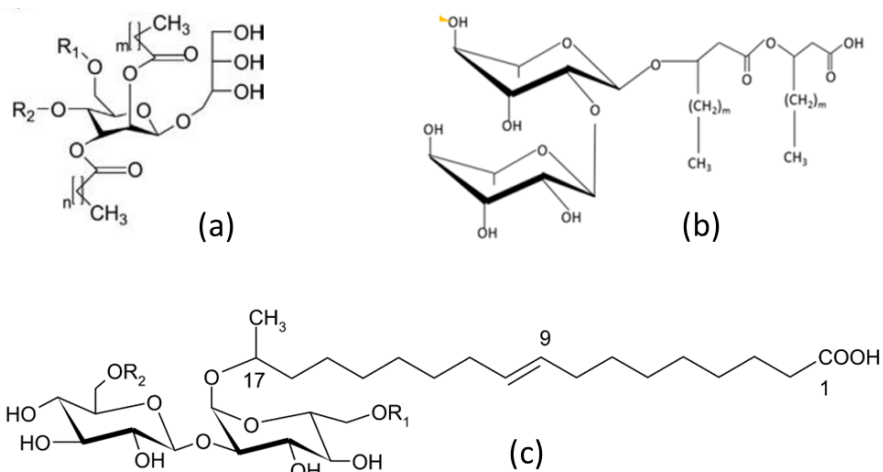


Figure 1: Examples of valuable glycolipid surfactants (a) mannosylerythritol lipids (Siebenhaller et al., 2018), (b) rhamnolipids (Chong & Li, 2017), and (c) sophorolipids (Kulakovskaya & Kulakovskaya, 2014)

1.2 Rhamnolipids as a valuable glycolipid surfactant

Rhamnolipids are one of the best explored microbial glycolipid surfactants. This group of compounds provides a wide range of industrial applications, for example in the food, pharmaceutical, cosmetics industry, in pollutant bioremediation, and as a cleaning agent (detergents) (Chong & Li, 2017; Soberon-Chavez et al., 2005). Rhamnolipids are naturally produced by *Pseudomonas* and *Burkholderia* (Caiazza et al., 2005; Rikalovic et al., 2017), whereby its production is controlled by the complex regulation of quorum sensing (Dusane et al., 2010). The tension-active properties of these compounds enable those bacteria to reduce the surface tension of hydrophobic substrates and generate emulsions, which increase the medium solubility. The ability of these bacteria to produce rhamnolipids broadens the range of carbon sources they can utilize as substrate (Nickzad et al., 2015; Wilhelm et al., 2007). The genes *rhlA* and *rhlB* are needed for the synthesis of mono-rhamnolipids. Those mono-

rhamnolipids can be combined by RhIC and are then termed di-rhamnolipids (Figure 2). The *rhlA* gene encodes the acyltransferase/HAA synthase (RhIA), which is responsible for the synthesis of the fatty acid dimers 3-(3-hydroxy-alkanoyl-oxy) alkanic acids (HAAs). They are formed via the esterification of two 3-hydroxy-fatty acids that are either linked to the acyl carrier protein (derived from de novo synthesis of fatty acids) or alternatively linked to the coenzyme A (derived from β -oxidation of fatty acid). The *rhlB* gene encodes the rhamnosyltransferase I (RhIB), which catalyzes the reaction of combining the HAA molecule with a dTDP-L-rhamnose (derived from glucose-6-phosphate) to produce mono-rhamnolipids. Furthermore, the *rhlC* gene encodes rhamnosyltransferase II (RhIC), which couples a second dTDP-L-rhamnose molecule to the mono-rhamnolipid to produce a di-rhamnolipid (Abdel-Mawgoud et al., 2014; Bahia et al., 2018; Wittgens et al., 2017). The microbial rhamnolipids are a mixture of different rhamnose residues and varying chain length of the β -hydroxy-fatty acid (indicated by the number after carbon atom). For example, the mono-rhamnolipid congeners produced by *Pseudomonas aeruginosa* consist of four compounds, which are Rha-C₁₀-C₁₀ (foremost), Rha-C₈-C₁₀, Rha-C₁₀-C₁₂, and Rha-C₁₀-C_{12:1}, containing an unsaturated carbon chain (Rendell et al., 1990; Tiso et al., 2017). On the other hand, the rhamnolipids produced by *Burkholderia* contain long-chain fatty acid, predominantly with C₁₄-C₁₄ (Wittgens et al., 2018).

The heterologous production of rhamnolipids using a recombinant host to avoid the employment of pathogenic bacteria has been well developed (Tiso et al., 2016; Tiso et al., 2017; Wittgens et al., 2018; Wittgens et al., 2011). One such host is, for example, *Pseudomonas putida* KT2440. However, scale-up production using common bioreactors requires strong aeration. This causes strong reactor foaming and reduces the yield, which is challenging to be overcome with conventional antifoam technologies (Beuker et al., 2016; Küpper et al., 2013). Hence, an alternative approach to facilitate the production of rhamnolipids by applying micro-aeration (oxygen-limited) reactor systems will be interesting and useful for foam-free rhamnolipids generation.

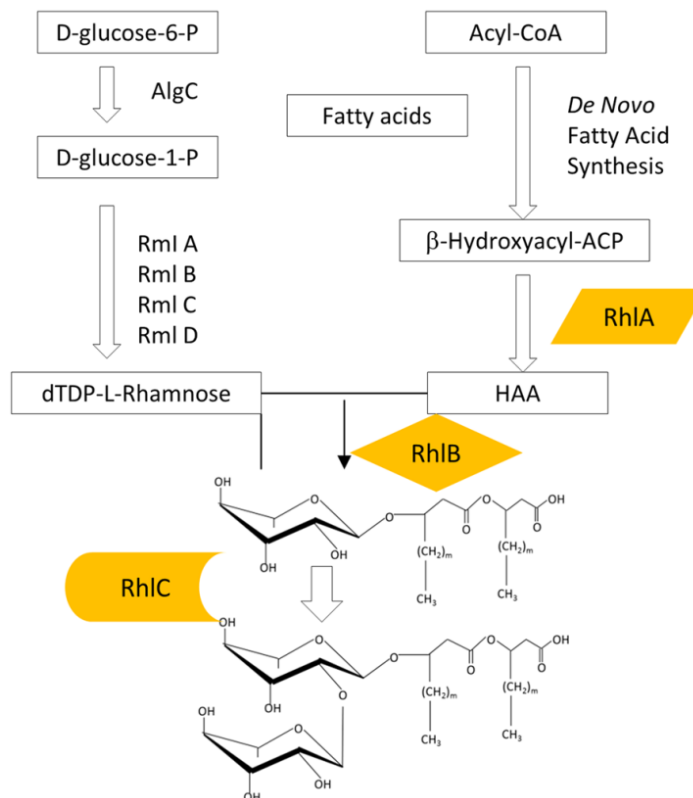


Figure 2: Rhamnolipid biosynthesis by *Pseudomonas*, adopted from Chong and Li (Chong & Li, 2017)

1.3 *Pseudomonas putida* KT2440 as multifaceted biocatalyst

Based on its GRAS (Generally Recognized As Safe) qualification, *P. putida* KT2440 is a non-pathogenic *Pseudomonas* species, which has emanated as a versatile recombinant host (Nikel & de Lorenzo, 2018). This bacteria stands out as a multifaceted biocatalyst due to the availability of extensive genetic and intrinsic metabolism information, combined with its tolerance to many chemical and biochemical substances (Loeschcke & Thies, 2015; Martinez-Garcia et al., 2014). This allows the strain to grow in the presence of various toxic chemicals and solvents (Calero & Nikel, 2019). Moreover, biocatalysis with this strain in organic systems allows for direct product removal of hydrophobic compounds, hence simplifying the purification process (Blank et al., 2008; Lang et al., 2014; Nikel et al., 2014).

Physiologically, *P. putida* KT2440 is a gram-negative saprophytic soil bacterium, which colonizes the rhizosphere (Fernandez et al., 2013). This bacterium is an obligately aerobic, as it employs

oxygen as the terminal electron acceptor. During its metabolism, it generates a high net NAD(P)H amount for enzymatic catabolism reactions, without the metabolic capacity for fermentation, anaerobic redox balancing or electron discharge (Escapa et al., 2012; Lai et al., 2016). The catabolism reaction of various substrates in *P. putida* KT2440 has been well studied. For example, the glucose metabolism is catalyzed by various enzymes, which are involved in several pathways, i.e. the Entner-Doudoroff pathway and the pentose phosphate pathway (Nikel et al., 2015; Sudarsan et al., 2014). The strain is able to accumulate biodegradable thermoplastic polymers, the poly-hydroxy-alkanoates (PHAs) as a carbon and energy storage material under growth-limited condition (Escapa et al., 2012).

Furthermore, the complete genome sequences and metabolomics studies of *P. putida* KT2440 are well established (Ballerstedt et al., 2007; Belda et al., 2016), opening the possibility for further genetic modifications. Hence, extends its usage for the heterologous production of valuable compounds. In comparison to *P. aeruginosa* PAO1, *P. putida* shares 85% similarity in the DNA sequence (Nelson et al., 2002). Therefore, *P. putida* KT2440 is a potential biocatalyst to be employed in the heterologous expression of various genes originating from *P. aeruginosa*.

1.4 Bioelectrochemical systems as a means of converting and conserving resources

The necessity of sustainable energy and environmental awareness propels the exploration and development of sustainable bioenergy resources. One of the biotechnological approaches to implement novel means of converting and conserving resources is the use of bioelectrochemical systems or BES. BES can thereby be utilized to generate bioelectricity from renewable (often waste) carbon sources or to sustainably produce platform chemicals through the interaction of microorganisms with a polarized electrode (Bajracharya et al., 2016). Therefore, BES is also a device that can be applied in the bioprocess of platform chemicals production.

As a bioprocessing system, BES involve microbial whole-cell biocatalysts to drive oxidation and reduction (redox) reactions at solid electrodes (Rosenbaum & Henrich, 2014). One example of a BES technology is the microbial fuel cell (MFC) (Figure 3b). In this system, the microorganism

catabolizes the organic matter and the electron produced from this catabolism reaction will be accepted by the BES anode. To generate the electricity, this electron moves through an external circuit to a cathode, where it combines with oxygen and protons to form water (Watanabe et al., 2009). In order to simplify the BES study in the laboratory, we are using a potentiostatically controlled BES (Figure a). In general, a potentiostatically controlled BES consists of the working electrode (anode), at which the microbial oxidation processes take place, a counter electrode (cathode), and a reference electrode, which has a stable and well-known electrode potential (Pant et al., 2012).

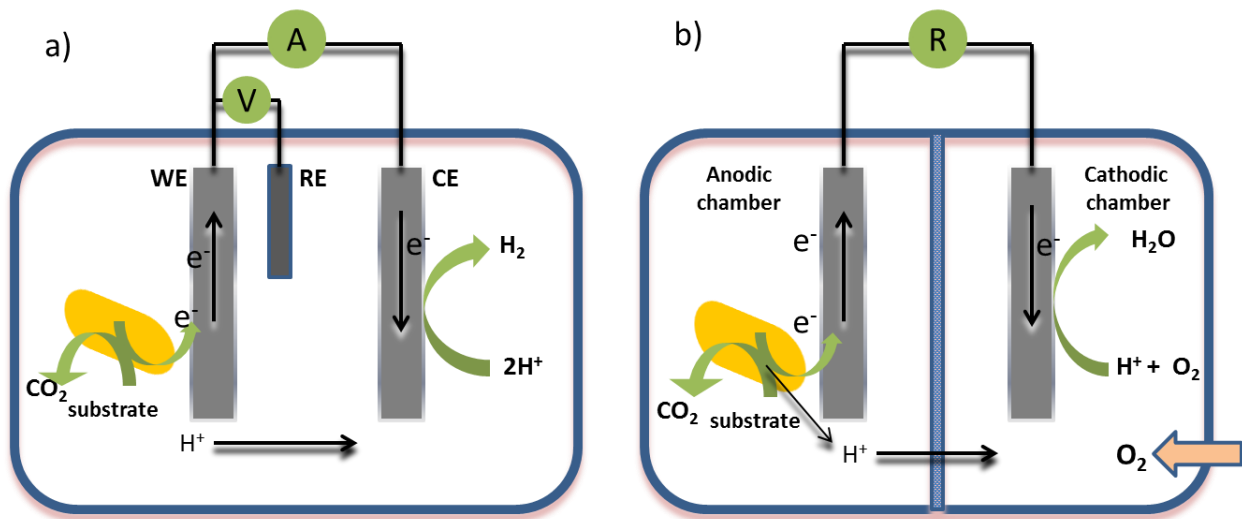


Figure 3: The general set up of a potentiostatically controlled BES and MFC. (a) is a schematic representation of a single-chambered BES, consisting of an anode as working electrode (WE), cathode as counter electrode (CE), and a reference electrode, which has a stable and well-known electrode potential (RE) and **(b)** a scheme of a two-chambered MFC separated by a proton exchange membrane (R: resistor). The schemes are modified from Logan *et al.* (Logan et al., 2006)

In relation to the presence of surfactants, it has been known that the addition of surfactant is efficiently increasing the current generation of MFC (Wen et al., 2010). Examples of synthetic surfactants have been tested to improve the MFC performance, particularly gaining the bacterial extracellular electron transfer, such as EDTA, polyethyleneimine, and Tween-80 (Liu et al., 2012; Wen et al., 2011). However, the addition of synthetic surfactant in the MFC can be toxic for the bacteria (Shen et al., 2014). Therefore, the study to understand the optimum concentration and condition of synthetic surfactant addition in the MFC is required.

Additionally, the surfactant produced by the bacteria so-called as biosurfactant, emerges less characteristic of toxicity to the bacteria, such as rhamnolipids and sophorolipids. However, the addition of exogenous biosurfactant resulted in the high cost of MFC operation. Ideally, the biosurfactant is endogenously produced by the bacterial MFC. It will be advantageous physiologically and economically for MFC performance. However, the biosurfactant synthesis by the natural biosurfactant producer bacteria is tightly controlled by the complex genetic regulatory network (quorum sensing). Therefore the production of surfactant using the recombinant host bacteria disconnecting the quorum sensing system will be more beneficial.

The extracellular electron transfer mechanism between microorganisms and electrodes can be differentiated in direct electron transfer (DET) and indirect (mediated) electron transfer. DET involves physical contact of the bacterial redox-active membrane with the anode of the BES, e.g. through nanowires and c-type cytochromes. On the other hand, MET involves a redox shuttling compound as the primary electron transfer pathway (Figure 4), which can either be exogenous (artificially added in the system) or endogenous (naturally synthesized by the microorganism) (Harnisch et al., 2011). Endogenous mediators, e.g., phenazines, have multiple advantages over exogenous mediators like methylene blue (Rahimnejad et al., 2011), neutral red (Popov et al., 2012) or ferricyanide (Hu et al., 2015). They do not require costly addition of chemical compounds and are likely produced throughout the process, while the production is linked to the activity of the producing microorganism. A disadvantage is that only certain microbial species are naturally equipped to produce endogenous redox mediators for extracellular electron transfer.

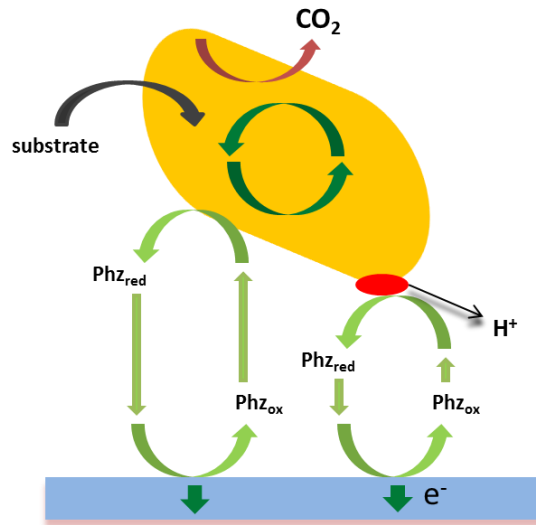


Figure 4: A scheme of extracellular electron transfer via redox shuttling compound, e.g., phenazines (Phz). The red dot indicated the membrane-bound compound involves in the mediated electron transfer. The scheme is modified from Harnisch *et al.* (Harnisch *et al.*, 2011)

1.5 Phenazines as electron shuttle compound in BES

One group of redox compounds studied for natural MET are microbial phenazines, which are produced by *Pseudomonas* species, especially by *Pseudomonas aeruginosa* (Figure 5) (Averesch & Kromer, 2018; Logan *et al.*, 2006). There are two types of phenazines; phenazine-1-carboxylic acid (PCA) and pyocyanin (PYO), which are predominantly produced by *P. aeruginosa* in oxygen-limited BES (Berger & Rosenbaum, 2017; Bosire *et al.*, 2016). In the environment, phenazines act as a virulence factor of *P. aeruginosa* by reducing the molecular oxygen into reactive oxygen species, which are toxic for other microbial species (Das *et al.*, 2015; Mentel *et al.*, 2009). On the other hand, the study of BES co-culture between *P. aeruginosa* and *Enterobacter aerogenes*, phenazines can promote synergistic interaction between species and be utilized further for electron discharge (Schmitz & Rosenbaum, 2018; Venkataraman *et al.*, 2011). The property and redox activity of the phenazines have been well studied, for example, PYO tends to be reactive with oxygen (at neutral pH)(Dietrich *et al.*, 2006), while PCA is more reactive to solid electron acceptors (Wang & Newman, 2008). Furthermore, a recent study revealed that the positive potential applied in the oxygen-limited BES of *P. aeruginosa* increased PCA production (Bosire & Rosenbaum, 2017). In the case of anaerobic cultivation, it has been revealed by Glasser *et al.*

that phenazine redox cycling enables *P. aeruginosa* to promote survival by coupling acetate and ATP synthesis (Glasser et al., 2014). The oxidation of glucose and pyruvate into acetate by acetate kinase activity found to be correlated with the ATP synthesis in the anaerobic survival mechanism (Eschbach et al., 2004). It shows that phenazines can facilitate energy generation, which might broaden the metabolic versatility of microorganisms.

The complex regulatory network of phenazine synthesis and the pathogenic nature of *P. aeruginosa* limit the application of phenazine redox mediation for specific biotechnological applications with this host (Dietrich et al., 2006). A successful initial proof-of-principle study has been reported by our lab in 2015 (Schmitz et al., 2015), introducing an engineered strain of non-pathogenic, aerobic *P. putida* KT2440, in which heterologous phenazine synthesis enables electron discharge to an extracellular anode under oxygen-limited conditions in BES. The heterologous expression of the nine phenazine synthesis genes from *P. aeruginosa* PAO1 (*phzA1-G1*, *phzM*, and *phzS*) in *P. putida* KT2440, resulted in the production of PCA and PYO. The derivative PYO was only fully synthesized when active aeration was applied during the initial growth phase since the final enzyme PhzS is dependent on molecular oxygen. During subsequent passive aeration via opened vent filter (i.e., strong oxygen limitation of the culture), metabolic activity sustained, and PCA was further synthesized and accumulated. Thereby, the total produced phenazine concentrations in BES were in the upper range of phenazine concentrations produced by the native producer *P. aeruginosa* (30–40 µg/mL for *P. putida* pPhz (Schmitz et al., 2015) vs. 22–25 µg/mL for *P. aeruginosa* PA14) (Bosire et al., 2016).

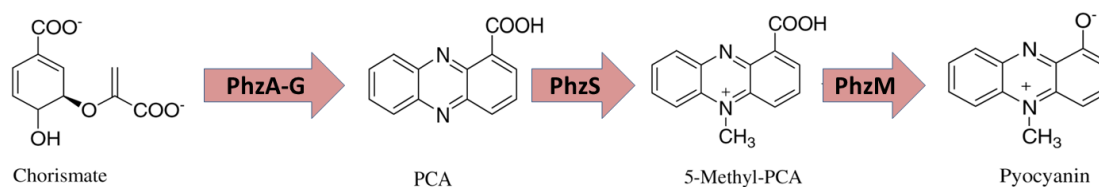


Figure 5: Phenazine biosynthesis pathways in *P. aeruginosa*. The scheme is modified from Parsons *et al.* (Parsons et al., 2007)

To develop an efficient *P. putida* biocatalyst for oxygen-limited bioelectrochemical production, it is necessary to explore further and optimize its heterologous production of phenazines. The work conducted by Bosire *et al.* showed for several carbon sources that *P. aeruginosa* PA14

produces more phenazines and results in higher anodic currents than *P. aeruginosa* PAO1 within an oxygen-limited BES setup (Bosire et al., 2016). This strain dependency of phenazine synthesis may be already encoded in the genetic origin for the phenazine synthesis genes in these strains. The original producer of phenazines, *P. aeruginosa*, encodes for two homologous operons; *phzA1-G1* (operon 1/*phz1*) and *phzA2-G2* (operon 2/*phz2*), which are responsible for the synthesis of PCA (Cui et al., 2016). It has been reported by Mavrodi *et al.* that the two phenazine gene operons of *P. aeruginosa* are 98% identical in DNA level, but differ distinctively in their promoter regions. The regulatory genetic element *las* box is present in the promoter region of the *phz1* operon, by which the quorum-sensing regulators LasR and/or RhIR recognize their target genes to initiate quorum-sensing-controlled gene expression. In contrast, for *phzA2*, the *las* box is not present in the promoter region (Mavrodi et al., 2001; Mavrodi et al., 2010). Furthermore, the two operons are also containing dissimilarities at DNA sequence level within *phzA1B1* and *phzA2B2*, while the regions from *phzC* to *phzG* of both operons are highly identical (Recinos et al., 2012). Therefore, both operons of phenazine genes from *P. aeruginosa* PAO1 and PA14 were deeper evaluated in this study. Base on the amino acid sequence comparison, each gene of phenazine operon from *P. aeruginosa* PAO1 and PA14 are containing dissimilarities between strains and operons as it is shown in Figure 6.

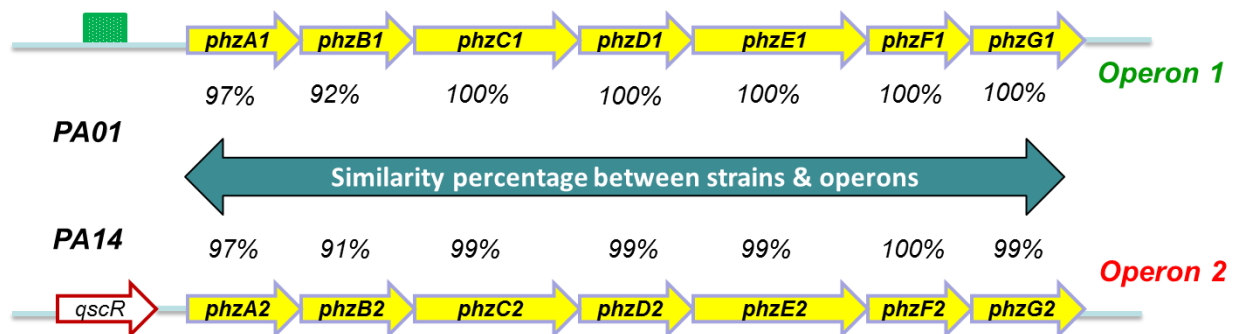


Figure 6: Amino acid sequence similarity of phenazine operon 1 and 2 in *P. aeruginosa* PAO1 and PA14 (Mavrodi et al., 2001; Recinos et al., 2012)

1.6 Scope and outline of the thesis

The purpose of this project is to develop an efficient engineered *P. putida* biocatalyst for oxygen-limited bioelectrochemical production, by employing phenazine electron shuttling to an anode as the main electron transfer pathway. Furthermore, to show the potential application, the heterologous production of rhamnolipids was combined with oxygen-limited phenazine redox balancing in the suitable *P. putida* host strain. The scope of the thesis is depicted in Figure 7.

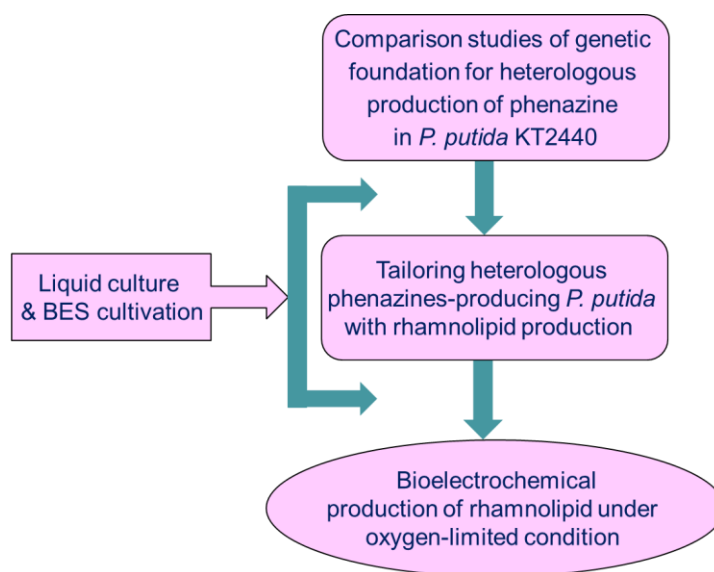


Figure 7: Research work flow in this study

Here in this study, we developed the concept of moving from an aerated to an oxygen-limited production process for rhamnolipids, where oxygen is only supplied in the headspace and/or via passive diffusion to prevent reactor foaming. With this approach, we aim to obtain the best heterologous *P. putida* phenazines producer for efficient biocatalysis in oxygen-limited BES. According to the motivation to generate *P. putida* KT2440 as an efficient biocatalyst for bioelectrochemical production, the following hypotheses have been proposed:

1. Heterologous phenazine production in *P. putida* can be tuned and enhanced by testing the natural gene variability of the native hosts

2. The heterologous phenazines production can be coupled to rhamnolipid biosynthesis by generating plasmid-based genetic engineered *P. putida*.
3. Oxygen-limited cultivations with redox balancing via phenazines in BES can be coupled to rhamnolipid biosynthesis.

Chapter 2

Materials and Methods

2.1 Strain engineering

2.1.1 Bacterial strains, media preparation, and strain cultivation

Pseudomonas putida strain KT2440 (DSM 6125) was used for heterologous expression of phenazine genes from *P. aeruginosa* PAO1 (DSMZ 19880) and PA14 (DSMZ 19882). *Escherichia coli* strain DH5 α (New England Biolabs) has been used as intermediary cloning recipient. Standard strain cultivations were performed in 250 mL shake flasks using LB medium (Carl Roth[®]) with or without antibiotics as required and were incubated at 30 °C (*P. putida*) or 37 °C (*E. coli*). For *P. putida* characterization in well plates, shake flasks and BES experiment, the strains have been cultivated at 30 °C in Delft mineral salt medium (Hartmans et al., 1989), with a final composition (per L) of 3.88 g K₂HPO₄ (22 mM), 1.63 g NaH₂PO₄ (14 mM), 2.00 g (NH₄)₂SO₄, 0.1 g MgCl₂·6H₂O, 10 mg EDTA, 2 mg ZnSO₄·7H₂O, 1 mg CaCl₂·2H₂O, 5 mg FeSO₄·7H₂O, 0.2 mg Na₂MoO₄·2H₂O, 0.2 mg CuSO₄·5H₂O, 0.4 mg CoCl₂·6H₂O, 1 mg MnCl₂·2H₂O, with 20 mM glucose (passive aeration) or 40 mM glucose (active aeration) and antibiotics as required (Kanamycin at 50 μ g/mL concentration or/and Gentamycin at 30 μ g/mL concentration).

2.1.2 Genetic engineering of *P. putida* for phenazine synthesis

Table 1 gives an overview of the strains and plasmids used for construct generation. The plasmid harboring operon *phzA1-G1* amplified from *P. aeruginosa* PAO1 genomic DNA (*O1.phz1*) was generated by Schmitz *et al.* The other three plasmids to synthesize PCA were newly constructed in this study; plasmid pBNT01.phz2 harboring *phzA2-G2* amplified from *P. aeruginosa* PAO1; the plasmid pBNT14.phz1 and pBNT14.phz2 harboring *phzA1-G1* and *phzA2-G2*, respectively, amplified from *P. aeruginosa* PA14. For plasmids assembly, the Gibson assembly method was used and performed according to the manufacturer's instruction (New England Biolabs-Gibson Assembly) (Gibson et al., 2009). Plasmid constructions were planned and conducted according to the New England Biolabs NEBuilder online tool (<http://nebuilder.neb.com/>). In Gibson cloning, DNA fragments are generated with special homologous primer-overlaps via polymerase chain reaction (PCR). Following vector linearization, all components were incubated with an enzyme mix, containing (i) a 5'-

exonuclease (digesting of the 5'-ends of the fragments in order to enable the annealing of the homologues parts), (ii) a DNA polymerase (refilling the gaps by extending the 3'-ends) and (iii) a DNA ligase (for sealing of nicks). For the assembly reaction, the linearized vector (50-100 ng) was mixed with a 2-fold excess of the amplified inserts, which contained the homologous overhangs (primers 1-6 Table 2). For insert amplification, the Q5[®] High-Fidelity DNA polymerase (NEB) was used. After adding the Gibson assembly master mix, the mixture was incubated at 50 °C for 30 minutes. The finished construct was transferred into chemically competent *E. coli* DH5 α cells.

Subsequently, all plasmids have been transformed into *P. putida* KT2440 via electroporation (Choi et al., 2006). For combined PCA and PYO synthesis, the best pre-selected strain producing PCA from each operon origin was transformed further with pJNN.phzM+S generated by Schmitz *et al.* Transformed cells were selected on LB agar plates with kanamycin (K, 50 μ g/mL) for PCA, while for PCA & PYO producers LB agar plates with kanamycin (same concentration) and gentamycin (G, 30 μ g/mL) were used. The constructs (Table 1) were verified using colony PCR, restriction digest analysis, and DNA sequencing with designed primers (Table 2). DNA plasmids sequencing analysis was performed using the Sanger sequencing method (GATC-Eurofins Genomics). The DNA sequencing products of the promoter and phenazine genes region were compared and verified with the reference plasmid map using Clone Manager Software. The successful expression of the *phzA-G* genes will show the PCA production by exhibiting yellow colour in Delft medium, while in combination with *phzM+S* genes, the bacterial culture will produce PCA and PYO appear in a greenish-blue color.

Table 1: Bacterial strains and plasmids used for genetic engineering of *P. putida* for phenazine synthesis

Strains/Plasmids	Characteristics	Source
Strains		
<i>P. aeruginosa</i> PAO1	Wildtype	DSMZ
<i>P. aeruginosa</i> PA14	Wildtype	DSMZ
<i>P. putida</i> KT2440	Wildtype	DSMZ
<i>P. putida</i> O1.phz1	harboring plasmid pBNT.O1.phz1	(Schmitz et al., 2015)
<i>P. putida</i> O1.phz2	harboring plasmid pBNT.O1.phz2	this study
<i>P. putida</i> 14.phz1	harbouring plasmid pBNT.14.phz1	this study

<i>P. putida</i> 14.phz2	harboring plasmid pBNT.14.phz2	this study
<i>P. putida</i> O1.phz1+	harboring plasmid pBNT.O1.phz1 and pJNN.phzM+S	(Schmitz et al., 2015)
<i>P. putida</i> O1.phz2+	harboring plasmid pBNT.O1.phz2 and pJNN.phzM+S	this study
<i>P. putida</i> 14.phz1+	harbouring plasmid pBNT.14.phz1 and pJNN.phzM+S	this study
<i>P. putida</i> 14.phz2+	harbouring plasmid pBNT.14.phz2 and pJNN.phzM+S	this study
<i>E. coli</i> DH5α	<i>fhuA2 (argF-lacZ)U169 phoA glnV44 80 (lacZ)M15 gyrA96 recA1 relA1 endA1 thi-1 hsdR17</i>	NEB

Plasmids

pBNT	ORI: ori/IHF for replication in <i>E. coli</i> and <i>Pseudomonas</i> ; Kanamycin resistance-cassette, salicylate-inducible <i>nagR/pNagAa</i> promoter	
pJNN	ori RO1600 for <i>Pseudomonas</i> and ori ColE1 for <i>E.coli</i> ; Gentamycin resistance-cassette, salicylate-inducible <i>nagR/pNagAa</i> promoter	
pBNT.O1.phz1	ORI: ori/IHF for replication in <i>E. coli</i> and <i>Pseudomonas</i> ; Kanamycin resistance-cassette, salicylate-inducible <i>nagR/pNagAa</i> promoter, <i>phzA1-G1</i> . PAO1 genes	(Schmitz et al., 2015)
pJNN.phzM+S	ori RO1600 for <i>Pseudomonas</i> and ori ColE1 for <i>E.coli</i> ; Gentamycin resistance-cassette, salicylate-inducible <i>nagR/pNagAa</i> promoter, <i>phzM+S</i> . PAO1 genes	(Schmitz et al., 2015)
pBNT.O1.phz2	ORI: ori/IHF for replication in <i>E. coli</i> and <i>Pseudomonas</i> ; Kanamycin resistance-cassette, salicylate-inducible <i>nagR/pNagAa</i> promoter, <i>phzA2-G2</i> . PAO1 genes	this study
pBNT.14.phz1	ORI: ori/IHF for replication in <i>E. coli</i> and <i>Pseudomonas</i> ; Kanamycin resistance-cassette, salicylate-inducible <i>nagR/pNagAa</i> promoter, <i>phzA1-G1</i> . PA14 genes	this study
pBNT.14.phz2	ORI: ori/IHF for replication in <i>E. coli</i> and <i>Pseudomonas</i> ; Kanamycin resistance-cassette, salicylate-inducible <i>nagR/pNagAa</i> promoter, <i>phzA2-G2</i> . PA14 genes	this study

Table 2: Primers used for genetic engineering of *P. putida* for phenazine synthesis

No	Primer	Sequence 5'→3'	Function
1	phz2.O1-f	GAAACAGGAGGTACCGCCTCGT CGCCTAGC	amplifying the <i>phzA2-G2</i> . PAO1 gene, with <i>EcoR1</i>
2	phz2.O1-r	CCTCTAGACTCGAGGGCGGTTG GATGGGTTTC	restriction site of overlapping regions for Gibson assembly
3	phz1.14-f	CCGACGTCGCATGCTCCTTGGC GTTATCCGCCATGAAAC	amplifying the <i>phzA1-G1</i> . PA14 gene, with <i>EcoR1</i> &
4	phz1.14-r	AGGAAACAGGAGGTACCGTCCT ACGTATGAACAATGCGC	<i>Xba1</i> restriction site of overlapping regions for Gibson assembly
5	phz2.14-f	GCCCGACGTCGCATGCTCCTGG GCTCCAAGGCCGCGTAG	amplifying the <i>phzA2-G2</i> . PA14 gene, with <i>EcoR1</i> &
6	phz2.14-r	ACAGGAAACAGGAGGTACCGG GTTACAAC TGGGTTTCAGGCCGA AAC	<i>Xba1</i> restriction site of overlapping regions for Gibson assembly
7	CP-f	GTCAACGCGAACATTTCC	amplifying the part of <i>phzG</i>
8	CP-r	CAACTGTTGGGAAGGCGATCG GTG	gene to ORI region of pBNT plasmid (colony PCR verification)
9	Seq_1	GCACCGGACTCCATATC	sequencing part of <i>phzG</i> gene to ORI region of pBNT plasmid
10	Seq_2	CACCATGCGAGAGTACC	sequencing part of ORI to Kanamycin resistance cassette of pBNT plasmid
11	Seq_3	GCTGTGGCGGTTTATGG	sequencing part of <i>nagR/pNagAa</i> promoter region of pBNT plasmid to part of <i>phzA</i> gene
12	Seq_4	GATCCTCAAGGGCTATG	sequencing part of <i>phzA</i> gene to part of <i>phzB</i> gene
13	Seq_5	GCGGCATTCCCGAAATC	sequencing part of <i>phzB</i> gene to part of <i>phzC</i> gene
14	Seq_6	GTTGCGCTTGCTCTACC	sequencing part of <i>phzC</i> gene
15	Seq_7	CGACAACCGCAAGGAAG	sequencing part of <i>phzC</i> gene to part of <i>phzD</i> gene
16	Seq_8	CGATGATCGCCAAGCAG	sequencing part of <i>phzD</i> gene to part of <i>phzE</i> gene
17	Seq_9	CGCATCCGCATCTTCAC	sequencing part of <i>phzE</i> gene
18	Seq_10	CCATGATGGGCGTCAAC	sequencing part of <i>phzE</i> gene to part of <i>phzF</i> gene
19	Seq_11	CACTGGCAGAGCATTAC	sequencing part of <i>phzF</i> gene to part of <i>phzG</i> gene

2.1.3 Tailoring heterologous rhamnolipid-producing *P. putida* with phenazine production

Table 3 shows the plasmids and strains used in construct generation. The plasmids harbor the *rhlA* and *rhlB* genes amplified from *P. aeruginosa* PAO1 genomic DNA. For plasmid assembly, the Gibson assembly method was used and performed according to the manufacturer's instruction (New England Biolabs-Gibson Assembly) (Gibson et al., 2009). The *rhlAB* genes were inserted into pJNN and pJNN.phzM+S plasmids to generate pJNN.rhlAB and pJNN.rhlAB.phzM+S, respectively. Subsequently, the pJNN.rhlAB and pJNN.rhlAB.phzM+S plasmids have been transformed into *P. putida* KT2440 via electroporation (Choi et al., 2006). The new strains named *P. putida* rhl and *P. putida* rhl-MS for further references. Transformed cells were selected on LB agar plates with gentamycin (G, 30 µg/mL).

The constructs were verified using colony PCR, restriction digest analysis, and DNA sequencing. DNA plasmid sequencing analysis was performed using the Sanger sequencing method (GATC-Eurofins Genomics). For verification, the DNA sequencing products of the promoter and rhamnolipid genes were compared with the reference plasmid map using Clone Manager Software. Primers used for DNA sequencing are described in Table 4. Cells were tested for gene expression on LB media containing antibiotic and pre-added autoinducer. Transformed cells were selected on LB agar plates with kanamycin (K, 50 µg/mL) and gentamycin (G, 30 µg/mL). Successful expression of the rhamnolipid production genes *rhlAB* was verified via HPLC (high-performance liquid chromatography).

Subsequently, pBNT14.phz2 plasmid has been transformed into *P. putida* rhl and *P. putida* rhl-MS via electroporation (Choi et al., 2006). The new strains named *P. putida* rhl-pca for PCA & rhamnolipid producer, and *P. putida* rhl-pyo for PCA, PYO, & rhamnolipid producer for further references. Transformed cells were selected on LB agar plates with kanamycin (K, 50 µg/mL) and gentamycin (G, 30 µg/mL). Successful expression of the rhamnolipid production genes *rhlAB* and phenazine/s were verified via HPLC.

Table 3: Bacterial strains and plasmids used for tailoring heterologous rhamnolipid-producing *P. putida* with phenazine production

Strains/Plasmids	Characteristics	Source
Strains		
<i>P. aeruginosa</i> PAO1	Wildtype	DSMZ
<i>P. aeruginosa</i> PA14	Wildtype	DSMZ
<i>P. putida</i> 14.phz2	harboring plasmid pBNT.14.phz2	this study
<i>P. putida</i> rhl	harboring plasmid pJNN.rhIAB	this study
<i>P. putida</i> rhl-pca	harboring plasmid pBNT.14.phz2 and pJNN.rhIAB	this study
<i>P. putida</i> rhl-MS	harboring plasmid pJNN.rhIAB.phzM+S	this study
<i>P. putida</i> rhl-pyo	harboring plasmid pBNT.14.phz2 and pJNN.rhIAB.phzM+S	this study
<i>E. coli</i> DH5 α	<i>fhuA2 (argF-lacZ)U169 phoA glnV44 80 (lacZ)M15 gyrA96 recA1 relA1 endA1 thi-1 hsdR17</i>	New England Biolabs
<i>P. putida</i> SK1	genome integrated <i>rhlAB</i> operon into the 16S rDNA sequence (the initial study of the anaerobic flask experiment)	(Kruth, 2017)
Plasmids		
pJNN.rhIAB	ori RO1600 for <i>Pseudomonas</i> and ori ColE1 for <i>E.coli</i> ; Gentamycin resistance-cassette, salicylate-inducible <i>nagR/pNagAa</i> promoter, <i>rhlA</i> and <i>rhlB</i> genes (<i>P. aeruginosa</i> PAO1)	this study
pJNN.rhIAB.phzM+S	ori RO1600 for <i>Pseudomonas</i> and ori ColE1 for <i>E.coli</i> ; Gentamycin resistance-cassette, salicylate-inducible <i>nagR/pNagAa</i> promoter, <i>phzM</i> , <i>phzS</i> , and <i>rhlA</i> and <i>rhlB</i> genes (<i>P. aeruginosa</i> PAO1)	this study
pBNT.14.phz2	ORI: ori/IHF for replication in <i>E. coli</i> and <i>Pseudomonas</i> ; Kanamycin resistance-cassette, salicylate-inducible <i>nagR/pNagAa</i> promoter, <i>phzA2-G2</i> genes (<i>P. aeruginosa</i> PA14)	this study

Table 4: Primers used for tailoring heterologous rhamnolipid-producing *P. putida* with phenazine production

No	Primer	Sequence 5'	Function
1	rhIAB-f	GTACCGAATTCCTCGAGTGGGCTC AACCTGGGAACTG	amplifying the <i>rhIAB</i> .PAO1 gene, with Xba1 restriction site with overlapping regions for Gibson assembly to pJNN plasmid
2	rhIAB-r	CCGACGTGCATGCTCCTCACCGCT ACACAGGAAATTC	amplifying the <i>rhIAB</i> .PAO1 gene, with Xba1 restriction site with overlapping regions for Gibson assembly to pJNN plasmid
3	rhIAB.MS-f	GTCTTTTTTCGGCCGCGTACCAGGA GGAGAGATG	amplifying the <i>rhIAB</i> .PAO1 gene, with Xba1 restriction site with overlapping regions for Gibson assembly to pJNN.M+S plasmid
4	rhIAB.MS-r	CTGGATCTGGCCTAGGACTCTAGA ATTCAGGACGC	amplifying the <i>rhIAB</i> .PAO1 gene, with Xba1 restriction site with overlapping regions for Gibson assembly to pJNN.M+S plasmid
5	CP.rhIAB-f	AGATGCGGCGCGAAAGTCTG	amplifying the part of <i>rhIA</i> gene to promoter <i>nagR/pNagAa</i> region of pJNN plasmid (colony PCR verification)
6	CP.rhIAB-r	CGCGCCTGCTCGTATTCGCC	
7	CP.M+S.rhIAB-f	CTAGGCCAGATCCAGCGG	amplifying the part of <i>rhIA</i> gene to promoter <i>nagR/pNagAa</i> region of pJNN.M+S plasmid (colony PCR verification)
8	CP.M+S.rhIAB-r	GCGGCCGAAAAAAGACCCGC	
9	Seq_rhIA	TGGCCGAACATTTCAACGTG	Sequencing the <i>rhIA</i> gene region
10	Seq_rhIB	CTGTTTCGACGGCAGTATCCC	sequencing the <i>rhIB</i> gene region

Eight clones of transformed *P. putida*, which were confirmed to produce both mono-rhamnolipid and phenazine/s, were tested in triplicates for aerobic strain characterization and evaluation, as described in section 2.1.5.

2.1.4 Plasmid sustainability experiments to determine the strain stability

To confirm whether the *P. putida* rhI-pca strain was still harboring the two plasmids expressing rhamnolipids and PCA, during the cultivation in the BES reactor, reactor samples were plated for cell counts at day 3, 6, and 9. They were diluted at the range of 10^{-2} – 10^{-6} , then 100 μ L of the diluted sample was streaked on the LB plate containing 50 μ g/mL of kanamycin only (selection for pBNT.14.phz2), LB plate containing 30 μ g/mL of gentamycin only (selection for pBNT.14.phz2), LB plate containing both of kanamycin and gentamycin (selecting for both plasmids), and LB plate without antibiotics (no selection = all viable cells). The plates were incubated at 30 °C overnight. The number of bacteria counted from the plate was expressed in

CFU/mL (CFU = colony-forming unit). Counts on plates with antibiotics (indicating colonies containing the plasmids) were related to the total cell counts on plates without antibiotics.

2.1.5 Aerobic strain characterization and evaluation

For evaluation of phenazine and/or rhamnolipid production, eight clones of each constructed strain were tested in triplicates in the multiplexed cultivation platform micro cultivation (CR1424d, EnzyScreen, Heemstede, The Netherlands), using 24 square-well plates filled with 5 mL Delft medium, 20 mM glucose, and supplemented with 50 µg/mL Kanamycin and/or 30 µg/mL Gentamycin. While the aerobic shake flask experiments were performed in 250 mL Erlenmeyer flasks; filled with 25 mL Delft medium. Both of the cultivations were starting at a uniform inoculation OD_{600} of 0.1. After three hours of incubation, 0.1 mM (for phenazine production) and 1 mM for rhamnolipid production) sodium salicylate was added as an inducer for gene expression. The incubation temperature was 30 °C, and the shaking frequency was 224 rpm (multiplexed cultivation) or 200 rpm (shake flasks experiment). The clone with the best growth behavior coupled with the best phenazine production of each constructed strain, during multiplex cultivation, was selected and further characterized in aerobic shake flasks- as well as BES experiments.

2.1.6 Anaerobic strain characterization and evaluation

To understand the effect of phenazines on the mono-rhamnolipid producing *P. putida*, a controlled study has been conducted. Here, the *P. putida* SK1 (genome integrated strain; Table 3) was cultivated in anaerobic serum bottles with artificial phenazine addition. The *P. putida* SK1 strain was cultivated in serum bottles (100 mL of Delft media in 220 mL bottles) closed with butyl septum and tightened with an aluminum cap. During initial growth, the *P. putida* SK1 + PYO_{synth} (~15 µg/mL) and *P. putida* SK1 + PCA_{synth} (~15 µg/mL,) were cultivated at 80 rpm, until the end of growth experiment (triplicate). The samples were taken once per day and measured for growth, synthetic phenazine concentration, and mono-rhamnolipid production.

2.2 Bioelectrochemical experiments

2.2.1 Oxygen-limited bioelectrochemical system experiments

Single chamber glass BES reactors (500 mL working volume) equipped with a water jacket for temperature control were used (Figure 8). The integrated three-electrode set-up included: (i) a 156.32 cm² graphite comb of high grade graphite (EDM-3, Novotec) as WE (anode), (ii) a 49.22 cm² graphite block as CE (cathode), and (iii) a Ag/AgCl, saturated KCl electrode (192 mV vs. SHE at 30 °C, pH 7) as RE. The BES reactor experiments were performed at 30 °C at 200 rpm stirring with a magnetic stirrer, and potentiostatically controlled by a potentiostat (VMP3, BioLogic) at 0.2 V vs. RE. The electrical currents signal was recorded continuously, including 24 h of blank media measurement. Sampling for determination of optical density at 600 nm, pH and HPLC analysis were performed daily, following inoculation. The duplicate BES reactor experiments were performed under two types of oxygen-limited condition: (i) active aeration (AA), in which the active aeration was applied via a sparger at 30 mL/minute flow rate for 48 hours, followed by passive aeration via two opened vent filters, and (ii) passive aeration (PA), in which only passive aeration via opened vent filters (~50 ppb dissolved oxygen) was applied for the entire experiment.

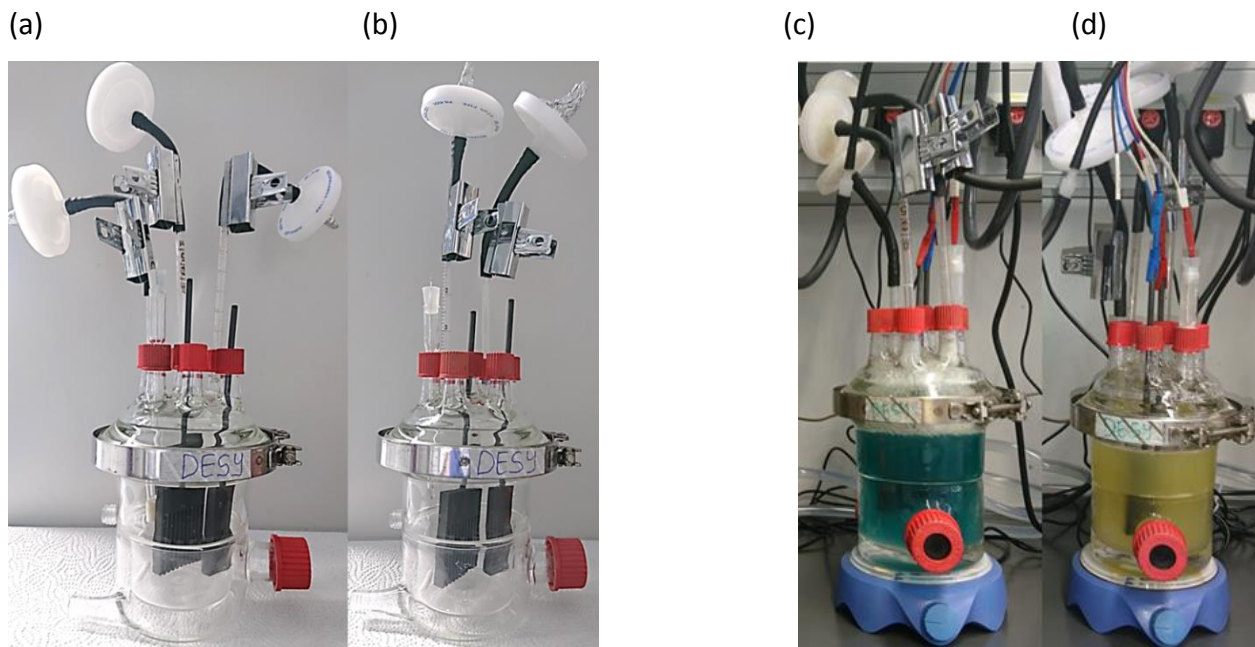


Figure 8: Image of bioelectrochemical reactors used in this study (a) Active aeration set-up (b) Passive aeration set-up (c) *P. putida* 14.phz2+ produced PCA and PYO indicated by blue pigment in the grown culture (d) *P. putida* 14.phz2 produced PCA indicated by yellow pigment in the grown culture.

2.2.2 Bioelectrochemical production of rhamnolipids under the oxygen-limited condition

The single-chamber reactors described in section 2.2.1 were applied in this experiment. To provide the best conditions for bioelectrochemical production of rhamnolipids, several different set-ups of BES experiments (triplicate) have been conducted as described in Table 5. The triplicate BES reactor experiments were performed under several types of oxygen-limited conditions: (i) active aeration via a sparger at 30 mL/minute flow rate for 48 hours, followed by either, passive aeration via two open vent filters (AA) or continued active aeration at 50 mL/minute (AA+). (ii) Passive aeration (PA), via open vent filters, applied for the entire experiment.

Table 5: Bioelectrochemical production of rhamnolipid set-ups

Strains	Set up (aeration mode, the presence of electrode)
<i>P. putida</i> rhl	AA, without and with electrodes (triplicate) PA, with electrodes (single)
<i>P. putida</i> rhl-pca	AA, without and with electrodes (triplicate) AA, with carbon cloth electrode as WE: 400 cm ² (duplicate) AA+, with electrodes (triplicate) AA+, with electrodes (single), plasmid sustainability experiment PA, with electrodes (triplicate) PA, with electrodes (triplicate, repetition experiment), plasmid sustainability experiment

2.3 Analytical methods

2.3.1 Bioinformatics analysis

Sequences and annotations of *Pseudomonas aeruginosa* PAO1 (assembly: GCA_000006765.1) and *Pseudomonas aeruginosa* PA14 (assembly: GCA_000014625.1) have been obtained from GenBank (Benson et al., 2005). Each strain contains two main operons of seven almost identical genes each, organized in an operon for PCA production. All these genes have been compared individually by multiple protein alignment, and the entire operons (excluding the promoter) have been compared by multiple nucleotide alignment. Clustal Omega 1.2.4 has been used to perform the alignments (Sievers & Higgins, 2018; Sievers et al., 2011). To detect changes between the codon usage among genes in the four operons, codon adaptation indices (Sharp &

Li, 1987) have been calculated for all genes using an index previously generated for *Pseudomonas putida* KT2440 (assembly: GCA_000007565.2). All calculations are performed using Biopython 1.72 (Cock et al., 2009). For all proteins involved in phenazines production (except PhzF and PhzM due to full sequence identity), a 3D-model has been created by homology modeling using MODELLER (Webb & Sali, 2014). All structures have been predicted in the same way, including those with an experimentally determined structure, to avoid bias. Models have been built as homodimers, except PhzS, which has been built as a monomer. The predicted protein structures have been superimposed and displayed using UCSF Chimera (Pettersen et al., 2004). RMSD (root-mean-square deviation of atomic positions) has been calculated to measure the difference between structures. Plots for codon adaptation index comparison and operon analysis have been created using RStudio (RStudio_Team, 2015).

2.3.2 Analysis of sugar metabolites

Analysis of glucose and secreted metabolites was performed using HPLC equipped with a 300×8.0 mm polystyroldivinylbenzol copolymer separation column (CS-Chromatographie), a UV/VIS detector at 210 nm and a refractive index (RI) detector at 35 °C. The separation was achieved at 60 °C with 5 mM sulphuric acid mobile phase at 0.8 mL/min isocratic flow rate. Analytical grade glucose, 2-ketogluconate, gluconate, and acetate (Carl Roth®) were used as standard solutions.

2.3.3 Phenazine analysis

The quantification of phenazines was performed using HPLC with a C₁₈ column (Waters Corporation) equipped with a photodiode array UV/VIS detector (LC-168, Beckmann), which detected and quantified the PCA at 366 nm and PYO at 280 nm. Separation was achieved with a gradient of 0.1 % trifluoroacetic acid (TFA) in acetonitrile (solution A) and 0.1 % TFA in water (solution B) as mobile phase (with solution A at 15 % for 2 min, 100 % for 15 min, and 5 % for 3 min) at a flow rate of 0.8 mL/min and a column temperature of 20 °C (Kern & Newman, 2014). Analytical grade PCA (Princeton Biomolecular) and PYO (Cayman Chemical) were used as standard solutions of phenazines.

2.2.1 Rhamnolipid analysis

The quantification of rhamnolipids was performed using reversed-phase high-performance liquid chromatography (RP-HPLC) elucidated in a NUCLEODUR C18 Gravity column (Macherey-Nagel GbH & Co. KG, Düren, Germany) (dimensions: 150x4.6 mm; particle size: 3 mm). The HPLC system Ultimate 3000 was equipped with a Corona-charged aerosol detector (CAD) (Thermo Fisher Scientific Inc., Waltham, MA, USA). The flow rate was 1 mL/min at 40 °C column oven temperature. Separation was achieved with a gradient of 100 % acetonitrile (eluent A) and ultra-pure water containing 0.2 % (v/v) formic acid (eluent B) as buffers (with eluent A at 70 % for 9 min, 100 % for 3 min, and 70 % for 3 min) (Tiso et al., 2016). Analytical grade of rhamnolipids consists of mono-rhamnolipids and di-rhamnolipids (C₈-C₁₂ congeners) (Sigma-Aldrich/AGAE Technologies) was used as standard solutions of rhamnolipids.

2.3.4 Rhamnolipid detection using thin-layer chromatography (TLC)

To verify the presence of rhamnolipids produced in the BES reactor, especially when the rhamnolipid concentration detected by HPLC was below 100 mg/L, TLC was applied. The samples from the reactors were extracted using ethyl acetate, in the ratio of 1:1 compared to the sample volume (3-5 times washed). The samples were subsequently evaporated using rotary dryer Scan speed 40™ connected to the SCANVAC Cooling Trap (LaboGene ApS, Lyngø, Denmark) at 1400 rpm and 45 °C, for one hour. The dried rhamnolipid samples were dissolved in 20 µL ethanol. All of the solutions were spotted on silica 60 TLC-plate (Macherey-Nagel, Düren, Germany). As a standard solution, 5 µL of a 0.1 % commercial rhamnolipid extract R90™ containing mono- and di-rhamnolipid (AGAE Technologies LLC, Corvallis, USA) was spotted as well. The running buffer was a mixture of chloroform, methanol, and acetic acid in the ratio of 65:15:2. For the visualization of the rhamnolipids, the TLC plate was layered with a solution mixture of acetic acid, sulfuric acid, and anisaldehyde in the ratio of 10:0.2:0.1. The TLC plate was incubated at >100 °C using the hot air gun (Einhell, Landau, Germany) until the bands became visible. The standard rhamnolipid mixture, as well as the samples, which contained rhamnolipids, were stained yellow by anisaldehyde.

Chapter 3

Results and Discussions

3.1 Boosting heterologous phenazine production in *Pseudomonas putida* KT2440 through the exploration of the natural sequence space

A version of this chapter is ready to be submitted for publication with the following distribution of work of the co-authors:

- Theresia D. Askitosari¹ – planned and conducted the experiments, analyzed the data and wrote the manuscript
- Santiago T. Boto² – performed the in silico sequence and structure analysis of the phenazine synthesis genes/proteins
- Lars M. Blank¹ – co-supervised the work, discussed the results and revised the manuscript
- Miriam A. Rosenbaum^{2,3*} – conceived the work, planned the experiments, discussed the results and revised the manuscript

¹Institute of Applied Microbiology IAMB, Aachen Biology and Biotechnology ABBt, RWTH Aachen University, Aachen, Germany

²Leibniz Institute for Natural Products Research and Infection Biology – Hans-Knöll-Institute, Jena, Germany

³Faculty of Biological Sciences, Friedrich-Schiller-University, Jena, Germany

*corresponding author: miriam.rosenbaum@leibniz-hki.de

3.1.1 Summary

Phenazine-1-carboxylic acid (PCA) and its derivative pyocyanin (PYO) are potential natural redox mediators in bioelectrochemical systems. The native producer *Pseudomonas aeruginosa* harbors two identical structured operons in its genome, which encode the enzymes responsible for PCA synthesis (*phzA1-G1* (operon 1), *phzA2-G2* (operon 1)). To optimize heterologous phenazines production in *Pseudomonas putida* KT2440, we compared PCA production from both operons originating from *P. aeruginosa* strain PAO1 (*O1.phz1* and *O1.phz2*) as well as from *P. aeruginosa* strain PA14 (*14.phz1* and *14.phz2*). Comparisons of phenazine synthesis and bioelectrochemical activity were performed between heterologous constructs with and without the combination with the genes *phzM* and *phzS* required to convert PCA to PYO. Despite a high

amino acid homology of all enzymes of more than 97 %, *P. putida* harboring *14.phz2* was found to produce 4-times higher PCA concentrations (80 µg/mL), which resulted in 3-times higher current density at maximum (12 µA/cm²) compared to *P. putida 14.phz1*. The respective PCA/PYO producer containing *14.phz2* was the best producer with 80 µg/mL of PCA, 11 µg/mL of PYO, and 22 µA/cm² of maximum current density. To elucidate the reason for this superior performance, a detailed structure comparison of the PCA-synthesizing proteins has been performed. The here presented characterization and optimization of these new strains will be useful to improve electroactivity in *P. putida* for oxygen-limited biocatalysis.

3.1.2 Introduction

One group of the redox compounds studied for natural MET are microbial phenazines, which are produced by *Pseudomonas* species, especially by *Pseudomonas aeruginosa*. The complex regulatory network of phenazine synthesis and the pathogenic nature of *P. aeruginosa* limit the application of phenazine redox mediation with this host for specific biotechnological applications (Venkataraman et al., 2011). Thus, to avoid *P. aeruginosa* as microbial host of phenazines production, the utilization of a non-pathogenic species would be an advantage for heterologous phenazines production and future biotechnological utilization. One of the non-pathogenic *Pseudomonas* species, which has emerged as a versatile recombinant host is *Pseudomonas putida* KT2440 (Wackett, 2003). This host stands out because of the availability of extensive genetic and intrinsic metabolism information, combined with its tolerance to many chemical and biochemical substances. Therefore, it has been very useful as a production host of various valuable compounds (Loeschcke & Thies, 2015).

As it has been described in Chapter 1, BES is also a device that can be applied in the bioprocess of platform chemicals production. To develop an efficient *P. putida* biocatalyst for bioelectrochemical production, it is necessary to explore further and optimize the heterologous production of phenazine. The work conducted by Bosire et al. showed for several carbon sources that *P. aeruginosa* PA14 produced more phenazines and resulting anodic currents than *P. aeruginosa* PAO1 in oxygen-limited BES. It is, therefore, clear that the phenazine production in *P. aeruginosa* is strain-dependent (Bosire et al., 2016).

Based on the successful initial proof-of-principle study has been reported in our lab 2015 (Schmitz et al., 2015), the heterologous production of phenazine in *P. putida* has been improved further. The original producer of phenazines, *P. aeruginosa*, encodes for two homologous operons; *phzA1-G1* (operon *phz1*) and *phzA2-G2* (operon *phz2*), which are responsible for the synthesis of PCA. Although the two phenazine operons of *P. aeruginosa* are 98% in DNA level identical (97% in amino acid level), they differ distinctively in their promoter regions. Moreover, it has been revealed by Mavrodi et al. that the two operons contain dissimilarities at DNA sequence level within *phzA1B1* and *phzA2B2*, while the regions from *phzC* to *phzG* of both operons are highly identical (Mavrodi et al., 2001). Base on the amino acid sequence comparison, each gene of phenazine operon from *P. aeruginosa* PAO1 and PA14 are containing dissimilarities between strains and operons, as it has been described in Figure 6 of Chapter 1. Hence, the heterologous expression of those two operons might be markedly different as well. Therefore, in this study, we generated new strains of *P. putida* expressing phenazine genes from three different gene sources as follows; *P. aeruginosa* PAO1 (operon 1) and *P. aeruginosa* PA14 (operons 1 and 2) to produce PCA (Supplementary information Figure S1). Those three new constructs were compared with the performance of the already existing constructs originating from *P. aeruginosa* PAO1 operon 1 (Schmitz at al., 2015). The PCA-producing *P. putida* strains were combined further with the *phzM+S* plasmid to produce PYO. All phenazine producer strains were characterized in two different oxygen-limited conditions BES; 48 hours active aeration then subsequently switched to passive aeration and fully passive aeration. With this approach, we aim to obtain the best heterologous *P. putida* phenazines producer for efficient biocatalysis under oxygen-limited condition BES.

3.1.3 Results and discussions

3.1.3.1 Phenazine gene origin determines the phenazine synthesis capacity in *P. putida*

In an initial study, we transferred the capacity to synthesize the phenazines PCA and PYO from the pathogen *P. aeruginosa* into the GRAS (“generally recognized as safe”) organism *P. putida* KT2440 (Schmitz et al., 2015). The gene origins in that work came from *P. aeruginosa* strain PAO1 (i.e., *O1.phz1* and *phzM+S*). Since it has been revealed in subsequent work that phenazine synthesis is much more active in *P. aeruginosa* strain PA14 compared to PAO1 (Bosire et al., 2016), the specific genetic origin effects on heterologous phenazine production are here evaluated further. Each *P. aeruginosa* strain contains two strongly homologous copies of a 7-gene operon responsible for PCA synthesis (*O1.phz1* and *O1.phz2* versus *14.phz1* and *14.phz2*) and each of these operons without their native promoter regions was inserted into the inducible plasmid pBNT. Since the PhzM protein shares 100% amino acid identity, while the PhzS protein shares 99% amino acid identity in the two strains (without impact on the active site of the protein) (Supplementary information Figure S2), the original plasmid construct for PYO synthesis (pJNN.phzM+S) with the genes originating from strain PAO1 was not changed in this study.

The comparison of phenazine synthesis of a strain version carrying only the PCA-production genes and the combination with the *phzM+S* genes also to synthesize PYO was studied (indicated by “+” after the construct name, e.g., *P. putida* O1.phz1 makes only PCA, and *P. putida* O1.phz1+ makes PCA and PYO). For each construct, eight colonies were picked from agar plates after transformation and compared in parallelized growth experiments on a micro-cultivation platform regarding the growth and yellow (PCA) or blue (PYO) pigment production (Figure 9 and Figure 10).

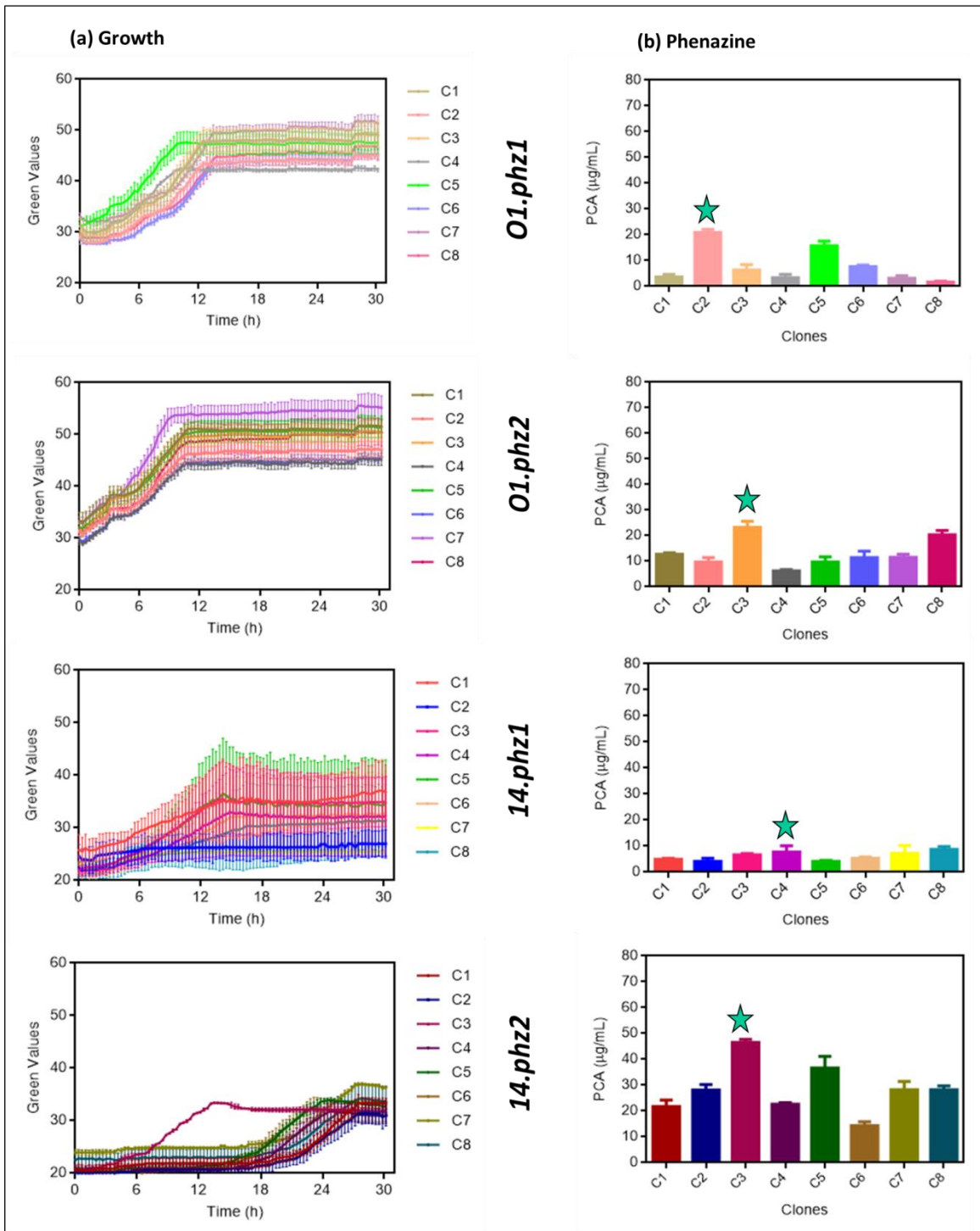


Figure 9: Growth curve (a) vs. PCA production (b) of eight individual clones of *P. putida* O1.phz1, O1.phz2, 14.phz1, and 14.phz2 in the micro cultivation experiment (triplicates for each). For this cultivation platform, the “green value” is the output signal for biomass density. The star symbol indicates the selected clone to be characterized in the flask & BES experiment.

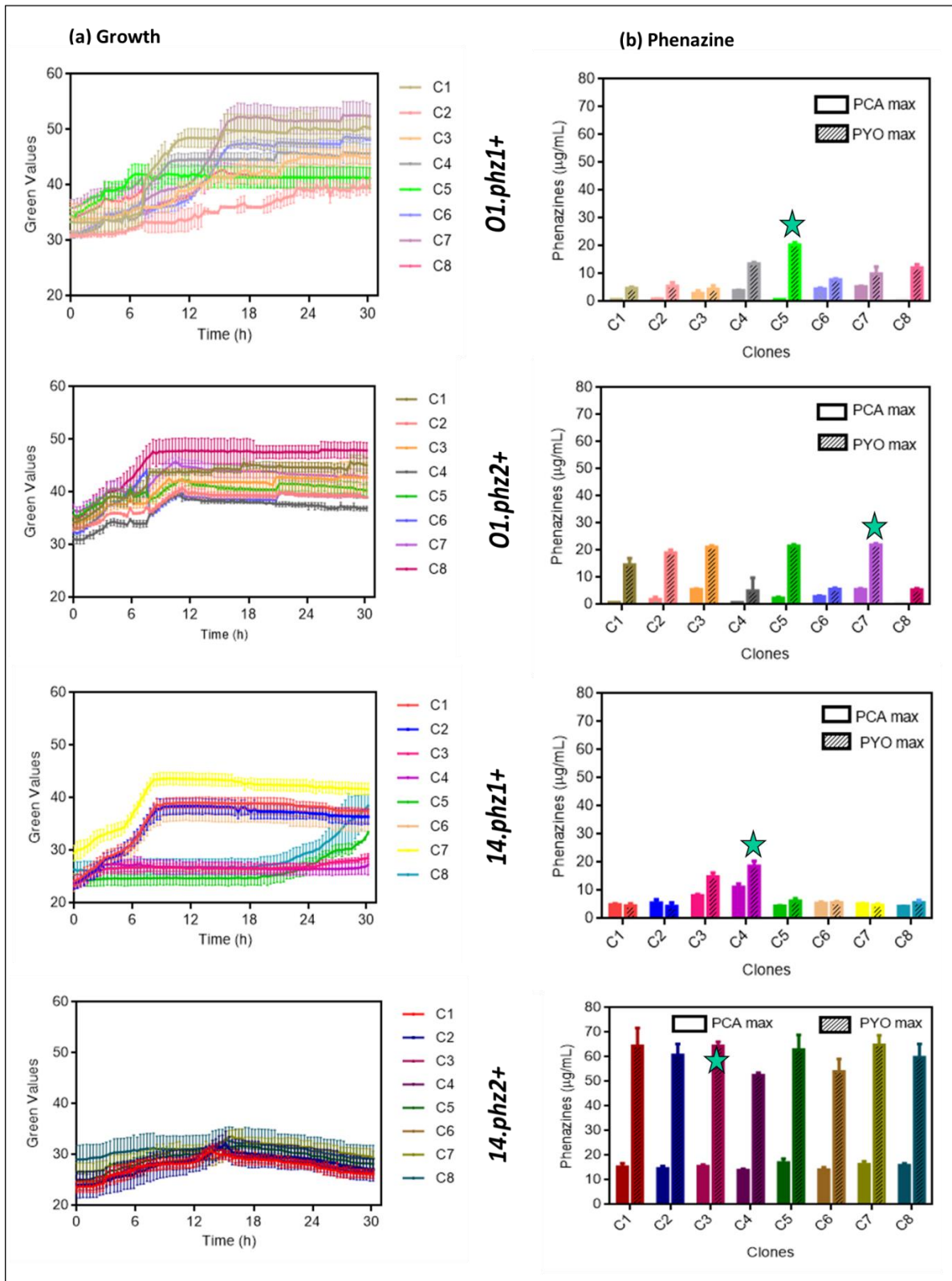


Figure 10: Growth curve (a) vs. PCA & PYO production (b) of eight clones of *P. putida* O1.phz1+, O1.phz2+, 14.phz1+, and 14.phz2+ in the micro cultivation experiment (triplicates for each). For this cultivation platform, the “green value” is the output signal for biomass density. The star symbol indicates the selected clone to be characterized in the flask & BES experiment.

For a more quantitative evaluation of phenazine synthesis, the best clone of each construct in the micro-cultivations was further cultivated in fully aerobic shake flask experiments (triplicate) (Figure 11 and Figure 12).

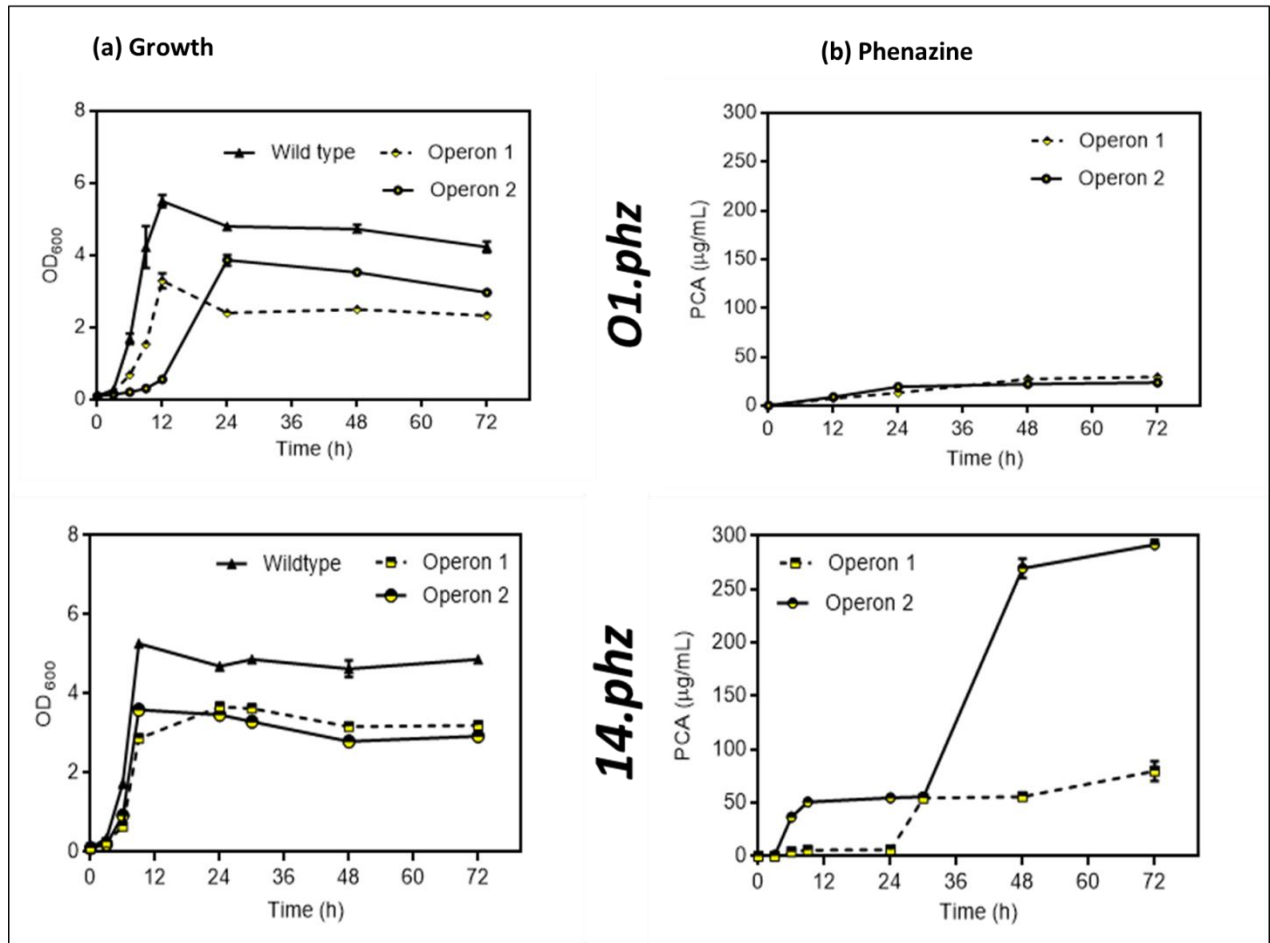


Figure 11: Growth curve (a) vs PCA production (b) of the selected *P. putida* O1.phz1, O1.phz2 (both top graphs), 14.phz1, and 14.phz2 (both bottom graphs) clone in the shake flask experiment (triplicates).

The strain constructs *P. putida* 14.phz2, and 14.phz2+ showed the most intense color formation compared to other strains (Figure 13) with the maximum phenazine quantification results shown in Figure 13b. The *P. putida* O1.phz1 strain was found to be the lowest PCA producer ($23.34 \pm 1.06 \mu\text{g/mL}$), and *P. putida* 14.phz1+ was identified to be the lowest PCA&PYO producer ($5.86 \pm 0.30 \mu\text{g/mL}$ and $0.60 \pm 0.15 \mu\text{g/mL}$, respectively). In comparison to the *P. putida* O1.phz1 strain, the expression of the 14.phz1 operon alone (without *phzM+5*) worked well to produce PCA at $79.79 \pm 9.09 \mu\text{g/mL}$. It showed that PCA production of *P. putida* expressing the 14.phz1

operon was higher than with the *O1.phz1* operon. However, the combination of both plasmids in *P. putida O1.phz1+* to produce PCA & PYO ($8.50 \pm 2.43 \mu\text{g/mL}$ & $12.10 \pm 1.25 \mu\text{g/mL}$, respectively) worked better than with *P. putida 14.phz1+*, although the growth curve of *P. putida 14.phz1+* was similar compared to *P. putida O1.phz1+* (Figure 12a). In *P. putida 14.phz1+*, the presence of the *phzM+S* genes negatively impacted the PCA synthesis, which resulted in low PYO production.

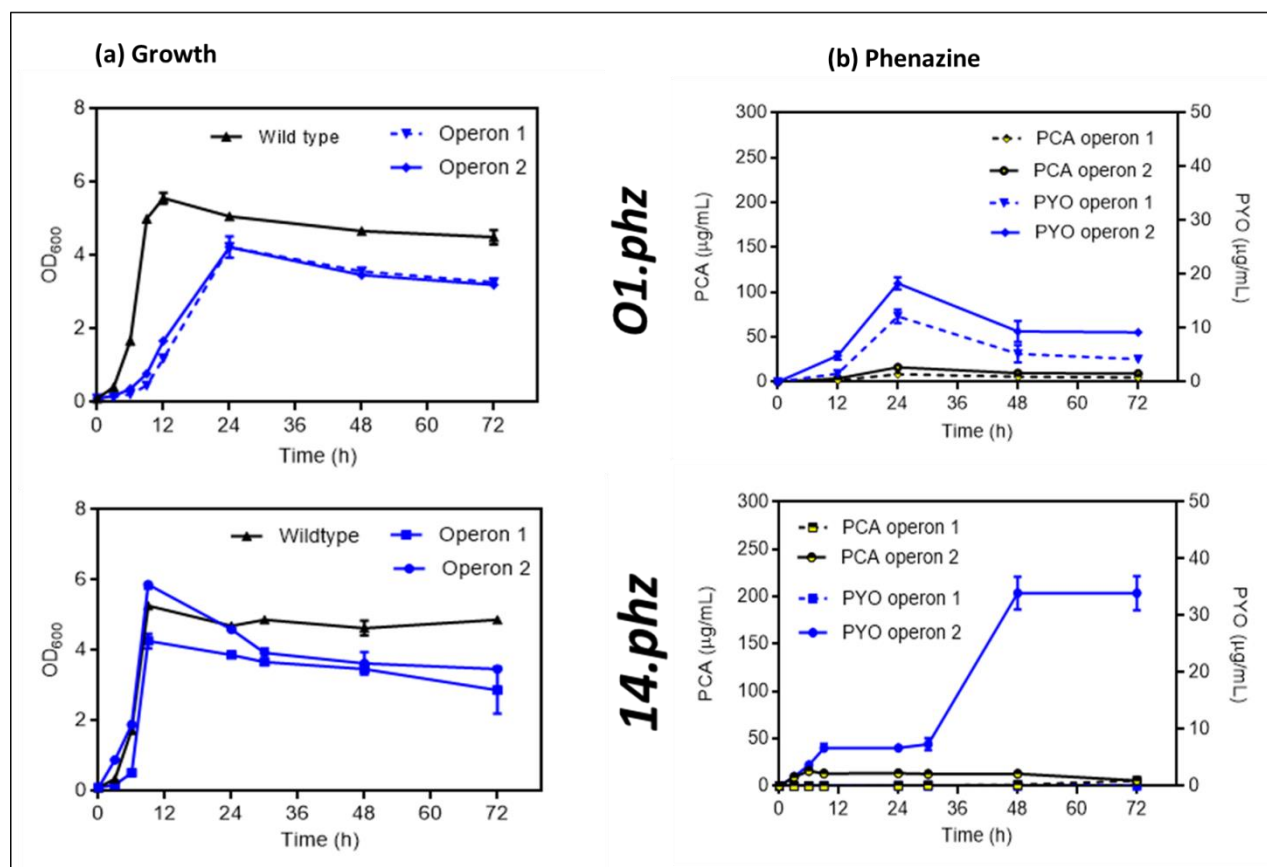


Figure 12: Growth curve (a) vs PCA & PYO production (b) of the selected *P. putida* O1.phz1+, O1.phz2+ (both top graphs), 14.phz1+, and 14.phz2+ (both bottom graphs) clone in the shake flask experiments (triplicates).

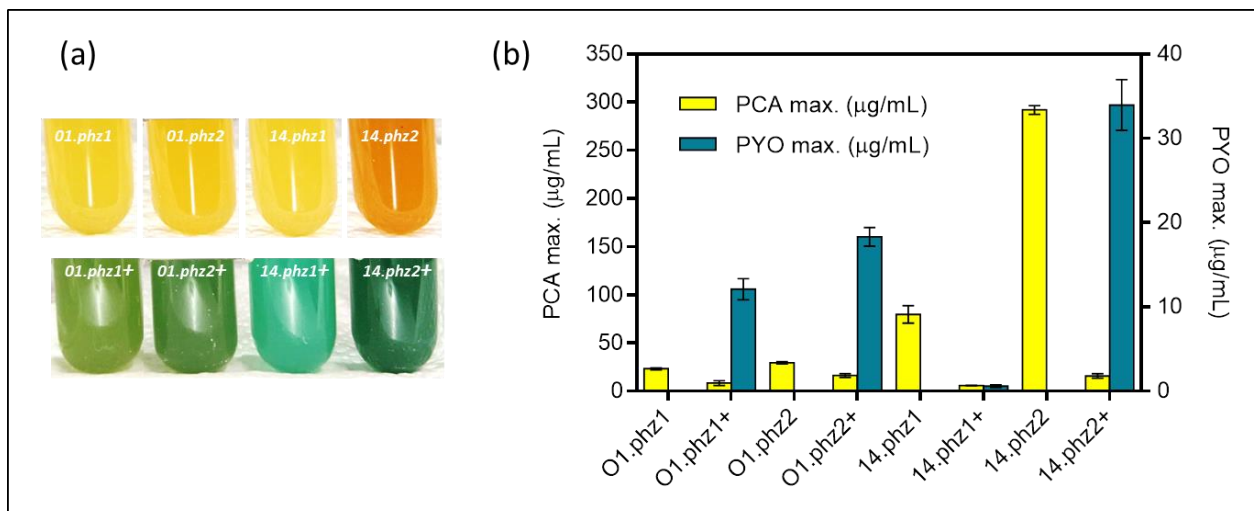


Figure 13: Heterologous expression of *phz* genes in *P. putida* KT2440. (a) *P. putida* cultures (from left to right) expressing O1.phz1, O1.phz2, 14.phz1, and 14.phz2 gene for PCA synthesis (top) and with combination of *phzM+S* genes for PCA & PYO synthesis PCA&PYO (bottom); (b) Phenazine production of engineered *P. putida* strains in triplicate shake flask experiments (fully aerobic), whereby the '+' in the strain designation indicates presence of *phzM+S* to convert PCA to PYO.

Moreover, *P. putida* O1.phz2 with 29.50 ± 1.29 µg/mL produced more PCA than *P. putida* O1.phz1, although the growth curve of *P. putida* O1.phz2 was lower compared to the other PCA producers strain (Figure 11a). It seems the high capacity of phenazine protein synthesis caused the growth reduction in *P. putida* O1.phz2. Furthermore, the *P. putida* 14.phz2 strain was found to be the most active PCA producer (292 ± 4.58 µg/mL) and *P. putida* 14.phz2+ to be the most active PCA & PYO producer (16 ± 2.31 µg/mL and 33.96 ± 3 µg/mL, respectively). The growth curve of *P. putida* 14.phz2 was similar to *P. putida* O1.phz1 and 14.phz1. It showed that the *phzA-G* operon 2 from *P. aeruginosa* PA14 was more active to produce PCA compared to operon 1. In *P. putida* 14.phz2+, although the PYO production was highest compared to the other strains, the PCA production was low. As the PCA production of the *P. putida* 14.phz2 strain was high, it was expected that *P. putida* 14.phz2+ would produce more PCA as well. However, we assumed that the two antibiotics burden also occurred in this strain caused low phenazines synthesis. And also, the presence of PYO may have a toxic effect on the cells since it is known to generate toxic oxygen radicals and therefore hinders the further PCA synthesis.

Overall, the experiments conducted under fully aerobic flask showed that the PCA synthesis of *P. putida* expressing the phenazine genes (same strain origin) from operon 2 of *P. aeruginosa* was higher than from operon 1. Furthermore, it was revealed that PCA production of *P. putida*

expressing the phenazine genes from *P. aeruginosa* PA14 was higher compared to PAO1. On the other hand, for combined PCA & PYO production, the phenazine production was affected by either the metabolic burden of the two antibiotics applied and/or a restricted total phenazine production with increased levels of PYO, which shows toxic behavior at higher concentration through the formation of reactive oxygen species (Mentel et al., 2009). In general, it showed that under fully aerobic condition, phenazine synthesis in engineered *P. putida* is strain template- and operon-dependent.

3.1.3.2 Phenazine gene origin determines performance in oxygen-limited BES

The motivation for engineering *P. putida* to produce phenazines is driven by the idea to capacitate this obligate aerobic bacterium for biocatalysis in the oxygen-limited BES. Phenazine producing *P. putida* will be able to utilize phenazines as the reversible redox mediator for the anodic discharge of metabolic electrons. In the future, this oxygen-limited metabolism will be coupled with valuable compound production in the BES. To characterize the potency of *P. putida* strains synthesizing phenazines from different gene origin, the BES performance of each engineered strain variant has been evaluated. In Figure 14, the left column shows the strain performance in BES under active aeration, while the right column shows the performance in BES under passive aeration. In the upper part (Figure 14a,b and e,f), the BES performance of the construct originating from the PAO1 genes shown, while the BES performance of genes templates from PA14 are shown in the lower part (Figure 14c,d-g,h). Under active aeration BES, the lowest PCA production and current generation were observed from *P. putida* O1.phz1, which only produced 9.38 µg/mL of PCA at maximum, corresponding to 1.68 µA/cm² of current density until day 7. The BES performance of this strain was in accordance with the flasks experiment, in which *P. putida* O1.phz1 also showed the lowest production of PCA. It has been observed in a control experiment where ~17 µg/mL of synthetic PCA has been added to the *P. putida* KT2440 wildtype in an oxygen-limited BES, that the PCA concentration sustained in the reactor until the end of the experiment, i.e., was not degraded or absorbed to the electrode, and produced a current density up to 8.57 µA/cm² (Figure 15a).

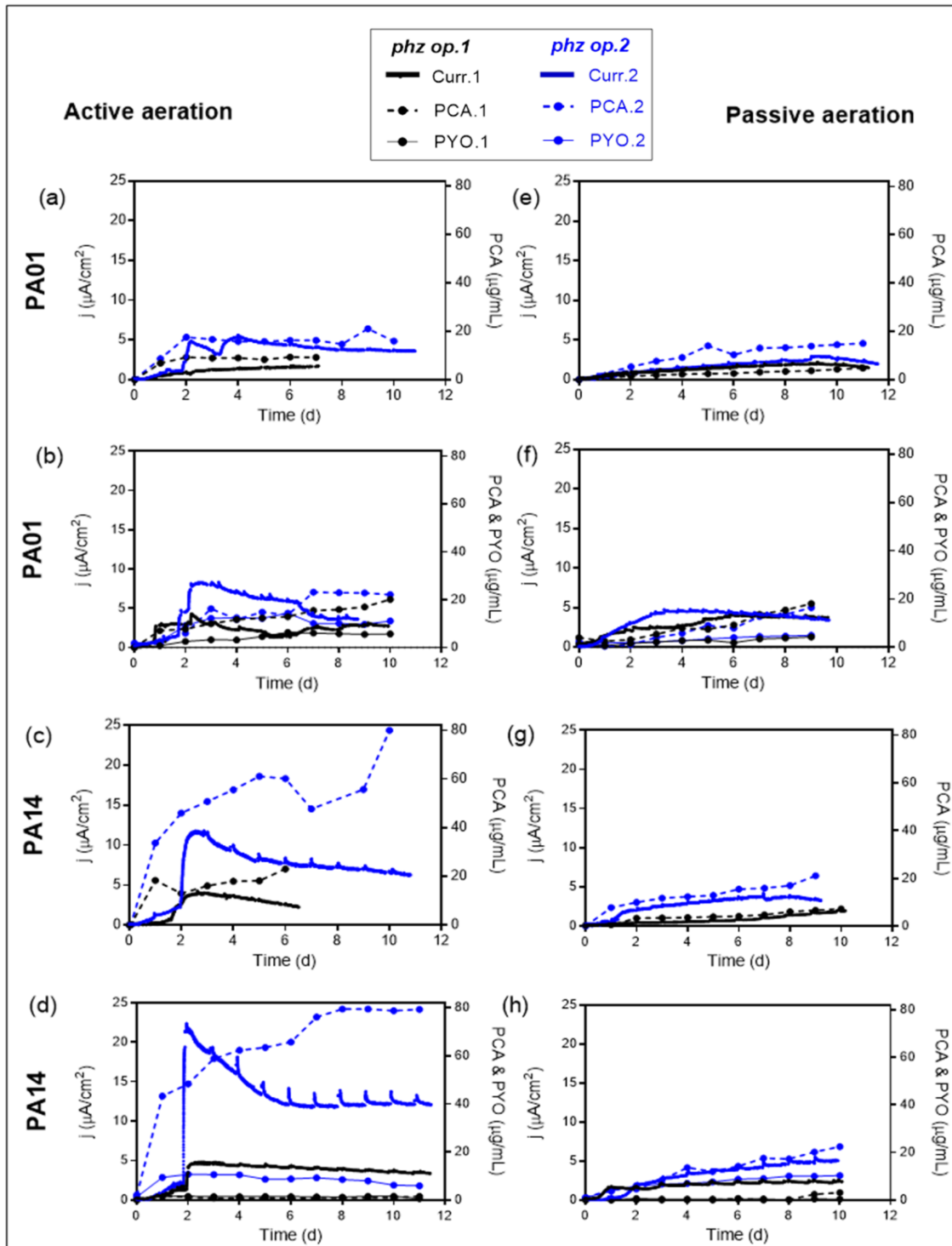


Figure 14: Heterologous phenazine production with *P. putida* under oxygen-limited conditions in a BES. Current densities generation and phenazine production of engineered *P. putida* KT2440 harbouring either *phz* operon 1 (blue curves) or operon 2 (black curves) originating from *P. aeruginosa* strains PA01 (a, b and e, f) or PA14 (c, d, and g, h). The left side shows data from actively aerated BES experiments and the right side refers to purely passively aerated BES. The highest currents generation and phenazine production were obtained from the engineered *P. putida* carrying operon 14.*phz2* under active aeration BES (Figure 7.d). The BES data are means from biological duplicates.

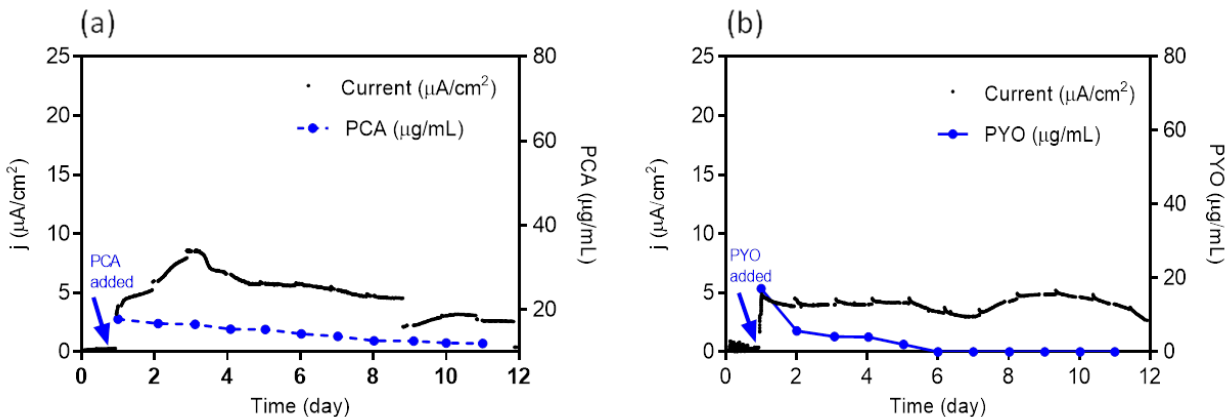


Figure 15: BES cultivation of *P. putida* KT2440 (wildtype) under passive aeration conditions. Synthetic PCA (a) or PYO (b) was added ($\sim 17 \mu\text{g}/\text{mL}$) after 24 hours inoculation (day 1).

Furthermore, by far the weakest PCA&PYO producer in actively aerated BES was *P. putida* 14.phz1+, which only produced 2.71 $\mu\text{g}/\text{mL}$ of PCA, 1.63 $\mu\text{g}/\text{mL}$ of PYO and 4.74 $\mu\text{A}/\text{cm}^2$ of maximum current density. This result also mirrored the feeble activity of the phenazine production of *P. putida* 14.phz1+ in the flasks experiment, where the combination of the 14.phz1 genes with the phzM+S genes leads to an almost complete suspension of phenazine production.

Moreover, the highest phenazine production and current generation were observed with *P. putida* 14.phz2, which produced 4-times higher PCA concentration, i.e., 80 $\mu\text{g}/\text{mL}$, resulting in 3-times higher maximum current density of 11.77 $\mu\text{A}/\text{cm}^2$ compared to the other PCA gene operons. Also, the combination of PCA & PYO produced with *P. putida* 14.phz2+ outperformed the other strains with 80 $\mu\text{g}/\text{mL}$ of PCA, 11 $\mu\text{g}/\text{mL}$ of PYO and 22.33 $\mu\text{A}/\text{cm}^2$ of maximum current density. Again, the performance in oxygen-limited BES of this strain was in accordance with the aerobic flasks experiment. It was observed in this study that the presence of PYO as a soluble redox mediator compound in the BES is significantly increasing the electron shuttling to the anode. From control experiments with the *P. putida* KT2440 wild type with $\sim 17 \mu\text{g}/\text{mL}$ of exogenous PYO added to an oxygen-limited BES, we know that the PYO concentration is not sustained over time, likely because of adsorption to the electrode (Figure 15b). However, here, we see a fairly stable concentration of PYO over the course of the experiment with a continuously increasing concentration of PCA. It means that PYO is continuously resynthesized from PCA when it is intrinsically produced.

Furthermore, in passively aerated BES, the lowest PCA production and current generation were observed from *P. putida* 14.phz1, which only produced 7.21 $\mu\text{g/mL}$ of PCA and generated 2 $\mu\text{A/cm}^2$ of current density. Also, in combination with *phzM+S* genes, *P. putida* 14.phz1+ was only able to produce 3.11 $\mu\text{g/mL}$ of PCA and 0.65 $\mu\text{g/mL}$ of PYO, resulting in 2.58 $\mu\text{A/cm}^2$ of current density. On the other hand, *P. putida* 14.phz2 was confirmed as the best PCA producer also under passive aeration conditions, where it produced 21.09 $\mu\text{g/mL}$ of PCA and, generated 4.12 $\mu\text{A/cm}^2$ of current density. Together with *phzM+S* genes, *P. putida* 14.phz2+ was able to produce 22.48 $\mu\text{g/mL}$ of PCA and 10.29 $\mu\text{g/mL}$ of PYO, resulting in 5.53 $\mu\text{A/cm}^2$ of current density.

Overall, the performance of the *P. putida* phenazine producing strains in oxygen-limited BES is well following the performance in flasks experiment. Also, it is confirmed for these cultivation conditions, that the phenazine synthesis in *P. putida* is strain origin- and operon-dependent. In direct comparison, the maximum produced amounts of PCA, however, are lower under oxygen-limited conditions compared to fully aerobic shake flasks because of the restricted energy availability. Notably, for the active aeration BES scenario, where the reactors were aerated for the first 48 hours of growth to enable faster growth and cellular energy generation followed by completely passive aeration with vent filters, a remarkable activity for PCA production resulting in roughly 1/3 of the concentrations of the aerobic cultivation was observed. This PCA production continued throughout the passive aeration phase, confirming results from Schmitz et al. that stringently oxygen-limited conditions enable biosynthesis in *P. putida* if an anode is made accessible for metabolic electron discharge (Schmitz et al., 2015). The concentration of PYO is not further increasing after switching from the active to the passive aeration phase because of the requirement of molecular oxygen for the enzymatic PYO synthesis.

3.1.3.3 Phenazine gene origin affected the carbon substrate utilization capacity

To further evaluate the metabolic activity of the phenazine producing *P. putida* strain under oxygen-limited conditions, we analyzed biomass formation, glucose consumption, metabolite production, and the efficiency of donating metabolic electrons derived from the substrate glucose to the anode, which is measured as coulombic efficiency. Table 6 summarizes all results. We did not observe any strong biofilm formation with *P. putida* in our BES, and the evaluations

at OD₆₀₀ are well suited to compare the growth performance of the strains. This is different from BES experiments with *P. aeruginosa* as described by Bosire et al., where we found very strong and variable biofilm formation in the experiments and a time-resolved estimation of growth was difficult (Bosire et al., 2016). The best growth, with the highest OD₆₀₀ of 2.45, was observed for *P. putida* 14.phz2 under active aeration which sustained throughout the stationary phase until day 11 after inoculation. The average OD₆₀₀ for active aeration was 1.95 compared to 1.57 for passive aeration, reflecting the very stringent oxygen availability during passive aeration. The glucose consumption is shown as the percentage of the provided glucose, which was 40 mM in active aeration BES and 20 mM in passive aeration BES. Most cultures showed a glucose consumption of approximately 80 % for active and about 70 % for passive aeration. The highest value of 88 % was observed for *P. putida* O1.phz2+ under active aeration BES. Notably, the lowest glucose consumption of only ~40 % for both active and passive aeration was found for strain *P. putida* 14.phz1. It has been reported before that *P. putida* produces several organic acids, such as 2-ketogluconate, gluconate, and acetate as side products from glucose degradation under oxygen-limited conditions (Nikel et al., 2015; Schmitz et al., 2015). For most strains, side product formation in these experiments stayed fairly low in the range of 0.1 to 2.9 mM. However, the best phenazine and most active current producer *P. putida* 14.phz2+ reached up to 4.80 mM gluconate. It is an exciting finding, since gluconate is a valuable biochemical product for industrial application, especially in food processing and pharmaceutical industry (Vandenberghe et al., 2018). This finding is also in line with bioelectrochemical studies of *P. putida* F1 with exogenous ferricyanide as an electron mediator, which shows a high efficiency of glucose to sugar-acid conversion under oxygen-limited BES conditions (Lai et al., 2016).

The estimation of energy retrieved from the carbon source in BES can be calculated as coulombic efficiency (Sleutels et al., 2011). Table 2 shows that overall, the coulombic efficiency observed from all strains was low. However, the most active strains *P. putida* 14.phz2 and *P. putida* 14.phz2+ showed a significantly increased coulombic efficiency of up to ~6 % for both active and passive aeration. This result indicates that already small changes in the strain design for phenazine synthesis can improve not only phenazine production but also the efficiency of bioelectrochemical interaction of this strain. For a further improvement of phenazine based electron discharge to the anode as the extracellular metabolic electron acceptor, specific

knowledge about the involved biochemical and energetic reaction pathways is required. However, this information is neither available yet, for *P. aeruginosa* nor *P. putida*. Work is ongoing in our group to elucidate the specific phenazine electron transfer pathways and their integration into the energetic pathways of the microorganisms.

In general, this study showed that *P. putida* expressing the phenazine gene origins from operon 2 of *P. aeruginosa* strain PA14 with or without the combination with the *phzM+S* genes, either underactive or passive aeration, was able to convert the carbon source to biomass, metabolite production, and anodic currents in BES at a high level. In contrast, surprisingly, the *P. putida* 14.phz1 strain showed the lowest level of carbon source utilization, biomass formation, metabolite production, and coulombic efficiency, either underactive or passive aeration BES. In combination with the *phzM+S* genes, the *P. putida* 14.phz1+ showed the same level of the carbon utilization to *P. putida* 14.phz1 strain. Overall, despite being highly homologous, we found that the specific gene origins play a crucial role in phenazine production and subsequently carbon source utilization and bioelectrochemical activity of *P. putida* in BES.

Table 6: Summary of glucose and metabolite evaluation of oxygen-limited BES experiments
(Data are means of biological duplicate)

O ₂	Strains	OD ₆₀₀ max	Glucose consumpt. (%)	Gluconate (mM)	2-Ketogluconate (mM)	Acetate (mM)	Coulombic effic. (%)
AA	O1.phz1	1.91	78	0.15	0.89	-	1.34
	O1.phz2	1.72	80	0.29	0.10	0.84	1.47
	14.phz1	1.74	44	0.08	1.12	0.65	1.12
	14.phz2	1.78	87	0.76	0.63	2.90	2.72
	O1.phz1+	1.90	63	0.59	2.30	1.53	1.45
	O1.phz2+	1.87	88	0.69	0.07	1.56	1.53
	14.phz1+	2.25	78	2.90	1.70	2.25	1.77
	14.phz2+	2.45	83	4.80	1.30	2.45	5.90
PA	O1.phz1	1.21	72	0.07	0.91	-	1.04
	O1.phz2	1.73	68	0.42	0.70	0.99	2.05
	14.phz1	1.02	39	1.91	0.55	1.38	0.77
	14.phz2	1.88	79	0.05	0.47	0.59	5.40
	O1.phz1+	1.70	65	0.38	0.29	0.63	3.38
	O1.phz2+	1.71	68	1.50	1.25	-	2.89
	14.phz1+	1.54	81	0.17	0.29	-	1.45
	14.phz2+	1.79	46	0.04	1.89	1.46	5.89

3.1.3.4 Deciphering the effects of operon and strain origin for heterologous production of phenazine in *P. putida*

To elucidate possible reasons for the difference in phenazine production capacity and resulting BES performance, we took a more in-depth look at the gene origins for PCA synthesis at DNA and protein level (Supplementary data Data S1). In all constructs, we omitted the native promoter region of the operons and cloned the genes in a uniform salicylic acid-inducible vector. Thus, any difference in performance and activity should be incorporated directly in the sequence information of the genes. All plasmids have been re-sequenced to confirm the correctness of the original sequence and exclude mutations. To obtain a deeper understanding of the gene characteristic and its impact to dictate the phenazine production, an *in silico* analysis of all genes origin used in this study has been conducted. Figure 16a-b shows the nucleotide alignment corresponding to two potential regulatory intergenic regions. These regions have enough length to allow the attachment of DNA-binding proteins, and they own ribosome binding sites (consensus sequence: 5'-AGGAGG-3'). The first regulatory element (Figure 16a) is located between the genes *phzA* and *phzB*. The RBS (ribosome binding sites) is slightly interrupted by a deletion in the operons 1 compared with operons 2, where the RBS are longer and more similar to the consensus sequence. It has been revealed that in the phenazine biosynthesis pathway, the PhzB protein plays an important role to accelerate the condensation of two molecules and of the intermediate product called 6-amino-5-oxocyclohex-2-ene-1-carboxylic acid (AOCHC) in the PCA formation (Blankenfeldt & Parsons, 2014). Thus, changes in the efficiency of PhzB protein synthesis will significantly influence overall phenazine synthesis. Furthermore, the second regulatory element (Figure 16b) is located between the genes *phzB* and *phzC*. There is an insertion observed in the operon 1 from strain PA14. The RBS in this operon seems to be slightly longer, but it is almost identical to the other ones. Other intergenic regions presenting RBS (Supplementary data Data S2) were also detected, but no differences observed among them. Those regions are located between *phzE* and *phzF* as well as between *phzF* and *phzG*.

Furthermore, one of the crucial aspects of the heterologous expression of specific genes is the fact that every organism is likely to prefer distinctive codons than others. In the genes of

different organisms, a non-random distribution of synonymous codons has been explicated by the comparative sequence analysis, the so-called codon bias (Quax et al., 2015). Instead of influencing the expression levels of protein, the codon bias is also affecting the protein folding and distinctive regulation of protein expression (Gingold et al., 2014; Pechmann & Frydman, 2013). It has been revealed that among genes in one genome, the codon usage is varied. To detect changes between the codon usages among genes in the four operons, codon adaptation indices have been calculated for all genes using an index previously generated for *P. putida* KT2440 (Sharp et al., 2005). Counting the cases in which each operon has a best or worst result, Figure 16c plots have been created to give an overall idea about the potential expression success of these operons. According to the results, operon 2 of PA14 would tend to have a better expression compared with the other constructs.

Moreover, a phylogenetic tree describing the relation between gene origins used in this study has been generated (Supplementary data Figure S3). It showed that the differences between operons are more prominent compared to the differences between strains. The amino acid comparison between operon 1 and 2, either in PAO1 or PA14, showed the same pattern. The overall amino acid alignment analysis indicated the biggest difference between operons 1 and 2 in the PhzB protein (91% identical), followed by the PhzA protein (97% identical). However, our structure analysis showed that these differences in the amino acids, which are located at the N- and C-terminus on the outer sphere of the protein, are likely not affecting the protein function. In general, regarding the structural analysis, mostly small conformation changes are detected in most of the enzymes involved in phenazine synthesis (Supplementary data Figure S4-S8). These changes are mainly located in the N-terminus, C-terminus and nearby loop regions, which could be the target of post-translational modifications and therefore these regions may not be present in the mature protein.

Nevertheless, in the protein, PhzE, relevant variations can be observed, which may be necessary in the activity of this protein (Figure 17). Structure differences are mainly occurring in PA14-PhzE2, probably due to two unique amino acid exchanges, which are the substitution of Leucine to Phenylalanine and another Leucine to Isoleucine. Those amino acids located close to each other and close to the enzyme catalytic site where the substrate chorismate binds. These exchanges likely yield the conformational shift, which our analysis predicts. PhzE protein plays a

vital role in the phenazine synthesis since it is the first protein of the synthesis pathway. It catalyzes the formation of 2-amino-2-desoxyisochorismate (ADIC) from the central metabolic intermediate chorismate (Spraggon et al., 2001). Therefore, the specific changes in the active site of this enzyme in the gene origin *PA14-phzE2* will likely have an impact on the overall phenazine synthesis and might be responsible for the superior performance of the *14.phz2* operon for PCA synthesis.

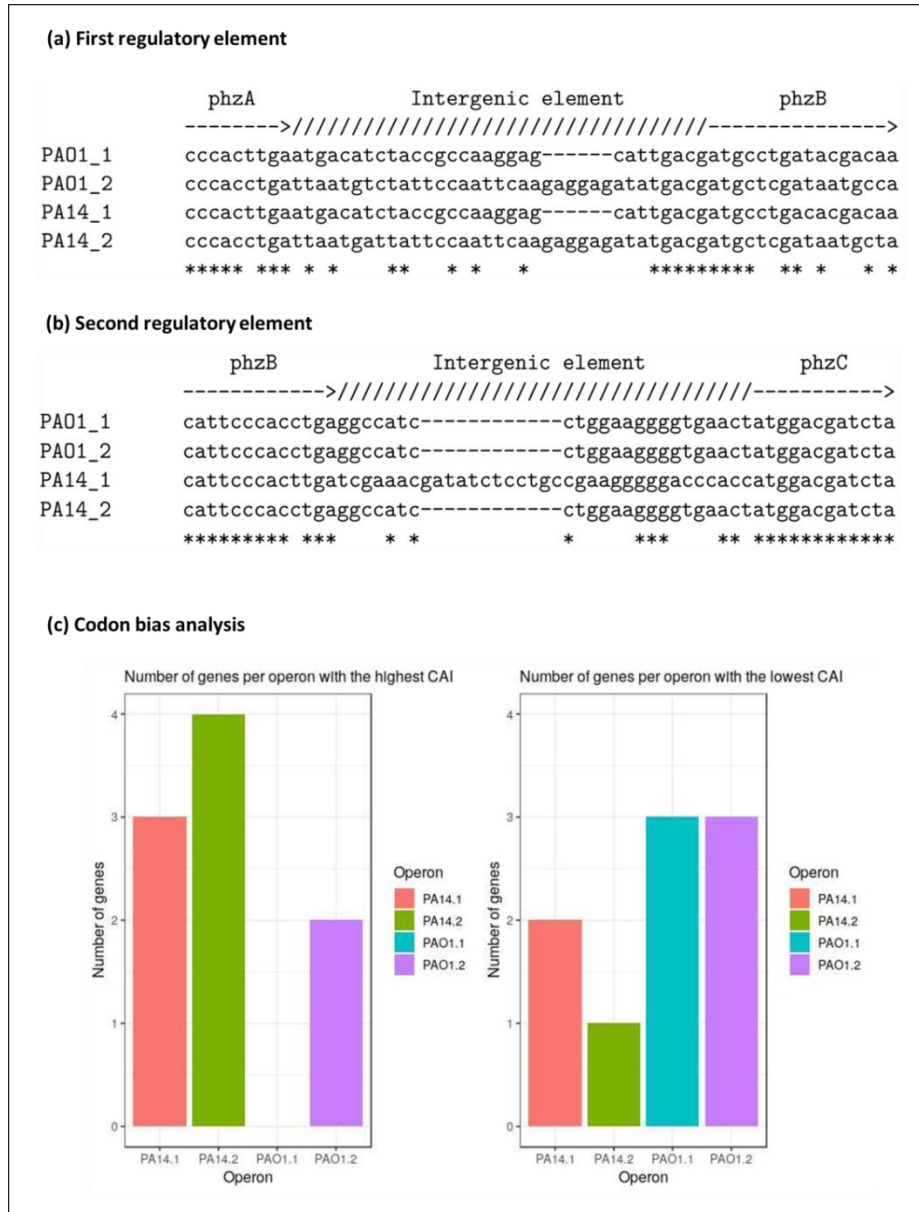


Figure 16: Nucleotide-based analysis of the phenazine operons. a) First regulatory element alignment overview. Deleted nucleotides are marked as a hyphen (-). Identical bases are marked as an asterisk (*). **b)** Second regulatory element alignment overview. Deleted nucleotides are marked as a hyphen (-). Identical bases are marked as an asterisk (*). **c)** Prediction of the expression tendency. Bars represent the number of times each operon has the highest or the lowest CAI.

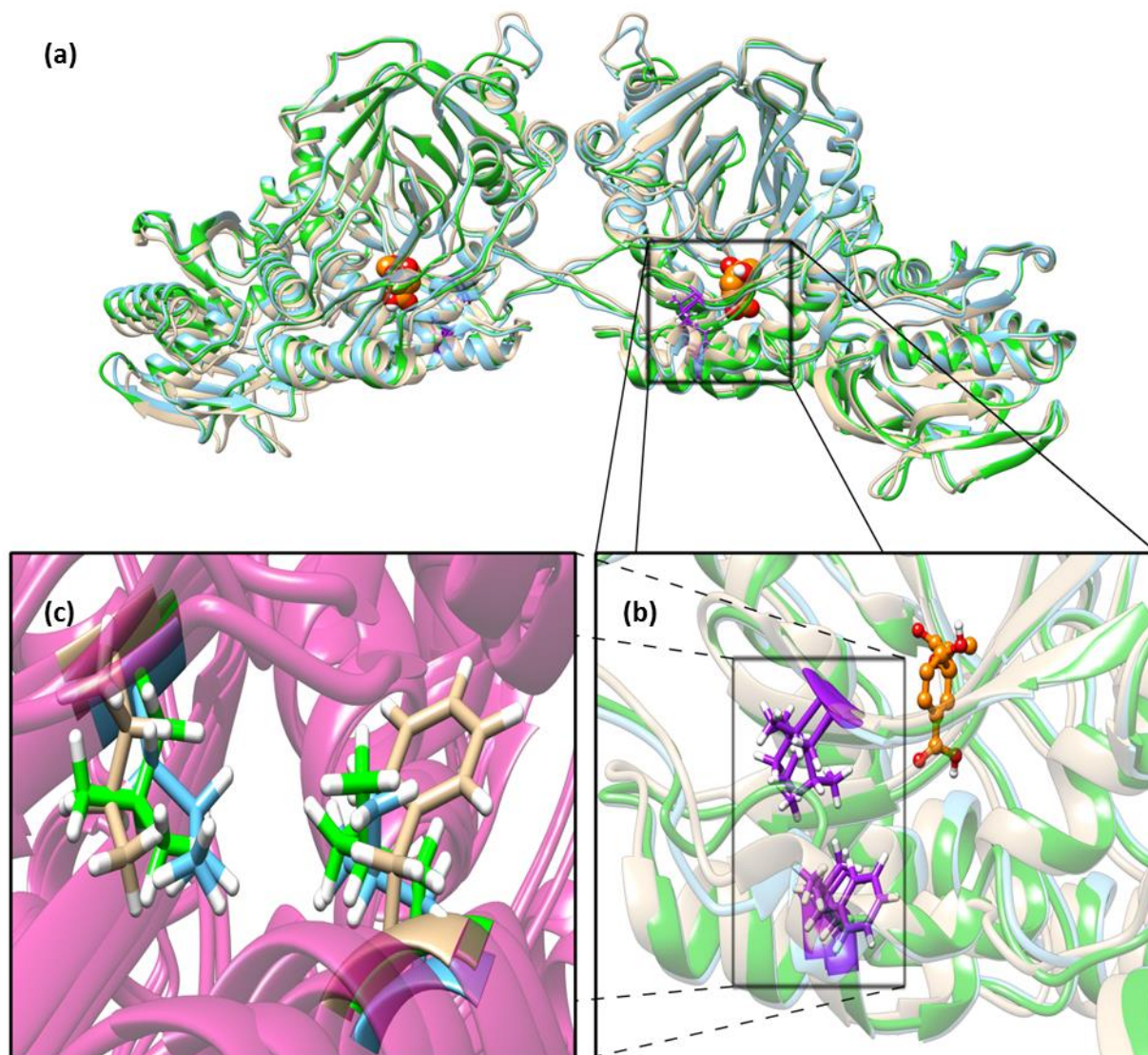


Figure 17: Structural analysis of PhzE. **a)** PA14-PhzE2 is used as the reference for the alignment (blue). RMSD for PA14-PhzE1 (yellow): 1.056 Å. RMSD for PAO1-PhzE1 (green): 0.836 Å. PAO1-PhzE2 is identical to PAO1-PhzE1. Unique amino acid changes regarding PA14-PhzE2 (p.[F231L; I266L]) are marked in purple. Substrate (chorismate) molecules are marked in yellow. **b)** Detail of the substrate-binding site vicinity. **c)** Detail of the unique amino acid changes in PA14-PhzE2 and location inside the structure.

3.1.4 Conclusions

The heterologous expression and comparative study of phenazine synthesis gene origins originating from two operons of *P. aeruginosa* strain PAO1 and PA14 in *P. putida* KT2440 revealed their distinctive activity. The gene origin dictates phenazine synthesis activity under fully aerobic flask experiments and oxygen-limited BES conditions, also affecting carbon

utilization. In this study, the *phzA-G* operon 2 from *P. aeruginosa* PA14 (*14.phz2*) carrying strain was found to be the best phenazine producer. *P. putida* 14.phz2 stunningly produced 4-times higher PCA concentrations as well as the respective PCA/PYO amounts compared to the other PCA synthesis operons, which resulted in 3-times higher maximum current density and 5-times higher coulombic efficiency than for the others. Through deciphering potential sequence-based reasons for this superior function, it has been revealed that the *14.phz2* genes contained distinctive regulatory elements.

Furthermore, the codon usage prediction, estimated by CAI, showed that operon 2 of strain PA14 differed, potentially supporting protein synthesis. Most importantly, for the PA14-PhzE2 enzyme, the 3D-protein structure analysis showed two unique amino acid changes in PA14-PhzE2 located close to the enzyme catalytic site where the substrate chorismic acid binds. This difference might promote higher PCA synthesis.

Here we show that *P. putida* 14.phz2 is a promising candidate to be employed as a biocatalyst in an oxygen-limited BES. The electric current generation can now be coupled with the bioelectrochemical production of valuable compounds. Example compounds that can be tailored further with phenazine production are rhamnolipids. These compounds are glycolipid biosurfactants, which offer many benefits for industrial application, for example as bio-detergent, bioremediation agent, and pharmaceutical additive agent. The production of rhamnolipid has been developed under fully aerobic conditions, in which the scale-up production using common bioreactors requires vigorous aeration. It causes strong growth medium foaming and reduces the yield, which is challenging to be overcome with conventional antifoam technologies (Beuker et al., 2016; Küpper et al., 2013). Hence a bioelectrochemical system involving phenazine as redox mediator could be applied as an alternative approach to produce foam-free rhamnolipids. Overall, the presented research findings will be useful to establish efficient, oxygen-limited biocatalysis of *P. putida* in BES.

3.2 Coupling the electroactive *P. putida* KT2440 with bioelectrochemical foam-free rhamnolipids production

*In this study, we used *P. putida* SK1 strain constructed by Kruth (Kruth, 2017) for control experiments

*The TLC experiment was assisted by Andreas Wittgens

3.2.1 Summary

Rhamnolipids are prospective microbial biosurfactants with eco-friendly properties. The metabolic engineering of *Pseudomonas putida* KT2440 as a recombinant host for rhamnolipid production has been already developed under aerobic conditions. However, costly aeration and the subsequent problems with strong reactor foaming are still technically challenging. Thus in this work, we are combining the phenazine-producing *P. putida* KT2440 with rhamnolipid production under the oxygen-limited condition in a bioelectrochemical system. For the first time, here we present the newly engineered *P. putida* *rhl-pca* strain harboring the *rhlAB* genes to synthesize mono-rhamnolipid (originating from *Pseudomonas aeruginosa* PAO1) with the *phzA-G* genes of operon two (originating from *P. aeruginosa* PA14) to synthesize phenazine-1-carboxylic acid or PCA as an electron shuttle in BES. Furthermore, we generated another genetically engineered *P. putida* *rhl-pyo* strain harboring the *rhlAB* genes along with *phzM+S* genes (originating from *P. aeruginosa* PAO1) and *phzA-G* genes of operon two from *P. aeruginosa* PA14 to synthesize mono-rhamnolipid, PCA, and pyocyanin (PYO), respectively. The new strain of *P. putida* *rhl-pyo* produced a shallow concentration of mono-rhamnolipid during the fully aerobic experiment (flasks), i.e., only 50 ± 0.00 mg/L mono-rhamnolipid, 130.80 ± 16.83 $\mu\text{g/mL}$ of PCA, and 33.96 ± 2.80 $\mu\text{g/mL}$ of PYO after 72 hours cultivation. On the other hand, *P. putida* *rhl-pca* was able to produce both mono-rhamnolipid and PCA under fully aerobic condition, i.e., 152 ± 1.22 mg/L of mono-rhamnolipid and 122.27 ± 12.49 $\mu\text{g/mL}$ of PCA after 72 hours cultivation. The *P. putida* *rhl-pca* was tested further for bioelectrochemical production under oxygen-limited BES cultivation. We observed that *P. putida* *rhl-pca* did not produce any mono-rhamnolipid on the BES reactors with active aeration, either for 48 hours (AA) or continuously (AA+) during the cultivation. In contrast, under passive aeration (PA) with the most stringent oxygen level in the reactor, this strain was able to produce mono-rhamnolipid at 20.67

± 0.15 mg/L and 11.23 ± 0.78 $\mu\text{g/mL}$ of PCA, which resulted in 8.07 ± 0.15 $\mu\text{A/cm}^2$ of maximum current density at a polarized anode, during 10 days cultivation. This result showed that the newly engineered *P. putida* rhl-pca is capable of being employed as a biocatalyst for bioelectrochemical production of foam-free mono-rhamnolipid. Moreover, this work also revealed that it is possible to produce glycolipid surfactants under oxygen-limited BES reactor.

3.2.2 Introduction

Rhamnolipids are one of the best explored microbial glycolipid surfactants. This compound is offering eco-friendly characteristics such as biodegradable, causing low eco-toxicity effect, and can be produced from renewable resources (Faivre & Rosilio, 2010), which make this compound considered as a prospective biosurfactant to be expanded in industrial scale. However, the production of rhamnolipids from the native producers, especially from pathogenic bacterium *P. aeruginosa*, is controlled by complex quorum sensing regulation. Hence, the studies of using a non-pathogenic bacterium as a recombinant host for rhamnolipid production will be beneficial. As a biocatalyst, the metabolic engineering of *P. putida* KT2440 for rhamnolipid production has already been developed under aerobic condition (Wittgens et al., 2011). However, costly aeration and the subsequent problems with strong reactor foaming are still technically challenging to be overcome (Küpper et al., 2013). Furthermore, those mentioned technical challenges are also hindering the scale-up process in the industrial production of rhamnolipids (Beuker et al., 2016). To reduce the drawbacks of aerobic growth, we explore an alternative approach for rhamnolipid production using *P. putida* as a biocatalyst under oxygen-limited growth in the bioelectrochemical system or BES. BES enabled the production of various valuable compounds, even using biomass waste. This bioprocess potentially reduces greenhouse gases emission and conserves energy simultaneously (Steinbusch et al., 2010).

The implementation of BES for rhamnolipid production is based on the successful heterologous production of phenazine redox mediators in *P. putida*. It was first reported by Schmitz *et al.* in 2015 and has recently been further optimized by myself, as it has been described in Chapter 3.1 (Schmitz et al., 2015). This work enabled a newly engineered strain of non-pathogenic, aerobic *P. putida* KT2440 (so-called as *P. putida* pPhz) to grow under oxygen-limited conditions in a BES through the electron discharge to an extracellular anode. All previous studies showed that the

best BES set up for phenazine and currents production is active aeration, in which the aeration via an air sparger was applied for 48 hours and then switched to passive aeration of the headspace until the end of cultivation. It has been revealed that during active aeration for 48 hours, *P. putida* pPhz produced mainly PYO, then subsequently during the passive aeration, PCA was predominantly synthesized and responsible for sustaining the current generation. Specifically, I determined in the previous chapter that the most successful heterologous phenazine production in *P. putida* was achieved with *P. putida* 14.phz2 to produce PCA compared to all other tested constructs. This strain also showed promising performance under oxygen-limited conditions in BES reactors.

To gain information on the overall performance and possible toxic effects of phenazine-based electron discharge in a rhamnolipid producing strain, we initially evaluated the growth of rhamnolipid producer strain in anaerobic cultivation. We worked with a genomic-integrated mono-rhamnolipid-producing *P. putida* SK1. The *rhIAB* genes in this strain were inserted in the 16S rRNA gene sequence of genomic DNA. In this anaerobic cultivation simulation, we added the synthetic commercially PCA and PYO and observed the growth as well as the mono-rhamnolipid production of the strain.

Furthermore, to evaluate the actual capacity of phenazine-based redox balancing in an oxygen-limited BES, this strain was now coupled with two newly constructed plasmids for heterologous production of rhamnolipids in *P. putida* (Supplementary information Figure S9). Furthermore, the production of both phenazine and mono-rhamnolipid from both strains were evaluated under fully aerobic condition (triplicate flasks experiment). The most potential strain that produced adequate amounts of both phenazine and mono-rhamnolipid has been further assessed for bioelectrochemical production under active aeration for 48 hours followed by passive aeration (AA), active aeration continuously (AA+), and passive aeration from the start (PA) in BES reactors (biological triplicates).

3.2.3 Results and Discussions

3.2.3.1 Tailoring heterologous mono-rhamnolipid synthesis with phenazine production in *P. putida*

The first new plasmid constructed in this study was a salicylate inducing-promoter pJNN plasmid carrying *rhlAB* genes, expressing mono-rhamnolipid. The second plasmid was the modification of the existing pJNN.phzM+S plasmid constructed by Schmitz *et al.* in which the *rhlAB* genes were inserted additionally to yield plasmid pJNN.rhlAB.phzM+S. Thus in this work, we generated two newly engineered strains. The first strain is *P. putida* rhl-pca carrying the pBNT.14phz2 and pJNN.rhlAB plasmids, which was able to produce mono-rhamnolipid and PCA. The second strain was *P. putida* rhl-pyo, carrying the pBNT.14phz2 and pJNN.rhlAB.phzM+S plasmids, which was able to produce mono-rhamnolipid, PCA, and PYO.

The introduction of the *rhlAB* operon, originating from *P. aeruginosa* PAO1, into *P. putida* KT2440 for the heterologous production of rhamnolipids has been previously successfully described. This non-pathogenic bacterium possesses both critical pathways for rhamnolipids precursor biosynthesis and grows well on glucose (Tiso *et al.*, 2016; Wittgens *et al.*, 2018; Wittgens *et al.*, 2011). In this study, the *rhlAB* operon was inserted in the pJNN plasmid and was transformed into *P. putida* KT2440. This strain was additionally equipped with the pBNT.14phz2 plasmid constructed for this thesis, enabling PCA production. This newly developed strain was termed *P. putida* rhl and was able to produce rhamnolipids and PCA in parallel. Additionally, a plasmid, in which the *rhlAB* operon was inserted in the pJNN.phzM+S plasmid (Schmitz *et al.*, 2015) was constructed and termed pJNN.rhlAB.phzM+S. In combination with the pBNT.14phz2 plasmid, a strain called *P. putida* rhl-MS, which was able to produce PCA, PYO, and mono-rhamnolipids was generated.

Moreover, the growth behavior of eight picked colonies was compared on a multiplexed micro-cultivation platform. The best performing *P. putida* rhl clone produced 730 mg/L mono-rhamnolipids on LB media containing 10 g/L of glucose after 30 h of cultivation (Figure 18a).

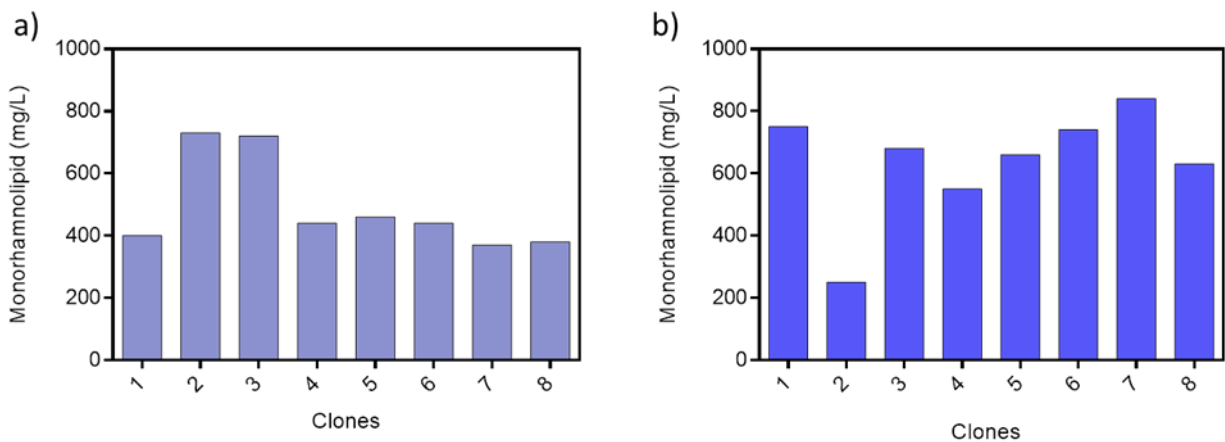


Figure 18: Characterization of rhamnolipid producing *P.putida*. Rhamnolipid production of eight clones of (a) *P. putida* rhl (carrying pJNN.rhlAB plasmid) (b) *P. putida* rhl-MS (carrying pJNN.rhlAB.phzM+S plasmid) cultivated in the micro cultivation platform in LB media for 24 hours.

Based on the HPLC quantification analysis, all of the four common mono-rhamnolipid congeners produced from *P. aeruginosa* were present, i.e., Rha-C₁₀-₁₀ (predominantly), Rha-C₈-C₁₀, Rha-C₁₀-C₁₂, and Rha-C₁₀-C_{12:1}. As it was described by Behrens *et al.*, in most of the cultivations that produced rhamnolipids, we found the same range of proportion from each congener (Behrens *et al.*, 2016). These eight clones were characterized further in Delft minimum media containing 10 g/L of glucose under the same cultivation condition, resulting in 360 ± 30 mg/L mono-rhamnolipid production after 30 h of cultivation (Figure 19). The best *P. putida* rhl-MS clone was able to produce a maximum of 840 mg/L mono-rhamnolipid on LB media (Figure 18b) and 400 ± 20 mg/L on Delft media, containing 10 g/L glucose (Figure 20). However, it was observed during the micro-cultivation experiment that some of the tested clones did not produce any mono-rhamnolipid. A possible explanation could be plasmid loss during the cultivation.

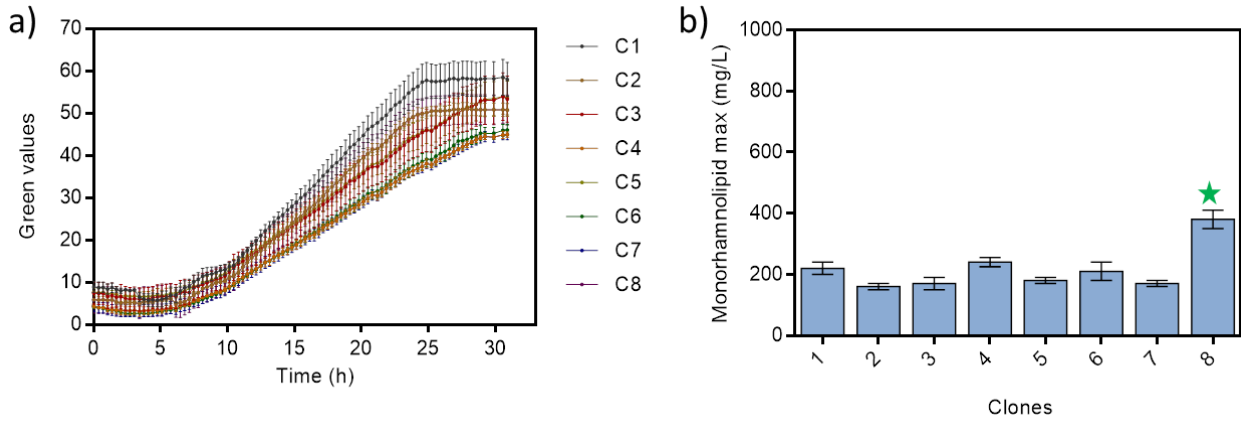


Figure 19: Growth curve (a) vs. mono-rhamnolipid production (b) of eight clones of the *P. putida* rhl strain in the micro cultivation experiment (triplicates for each) in Delft media with 10 g/l glucose. For this cultivation platform, the “green value” is the output signal for biomass density. The star symbol indicates the selected clone to be characterized in the flask & BES experiment.

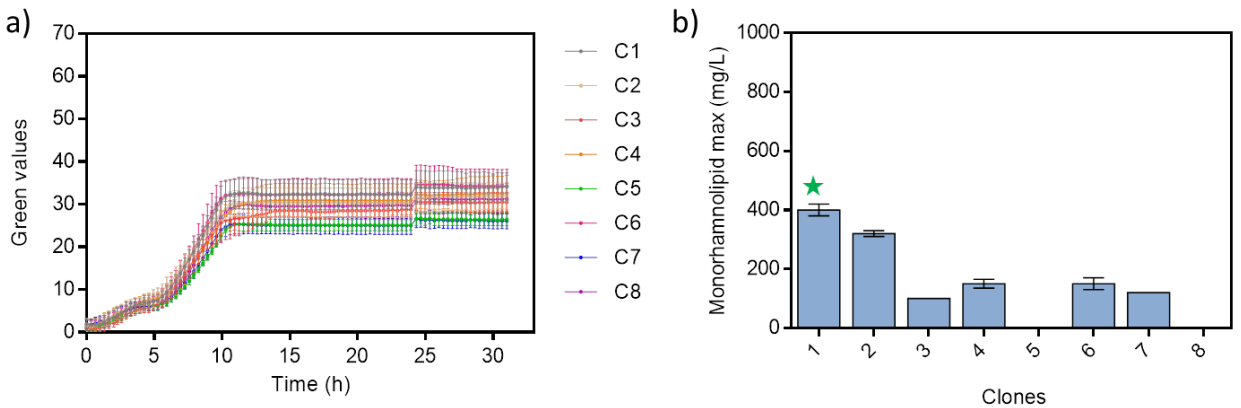


Figure 20: Growth curve (a) vs. mono-rhamnolipid production (b) of eight clones of the *P. putida* rhl-MS strain in the micro cultivation experiment (triplicates each) in Delft media with 10 g/L glucose. For this cultivation platform, the “green value” is the output signal for biomass density. The star symbol indicates the selected clone to be characterized in the flask & BES experiment.

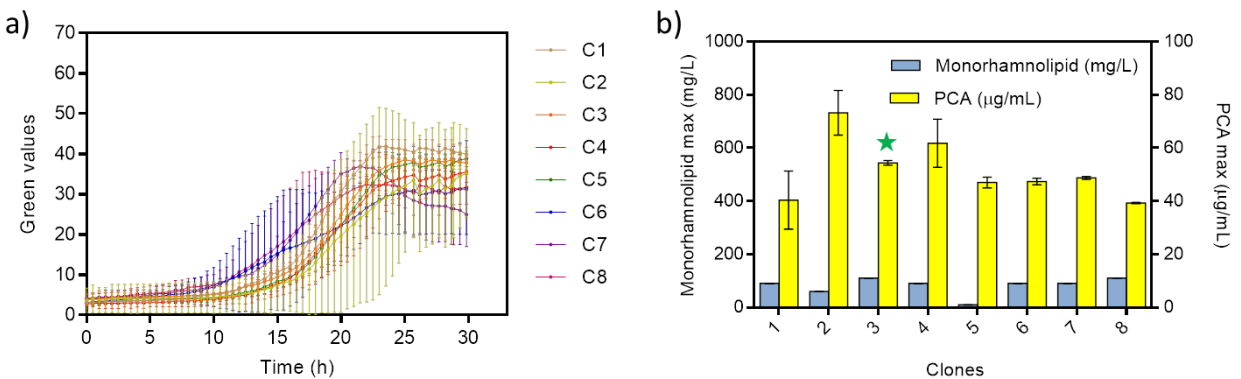


Figure 21: Growth curve (a) vs. mono-rhamnolipid & PCA production (b) of eight clones of the *P. putida* rhl-pca strain in the micro cultivation experiment (triplicates) in Delft media with 10 g/L glucose. For this cultivation platform, the “green value” is the output signal for biomass density. The star symbol indicates the selected clone to be characterized in the flask & BES experiment.

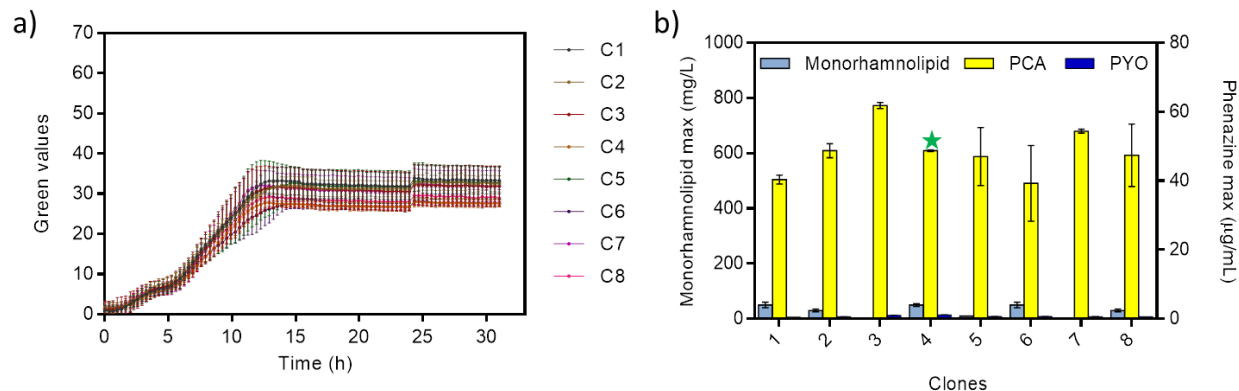


Figure 22: Growth curve (a) vs. mono-rhamnolipid, PCA & PYO production (b) of eight clones of the *P. putida* rhl-psy strain in the micro cultivation experiment (triplicates each) in Delft media with 10 g/L glucose. For this cultivation platform, the “green value” is the output signal for biomass density. The star symbol indicates the selected clone to be characterized in the flask & BES experiment.

Several studies have been conducted to generate a recombinant host for rhamnolipid production. For example, Ochsner *et al.* established recombinant strains of *P. fluorescens*, *P. putida*, *P. oleovorans*, and *E. coli* to produce mono-rhamnolipid using glycerol as a substrate. Recombinant strains of *P. fluorescens* produced 250 mg/L, 600 mg/L of rhamnolipid from *P. putida* KT2440, but no mono-rhamnolipid was synthesized in *E. coli* and *P. oleovorans* (Ochsner *et al.*, 1994). Another study conducted by Cabrera-Valladares *et al.* also reported the heterologous production of mono-rhamnolipids in *E. coli* W3110 that expressed the *P. aeruginosa* operons *rhlAB* and *rmIBDAC* (responsible for the dTDP-L-rhamnose synthesis pathway). By using glucose as a substrate, this strain produced 120 mg/L mono-rhamnolipid (Cabrera-Valladares *et al.*, 2006). Notably, by utilizing soybean oil as substrate, Cha *et al.* reported on the expression of the *rhlAB* genes from *P. aeruginosa* in *P. putida* KCTC1067, resulting in 7.3 g/L mono-rhamnolipid (Cha *et al.*, 2008). In general, *P. aeruginosa* produces rhamnolipid in highest rate on plant oils as a carbon source. However, it leads to unbeneficial and complicated procedures in the downstream processing of rhamnolipid production. More recently, heterologous rhamnolipid production from glucose with strain *P. putida* KT2440 pVLT33_rhlAB conducted by Wittgens *et al.* produced 220 mg/L mono-rhamnolipid (Wittgens *et al.*, 2011). Moreover, in work performed by Tiso *et al.* of the genetically optimized strain, *P. putida* pSynPro8 was generated, which was able to produce up to 3 g/L rhamnolipid (Tiso *et al.*, 2016). In comparison with these other efforts for heterologous rhamnolipid production, the

here generated strains *P. putida* rhl and *P. putida* rhl-MS produced moderate amounts of mono-rhamnolipid titer in aerobic cultivations on LB containing glucose.

The best performing clone of the *P. putida* rhl as well as *P. putida* rhl-MS strain was sequentially further transformed with the pBNT.14phz2 plasmid expressing PCA, to generate the PCA- or PYO-expressing strains *P. putida* rhl-pca and *P. putida* rhl-pyo, respectively. The *P. putida* rhl-pca strain was characterized in a micro-cultivation under the same cultivation conditions, where it produced a maximum of 110 ± 0.52 mg/L mono-rhamnolipids and 54.38 ± 8.41 μ g/mL PCA (Figure 21). *P. putida* rhl-pyo, on the other hand only produced a maximum of 50 ± 10 mg/L mono-rhamnolipids, 48.76 ± 0.24 μ g/mL PCA, and 14.66 ± 0.35 μ g/mL PYO (Figure 22). Hence, its performance concerning mono-rhamnolipid was rather low. It is likely that the introduction of both plasmids, each carrying different antibiotic, caused big stress to *P. putida* rhl-pyo strain. Notably, inserting the *rhlAB* genes in the pJNN plasmid containing *phzM* and *phzS* genes without the presence of the PCA producing plasmid (*P. putida* rhl-MS) showed enhanced rhamnolipid production compared to the strain without the *phzM* and *phzS* genes. Subsequently, the best performing *P. putida* rhl-pca and *P. putida* rhl-pyo clones, obtained from the micro-cultivation selection, were further characterized under aerobic conditions in shake flasks (Figure 23).

As can be seen in Figure 23a, the best performing clone of *P. putida* rhl-pca was able to produce a maximum of 141 mg/L mono-rhamnolipids and 57.70 ± 18.41 μ g/mL PCA after 48 hours of fully aerobic cultivation. Hence, the mono-rhamnolipid production of *P. putida* rhl-pca was higher than the production of the *P. putida* rhl strain, which only produced 110 ± 0.3 mg/L mono-rhamnolipids. By doubling the salicylate concentration during cultivation (2mM), mono-rhamnolipid and PCA productions were further increased up to $152 \pm 1,22$ mg/L and 122 ± 12.49 μ g/mL, respectively. On the other hand, as it can be seen in Figure 23b, the *P. putida* rhl-pyo only produced mono-rhamnolipids at 50 ± 0.00 mg/L, PCA at 67.22 ± 7.80 μ g/mL, and PYO at 33.96 ± 2.8 μ g/mL. By increasing the salicylate concentration, it was only possible to increase the PCA concentration up to 130.80 ± 16.83 μ g/mL, yet it did not markedly increase the mono-rhamnolipid concentration. Based on this result, we assumed that PYO production caused cell toxicity and negatively affected mono-rhamnolipid production. It is also supported by the lower OD₆₀₀ observed from *P. putida* rhl-pyo compared to *P. putida* rhl-pca and *P. putida* rhl (Figure

24). This growth trend was also observed in *P. putida* 14.phz2+ strain (Chapter 3.1), which is also carrying two plasmids to produce PCA and PYO.

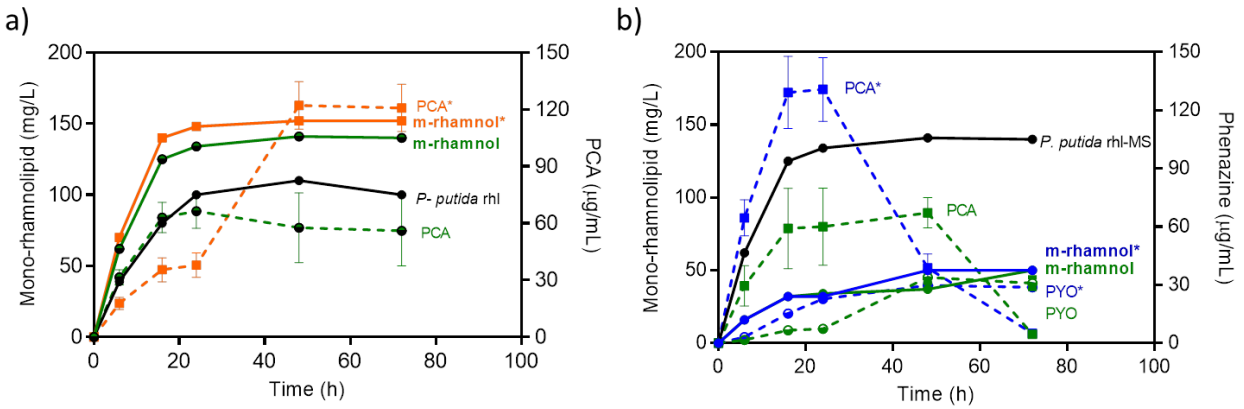


Figure 23: Fully aerobic flasks cultivation (triplicates) for mono-rhamnolipid (m-rhamnol) and phenazine production (PCA and PYO). (a) *P. putida* rhl-pca and (b) *P. putida* rhl-pyo in Delft minimum media containing 10 g/L glucose. The sign "*" followed after the strain name indicating two times of salicylate concentration given as plasmid inducer in the experiments.

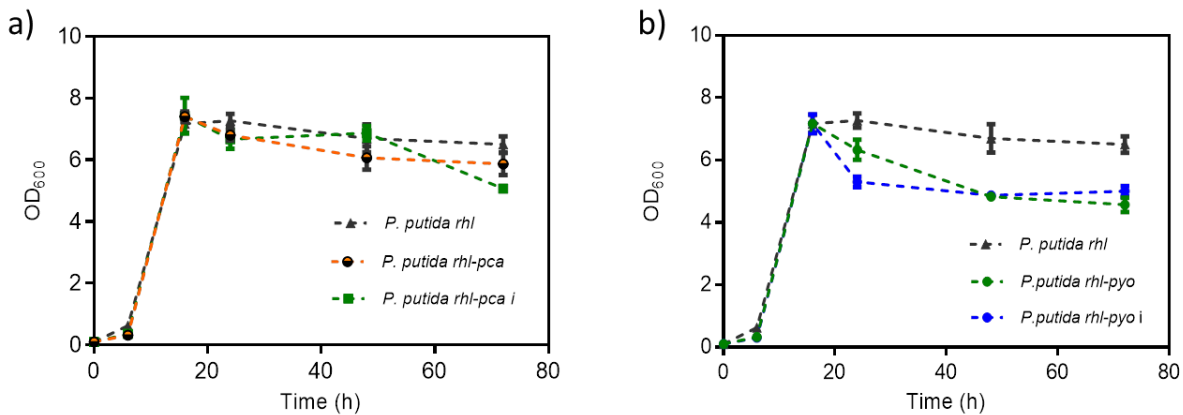


Figure 24: Fully aerobic flasks cultivation (triplicates) for growth observation (OD₆₀₀). (a) *P. putida* rhl-pca and (b) *P. putida* rhl-pyo in Delft minimum media containing 10 g/L glucose. The letter "i" followed after the strain name indicating two times of salicylate concentration given as plasmid inducer in the experiments

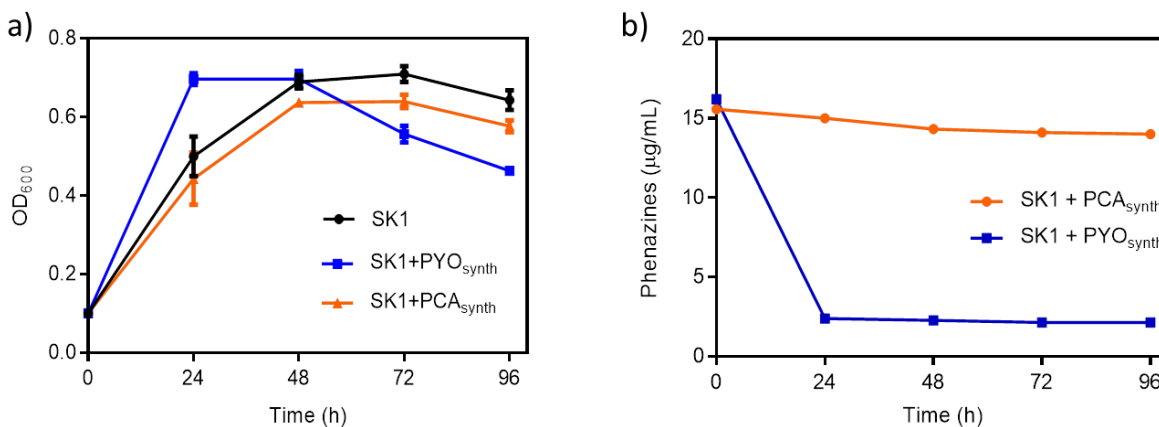


Figure 25: Anaerobic flasks experiment (triplicate) of *P. putida* SK1 with synthetic PCA and PYO added. Growth curve (a) Synthetic PCA & PYO concentration changes during the cultivation (b).

In order to gain the understanding of phenazine effect to the mono-rhamnolipid-producing *P. putida* under oxygen-limited cultivation, a controlled study has been conducted by cultivating *P. putida* SK1 (genome integrated strain) in the anaerobic flask with synthetic phenazines added (Figure 25). Based on the growth observation, during the exponential phase, *P. putida* SK1 + PYO_{synth} culture grew faster compared to *P. putida* SK1 + PCA_{synth} culture and *P. putida* SK1 without any phenazine culture. After 48 hours, *P. putida* SK1 + PYO_{synth} culture stopped growing and sustaining faster, due to the remaining oxygen in the headspace of serum bottle has been consumed faster as well. On the other hand, *P. putida* SK1 + PCA_{synth} and *P. putida* SK1 only cultures were still sustained the stationary phase up to 72 hours. None of the cultures produced mono-rhamnolipid. In these tests, the grown culture depends on how long the initial oxygen lasts to survive. The phenazines cannot be used for electron discharge since they are not regenerated at an anode.

Regarding the phenazines analysis, the PCA was more sustained in the cultures compared to PYO, which was quickly gone after 24 hours. Since no electrode was present in these experiments, removal of the PYO from the solution through adsorption processes to the electrode is not possible. It showed that PCA was more potential to be employed as an electron shuttle in the BES reactor, combined with the rhamnolipid production. Therefore, from the strain evaluation in the aerobic and anaerobic flask cultivation, *P. putida* rhl-pca was chosen to be characterized further for bioelectrochemical production of rhamnolipids in the BES reactor.

3.2.3.2 Bioelectrochemical production of rhamnolipid in oxygen-limited BES

3.2.3.2.1 Applying active aeration in BES

Initially, as the controls experiments, the *P. putida* rhl (producing mono-rhamnolipid only) has been characterized in actively aerated BES reactors with and without electrode (Supplementary information Figure S10 and S11). Those experiments showed that there was no mono-rhamnolipid produced in those reactors. Subsequently, the *P. putida* rhl-pca strain has also been characterized in actively aerated BES reactors without electrode (Supplementary information Figure S12), and it also showed the absence of mono-rhamnolipid production. From these control experiments, we expected the presence of a poised electrode in the oxygen-limited BES for *P. putida* rhl-pca cultivation would be beneficial as an alternative electron acceptor to support the rhamnolipid production.

From the characterization of *P. putida* rhl-pca in aerobic shake flasks, we knew this strain was able to produce mono-rhamnolipid and PCA. And also, based on the work presented in the previous chapter, we knew that the highest PCA production and currents generation was obtained with *P. putida* carrying the phenazine genes from *P. aeruginosa* PA14 operon two under active aeration (AA). Therefore, we firstly tested the performance of *P. putida* rhl-pca in a polarized BES at 0.2 V vs. the reference electrode by applying active aeration at 30 ml/minute flow rate for 48 hours and then continued to passive aeration via opened vent filter (Figure 26). As it is shown in Figure 26a, the PCA production of the *P. putida* rhl-pca strain was 75.75 ± 13.76 $\mu\text{g/mL}$, resulting in 10.65 ± 3.26 $\mu\text{A/cm}^2$ of currents density. This PCA production was in the same range with the BES performance of the *P. putida* 14.phz2 strain (PCA producer only) presented in the previous chapter, i.e., there 80 $\mu\text{g/mL}$ of PCA resulted in 11.77 $\mu\text{A/cm}^2$ of currents generation. This result showed that pBNT.14phz2 plasmid stayed active expressing PCA. The glucose consumption was up to 89%, which was also in the same range compared to *P. putida* 14.phz2 strain (87%). Moreover, the *P. putida* rhl strain produced higher 2-ketogluconate (predominantly) during the first three days of cultivation in BES reactor, which was up to 2.76 ± 0.51 mmol/L (compared to 0.63 mmol/L with *P. putida* 14.phz2, as described in Chapter 3.1). It is an interesting finding since 2-ketogluconate is also a potential compound for industrial application, such as in the pharmaceutical and cosmetics industries (Sun et al., 2018).

However, in this BES reactor set up, the *P. putida* rhl-pca strain did not produce any mono-rhamnolipid until the end of the cultivation time (10 days).

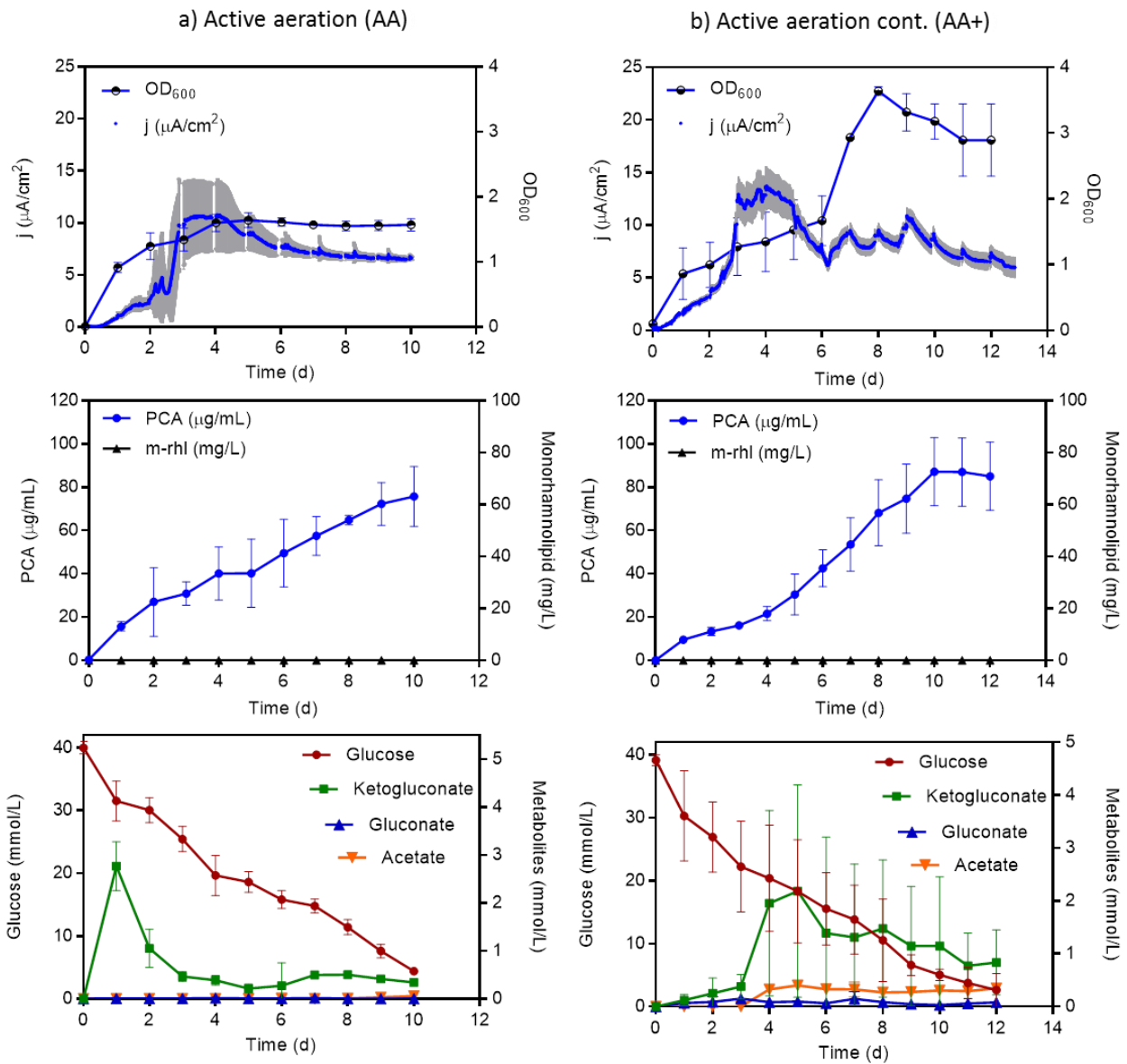


Figure 26: BES performance of *P. putida* rhl-pca at an applied potential of 0.2 V vs. RE. BES set up under (a) Active aeration, AA, at a flow rate of 30 ml/minute for 48 hours, then continued with passive headspace aeration (b) Active aeration plus, AA+, at a flow rate of 50 ml/minute continuously until the end of the experiment. The BES data are means from biological triplicates

Therefore, another set up of BES reactor has been conducted by applying a higher airflow rate of 50 mL/minute continuously until the end of cultivation (AA+). The AA+ set up aimed to give more oxygen in the reactor, which serves an electron acceptor in the cellular catabolic reaction

to gain more energy for the cellular metabolism and with that to support the mono-rhamnolipid production in the BES culture. As can be seen in Figure 26b, the PCA production of AA+ reactors was increased by 16% compared to AA reactors, which resulted in a 30% increase of current density. The glucose consumption was up to 93%, with the production of 2-ketogluconate as a side product, which was in the same range compared to AA reactors. There was still no mono-rhamnolipid produced in those BES reactors set up. It is likely that in AA and AA+ reactors, most of the electrons likely go to oxygen respiration as the easiest and the most energy delivering route. Additionally, it showed that oxygen level in AA and AA+ reactors were not the limiting factors for bioelectrochemical production of mono-rhamnolipid in BES.

3.2.3.2.2 Applying passive aeration BES

Since it has been revealed that oxygen was not the main limiting factor for rhamnolipid production in AA, BES reactors were operated by only applying passive aeration of the headspace during the cultivation time. Figure 28 shows the performance of the *P. putida* rhl-pca strain in passively aerated BES (PA). Under stringent oxygen condition, this strain was able to produce 11.23 ± 0.78 $\mu\text{g/mL}$ of PCA, which resulted in 8.07 ± 0.15 $\mu\text{A/cm}^2$ current density. Although the glucose consumption (58.67 ± 2.08 %), as well as the metabolite production, was low, this strain surprisingly was able to produce the mono-rhamnolipid in low concentration, i.e. 20.67 ± 0.15 mg/L at maximum. It is likely that in the absence of oxygen, the electron pressure becomes very high and activates the rhamnolipid production. The presence of mono-rhamnolipid produced in the passively aerated BES reactors has been confirmed independently through TLC analysis for each of the reactors (Figure 27). We investigated three samples for the TLC analysis, each from a different reactor and cultivation time to scan the production range. The mono-rhamnolipids detected with the HPLC for reactor 1 during early cultivation (9 mg/L , day 1 of cultivation time) did not appear in the TLC plate. Probably the extraction method applied in this study was not able to extract this low concentration of mono-rhamnolipid. Based on the HPLC analysis, there were only two congeners of mono-rhamnolipid produced from this BES cultivation, i.e., Rha-C₁₀-C₁₀ and Rha-C₁₀-C₁₂, probably due to the low titer of rhamnolipid production. Additionally, the low rhamnolipid production in the passively aerated BES was in

accordance with the low cell density (OD_{600} : ~1) observed during the cultivation of *P. putida* rhl-pca.

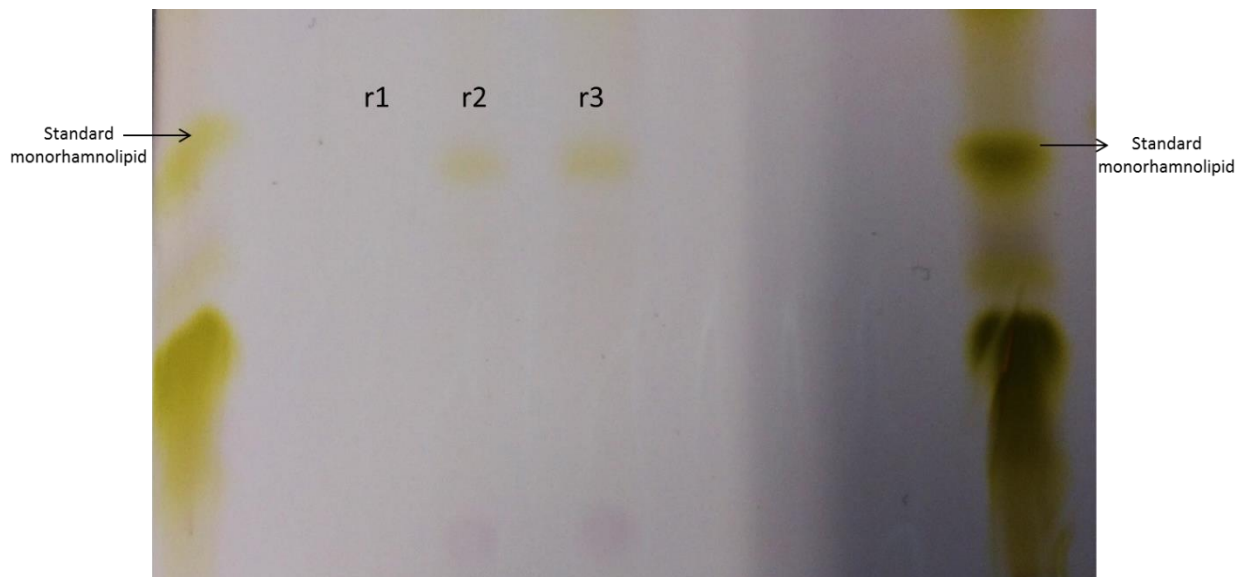


Figure 27: Thin-layer chromatography (TLC) analysis of the samples were taken from the second experiment BES reactors of *P. putida* rhl-pca strain under PA condition. Measured by HPLC quantitatively, r1: 9 mg/L (reactor 1, day 1), r2: 13 mg/L (reactor 2, day 3), and r3: 23 mg/L (reactor 3, day 7) of mono-rhamnolipid.

The repetition of the experiment with the same setup and again in triplicates showed the same range of results for all of the parameters (Supplementary information Figure S14). It showed that the passive aeration set up is more suitable to be applied for bioelectrochemical production of rhamnolipid from *P. putida* rhl-pca, compared to actively aerated reactors. It is likely that under these most stringent oxygen levels, the need to get rid of electrons was higher and led the *P. putida* rhl-pca culture to store them in the form of rhamnolipids.

To estimate the electrical energy retrieved from the glucose substrate in BES, we evaluated the coulombic efficiency from each BES set up, as shown in Figure 28d. The BES reactors of *P. putida* rhl-pca strain under PA condition had lower coulombic efficiencies (4.27 ± 1.73 %) compared to the AA (4.83 ± 0.68 %) and AA+ reactors (8.68 ± 3.83 %). However, this coulombic efficiency was in the same range as the passively aerated BES cultivation of *P. putida* 14.phz2, which produced PCA only, as described in Chapter 3.1.

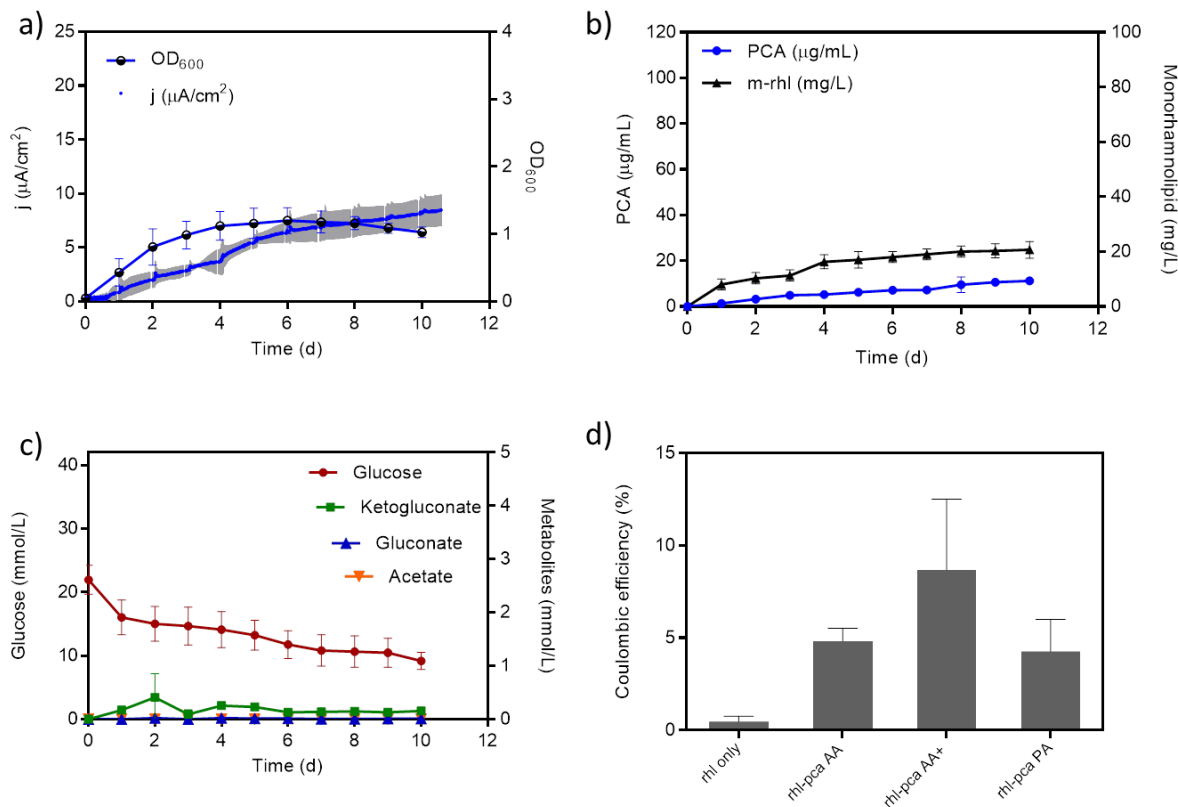


Figure 28: BES performance of *P. putida* rhl-pca at an applied potential of 0.2 V vs. RE. (a-c) BES set up under passive aeration. The BES data are means from biological triplicate. (d) Coulombic efficiency comparison between the BES reactors of *P. putida* rhl (control), *P. putida* rhl-pca AA, AA+, and PA.

3.2.3.3 Plasmid sustainability evaluation in the BES reactors

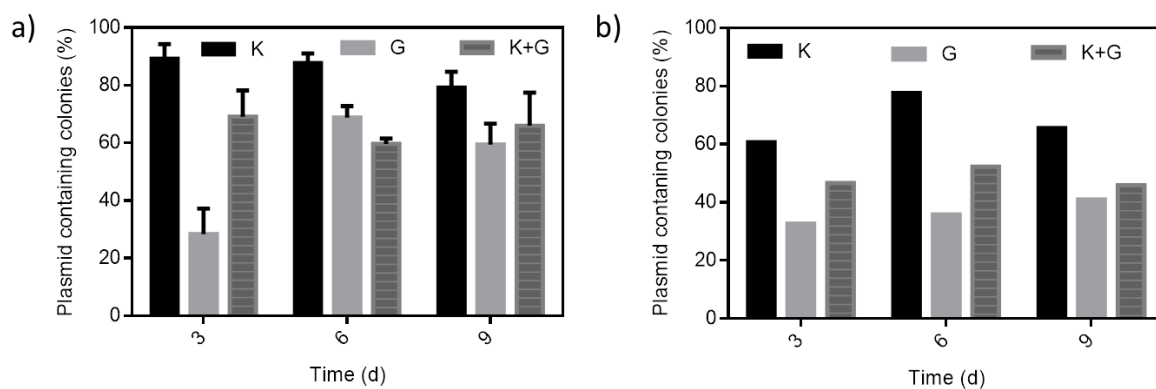


Figure 29: Plasmid sustainability evaluation of *P. putida* rhl-pca strain BES reactors. (a) BES operation under PA conditions (triplicate), (b) BES operation under continuous active aeration, AA+ (single). **K**; indicating the percentage of colonies which grew on the LB+Kanamycin plate (carrying plasmid pBNT. 14phz2), **G**; indicating the percentage of colonies which grew on the LB+Gentamycin plate (carrying plasmid pJNN.rhIAB), and **K+G**; indicating the percentage of colonies which grew on the LB+Kanamycin+Gentamycin plate (carrying plasmid pBNT. 14phz2 and pJNN.rhIAB).

To verify if *P. putida* rhl-pca sustained to carry both of the plasmid expressing PCA and mono-rhamnolipid during the cultivation in BES, a plasmid stability evaluation via positive selection plate counts has been conducted (del Solar et al., 1987). Figure 29a showed the plasmid evaluation of passively aerated BES reactors (triplicate from the second experiment) every 3 days during the cultivation. It revealed that on day 3, the cells carrying plasmid pBNT.14phz2 (selected through kanamycin resistance - K) were still above 80% and predominant, while the cultures carrying plasmid pJNN.rhIAB (selected through gentamycin resistance - G) were only 28.37 ± 8.81 % and the cultures carrying both plasmids (K + G) were at ~70%. It might be the reason why the production of mono-rhamnolipid in the passively BES reactors was only 15% of the production under a fully aerobic condition in the flasks experiment. During the exponential growth (day 6), the percentage of the cultures in every selective antibiotic plate were increasing and sustained until stationary phase (day 9). Base on the proportion of the grown colonies from each selective plate, it can be seen that this method is not suitable to be applied for the plasmid sustainability determination during the BES cultivation. It is not explainable why the more colonies grew on the G+K plates than on the G only plates. Therefore, we could only use this method as tendency information for the likelihood of cells not carrying a plasmid during cultivation rather than for an exact quantification.

In the meantime, a single BES reactor under AA+ aeration was also investigated for plasmid stability (Supplementary information Figure S13). As it can be seen in Figure 29b, the percentage of the cells in AA+ reactors for each selective antibiotic plate was lower compared to PA reactors. The cells carrying the pBNT.14phz2 plasmid was also predominant. Compared to the BES reactors under PA condition, the percentage of the cells which lost their plasmid was higher under AA+. The results showed that the density of *P. putida* rhl-pca cultures carrying the pJNN.rhIAB plasmid was below 50% during the cultivation in AA+ reactors. It might be one of the reasons for the absence of mono-rhamnolipid production in BES under AA/AA+ condition. However, the correlation between the oxygen level and the plasmid sustainability in the BES reactors AA+ is still unclear.

3.2.4 Conclusions

In this study, we show that oxygen-limited biocatalysis of *P. putida* in BES has been established. We successfully generated a non-pathogenic strain, which was able to produce two compounds, i.e. phenazines and rhamnolipids, in which a complex quorum sensing network tightly controls their synthesis. For the first time, this study proved the concept that anodic bioproduction from glucose under strong oxygen limitation is possible by employing an engineered, obligately aerobic bacterium in BES. Under passively aerated conditions in a BES, survival through bioelectrochemical electron discharge to an anode was able to be coupled with the bioelectrochemical production of foam-free mono-rhamnolipids, by involving phenazines as redox mediator. This research finding opens the possibility to produce other types of glycolipid surfactant or other valuable amphiphilic compounds in BES reactors. The titer of mono-rhamnolipids produced in the BES reactors could be increased by further improving the strain performance through genetic engineering, for example, by introducing strong promoters in the expression plasmid. By developing this approach with suitable BES operation, this could be a powerful strategy to produce valuable compounds and fuels from renewable resources in high carbon yield.

Chapter 4

General Discussion

4.1 State-of-the-art in rhamnolipid production for bio-detergents industry

One of the industrial applications of rhamnolipids is their utilization as an additive compound for cleaning agents and detergents, as they are suitable natural emulsifiers and tension-active agents (Parry & S., 2013). The production of rhamnolipids in pilot-scale as an additive compound to cleaning products and detergents has already been conducted by several companies, such as Tee Gene Biotech (UK), Jeneil Biosurfactant Co. LLC (USA), and Henkel (Germany) (Sekhon Randhawa & Rahman, 2014). However, the cash flow for rhamnolipid scale-up production is still far too low to consider this biosurfactant as an alternative to synthetic surfactants, due to the high cost of raw materials and processing (Gong et al., 2015; Sekhon Randhawa & Rahman, 2014). Several studies have been conducted to replace oil-based substrate with, for example, glucose, which resulted in a competitive titer and carbon yield (Tiso et al., 2016; Wittgens et al., 2011). However, the existing strategy of the rhamnolipid production process has not been effectively applied yet. It is due to the complex metabolic regulation of the rhamnolipid production and strong foam formation in the fermenter during aerobic cultivation (Beuker et al., 2016; Díaz De Rienzo et al., 2016; Muller et al., 2010). Rhamnolipid production with an efficient biocatalyst in an operating system that enables the conversion and conservation of renewable resources is very beneficial and therefore, a current focus in the process development. Furthermore, the foam-free rhamnolipid production will simplify the downstream processing while maintaining the production yield.

In this study, I successfully generated a newly engineered strain of *P. putida* to synthesize phenazine redox mediators (*P. putida* 14.phz2), which was able to produce ten times higher PCA titers compared to the existing strain (Schmitz et al., 2015). Furthermore, I also successfully combined the mono-rhamnolipid synthesis with phenazine production by generating the *P. putida* rhl-pca strain, which has the genetical capacity to be employed as a biocatalyst for the bioelectrochemical production of rhamnolipids (Chapter 3.2). During the cultivation of *P. putida* rhl-pca in the passively aerated BES, we did not observe the foam formation within the bioreactor that is otherwise typical in non-BES rhamnolipid fermentation. At the end of the experiment, we applied vigorous aeration via a big sparger (500 L/minute), leading to the slight

formation of rainbowish bubbles within the reactor (Figure 31). However, the maximum titer of mono-rhamnolipids was quite low in both, the aerobic shake flask cultivations and the passively aerated, strongly oxygen-limited BES cultivations. We determined the keys factors to enhance bioelectrochemical foam-free mono-rhamnolipid production to be a further improvement of the recombinant rhamnolipid productivity and optimization of the bioelectrochemical production. Additionally, this study opens the path to the production of other types of glycolipids surfactant with oxygen-limited BES.

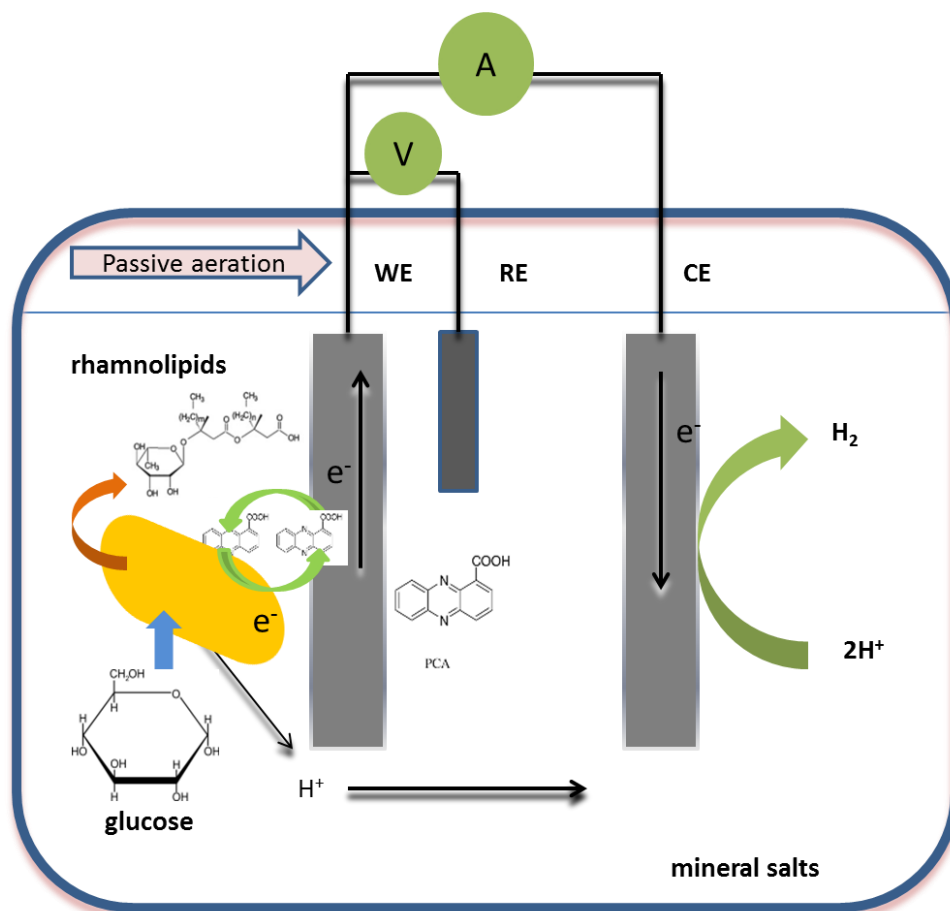


Figure 30: Scheme of bioelectrochemical production of mono-rhamnolipid *P. putida* rhl-pca using glucose as substrate, facilitated by PCA as an electron shuttle in passively aerated-BES at an applied potential of 0.2V vs. RE



Figure 31: Bubble formation in the passively aerated BES (reactor 1), after being sparged with vigorous aeration at a flow rate 500 mL/minute (at the end of the experiment, day 10).

4.2 Evaluation of the productivity of the recombinant rhamnolipid strain

In our initial study (Chapter 3.2), we attempted to obtain a stable recombinant host for rhamnolipid production by combining *P. putida* SK1 (contains genome integration of *rhIA* and *rhIB*) (Wittgens et al., 2011) with our new pBNT.O1phz2 plasmid. The new transformed strain produced no mono-rhamnolipids, although the PCA production was 4-times higher than in the *P. putida* O1.phz2 strain (expressing PCA only), i.e., $140 \pm 30 \mu\text{g/mL}$ (Kastenholz, 2017). Likely, the introduction of the phenazine-expressing plasmid in the *P. putida* SK1 strain repressed *rhIAB* genes expression. In this strain, the operon is inserted into the genomic 16S rDNA sequence.

Nonetheless, the production of both PCA and mono-rhamnolipid was successfully coupled in the plasmid-based *P. putida* rhl-pca strain. The ability of this strain to produce both of the compounds enables the bioelectrochemical production of mono-rhamnolipids as model compounds. Although they might be genetically-less stable, the plasmid-based strains generated in this study were a better approach compared to the initial genome integrated

strategy. *P. putida* rhl-pca was able to cope with two introduced plasmids, which contain two different antibiotic resistance gene cassettes (kanamycin and gentamycin). However, the strains generated in this study produced lower maximum titers of rhamnolipids in both anaerobic flasks and passively aerated BES cultivations, when compared to other recombinant rhamnolipid producers (Table 7). For comparison, *P. putida* KT2440 pSynPro8 is a good example of recombinant host improvement. The new synthetic constitutive SynPro promoter and the *rhlAB* genes inserted in the pBBR1MSC-3 vector backbone proved to increase the rhamnolipid titer to up to 3 g/L in LB aerobic shake flasks (Tiso et al., 2016). In the future, an optimization of the bioelectrochemical rhamnolipid production could be achieved by further engineering the strain with this more advanced plasmid system and synthetic constitutive promoters.

Table 7: Recombinant rhamnolipid producer strains in this study compared to other strains

Organism	Medium	Substrate	Substrate conc. (g/L)	Maximum titer (g/L)	Carbon yield (Cmol _{rhamnolipid} /Cmol _{substrate})	Growth condition	Reference
<i>P. aeruginosa</i> PAO1 (wt)	Mineral Salts (MS)	Sunflower oil	250	39	0,07	aerobic fermenter	(Muller et al., 2010)
<i>P. putida</i> KCTC 1067	MS	Soybean oil	20	7,3	0,17	aerobic flask	(Cha et al., 2008)
<i>P. putida</i> KT42C1 pVLT31_rhIAB	LB	Glucose	10	1,5	0,23	aerobic, flask	(Wittgens et al., 2011)
<i>P. putida</i> KT2440 pSynPro8	LB	Glucose	10	3	0,40	aerobic, flask	(Tiso et al., 2016)
<i>P. putida</i> SK1	LB	Glucose	10	1,25	0,19	aerobic, shaking flask	(Kruth, 2017)
<i>P. putida</i> rhI	LB	Glucose	10	0,73	0,11	aerobic, flask	this study
<i>P. putida</i> rhI	Delft	Glucose	10	0,36	0,06	aerobic, multiplex well	this study
<i>P. putida</i> rhI-pca	Delft	Glucose	10	0,11	0,02	aerobic, multiplex well	this study
<i>P. putida</i> rhI-pca	Delft	Glucose	10	0,141	0,02	aerobic, flask	this study
<i>P. putida</i> rhI-pca	Delft	Glucose	10	0,152	0,02	aerobic flask, 2x induction	this study
<i>P. putida</i> rhI-MS	LB	Glucose	10	0,84	0,13	aerobic, flask	this study
<i>P. putida</i> rhI-MS	Delft	Glucose	10	0,4	0,06	aerobic, multiplex well	this study
<i>P. putida</i> rhI-pyo	LB	Glucose	10	0,05	<0,01	aerobic, multiplex well	this study
<i>P. putida</i> rhI-pyo	Delft	Glucose	10	0,05	<0,01	aerobic, flask	this study
<i>P. putida</i> rhI-pyo	Delft	Glucose	10	0,05	<0,01	aerobic, flask, 2x induction	this study
<i>P. putida</i> rhI-pca	Delft	Glucose	5	0,02	0,22	oxygen-limited BES (PA)	this study

4.3 Bioelectrochemical production optimization

The process operation of the BES can be further explored and optimized to enhance bioelectrochemical productions. For example, by changing the size or shape of the working electrode (WE), we expect to get more current to support the bioelectrochemical production. In our study, we attempted to improve the rhamnolipid production of *P. putida* rhl-pca in the BES reactor by increasing the surface area of the WE to provide a larger surface for bioelectrochemical interaction. Therefore, a woven carbon cloth (400 cm² surface area) was used in duplicate actively aerated BES (AA). However, this approach did not yield the proposed results (Figure 32). The culture stopped growing on day 4, no mono-rhamnolipids were produced, and the current generation was lower than in the cultivation of *P. putida* rhl-pca using the solid carbon comb electrode under the same set up (AA). It shows that in the case of a single chamber BES reactor, increasing the surface area of the WE does not effectively work to increase the current generation with this strain.

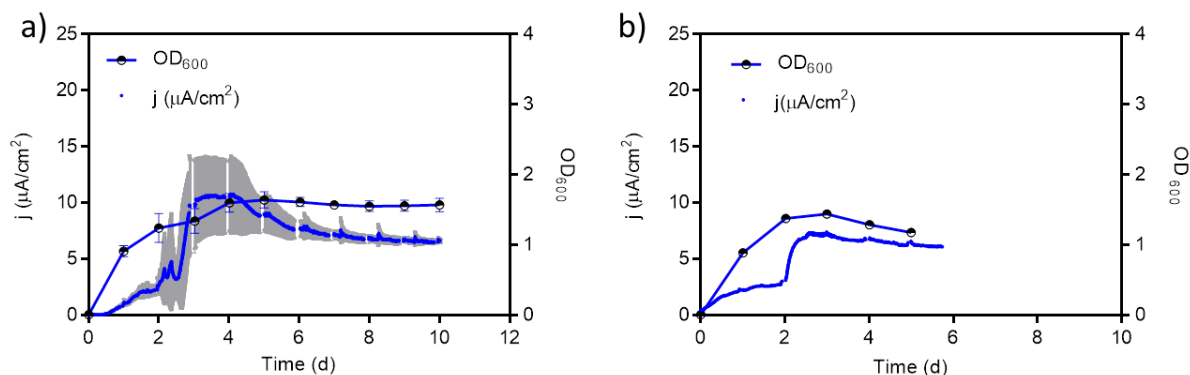


Figure 32: Comparison of BES performance of *P. putida* rhl-pca at an applied potential of 0.2 V vs. RE using carbon comb and carbon cloth as WE. (a) BES set up with a carbon comb electrode (400 cm²) under active aeration, AA, at a flow rate of 30 ml/minute for 48 hours, then continued with passive headspace aeration. The BES data are means from biological triplicates, taken from Chapter 3.2 (b) BES production of *P. putida* rhl-pca (biological duplicate) using a woven carbon cloth (400 cm²) as working electrode and the same aeration conditions as (a).

The ability of the *P. putida* rhl-pca strain to produce a redox mediator and the target product enables the bioelectrochemical production of mono-rhamnolipids as model compounds, which in the future can be developed further towards productivity optimization. The bioproduction under anaerobic condition will potentially be an economic advantage, due to the reduced

substrate loss in the form of CO₂ during anaerobic metabolism and the resulting higher carbon yield (Tashiro et al., 2015). The carbon yield of *P. putida* rhl-pca in passively aerated BES was 0.22 C_{mol rhamnolipid}/C_{mol substrate}, which is higher than the best production with this strain under aerobic cultivation (highlighted blue colour in Table 7) and comparable to strains engineered in other studies (Beuker et al., 2016; Sekhon Randhawa & Rahman, 2014).

In this study, we showed the production of rhamnolipid by providing an extracellular electron sink to *P. putida* rhl-pca in the form of electrodes and redox mediators in passively aerated BES. However, a more detailed study to understand and enhance the respiration tendency through phenazines in *P. putida* rhl-pca is necessary to reduce the cellular metabolic constraint that is hindering utilization of the substrate in stringent oxygen-limited BES. In chapter 3.2, it is shown that the coulombic efficiency of *P. putida* rhl-pca was only at 4.27 ± 1.73 % in passively aerated BES. It means that at this point only ~4.27 % of the electrons provided by the substrate were shuttled (respired) via the phenazines to the anode, while the rest of the electrons were passed to oxygen as the main electron acceptor. Thus, the electron discharge efficiency of *P. putida* to the anode is very low. A central question for any rational improvement of this anodic electron discharge process will be the clarification of the electron transfer pathways from the cellular metabolism to the phenazines as electron shuttles. Therefore, a study to gain an understanding of why *P. putida* KT2440 could not discharge more electrons via the phenazine needs to be conducted. This already ongoing investigation deals with the following questions: (i) how are the phenazine currently linked within the *P. putida* KT2440 metabolism, and (ii) how should they ideally be linked in to trigger a more efficient phenazine based respiration. Therefore, a more in-depth flux balance analysis related to the NADP⁺/NADPH ratio in oxygen-limited BES is needed. Furthermore, when considering energy generation, a deeper flux balance analysis can help to predict the rate of ATP synthesis through ATP synthase, which is depending on the available proton gradient (Lai et al., 2016). As it has been reported by Glasser et al. (Glasser et al., 2014) that phenazines play a role in anaerobic survival mechanism, the ATP synthesis in *P. putida* rhl-pca might be changed into a different rate. Understanding the total energy involved in rhamnolipid formation (or any other valuable product) will support the optimization of anodic oxidation from the carbon substrate in passively aerated BES. This investigation will be very

beneficial to sustain more active biocatalysis, as well as the viability of the cells in the strongly oxygen-limited BES.

4.4 Expanding the concept to the heterologous production of other types of glycolipid surfactants

As introduced in Chapter 1, glycolipid surfactants are highly attractive compounds for industrial application. Therefore, the bioelectrochemical production of rhamnolipids from *P. putida* rhl-pca in passively aerated BES is an essential initial study. The findings of this study showed that it is possible to electrochemically produce foam-free glycolipid surfactants, at a stringent level of oxygen, by employing phenazines as redox shuttle compound.

Several glycolipid surfactants have been intensively studied from their native producer. For example, the gene operon involved in the synthesis of mannosylerythritol lipids originating from *Pseudozyma* (Morita et al., 2014; Saika et al., 2016) and *Ustilago maydis* (Hewald et al., 2006) has been fully characterized. A study of mannosylerythritol lipids production in anaerobic fermenter showed the same problem as in the production of rhamnolipids, i.e., the formation of excessive foam and therefore required a complicated method in the downstream processing (Rau et al., 2005). Additionally, another type of potential glycolipid surfactant, so-called sophorolipids are also well-studied. The functional gene responsible for sophorolipids synthesis in *Candida bambicola* (Solaiman et al., 2014) and *Starmerella bambicola* (Geys et al., 2018) has been characterized. Although sophorolipids are considered low-foam forming biosurfactant, compared to mannosylerythritol lipids (Hirata et al., 2009), my work could be useful to design new bioprocess strategies for the heterologous production of mannosylerythritol lipids as well as sophorolipids. The heterologous production of these compounds could be tailored further with our phenazine plasmid to develop a bioelectrochemical production in BES, with high carbon yield and purity.

Chapter 5

Concluding remarks and Outlook

5.1 Concluding remarks

In this study, we showed that the heterologous phenazine production in *P. putida* could be tuned and enhanced by exploring the natural gene variability of the native hosts. Following the work from Schmitz *et al.*, we successfully expressed the other three phenazine synthesis gene origins originating from operon 2 of *P. aeruginosa* PAO1, operon 1 of *P. aeruginosa* PA14, and operon two of *P. aeruginosa* PA14. Notably, the phenazine-1-carboxylic acid synthesis operon two from *P. aeruginosa* PA14 was found to be the most active in the heterologous phenazine production in *P. putida*, both in the aerobic shake flask and oxygen-limited BES cultivation. This gene origin was chosen to be tailored further with rhamnolipid production.

By applying a plasmid-based genetic engineering strategy, new strains of *P. putida* was successfully generated and produced mono-rhamnolipid, i.e., *P. putida* rhl and *P. putida* rhl-MS. Hereinafter, the heterologous mono-rhamnolipid production in *P. putida* has been successfully coupled with the phenazine production to create strain *P. putida* rhl-pca (produces PCA and mono-rhamnolipid) and *P. putida* rhl-pyo (produces PCA, PYO, and mono-rhamnolipid). Based on the maximum titer of mono-rhamnolipid produced in aerobic shake flasks, *P. putida* rhl-pca was chosen for bioelectrochemical production.

The oxygen-limited cultivations with redox balancing at an anode via phenazines can be coupled to rhamnolipid biosynthesis by employing plasmid-based genetic engineered *P. putida*. The oxygen-limitation level applied in the BES reactor was evaluated for bioelectrochemical production of rhamnolipid. The result of our study showed that passive headspace aeration of BES was suitable to be applied for bioelectrochemical production of foam-free rhamnolipid from *P. putida* rhl-pca. The increased carbon yield obtained from *P. putida* rhl-pca in passively aerated BES showed a potential economic advantage for the glycolipid surfactant bioproduction. However, further strain improvement for higher rhamnolipid titer production, optimizing the BES reactor set-up and investigating the main metabolic aspect to increase the tendency to respire with phenazine as an alternative electrons acceptor, are necessary for the bioelectrochemical production. Overall, this work is an initial study showing that the

bioelectrochemical production of foam-free glycolipid surfactants by employing phenazines as electron shuttle is possible.

5.2 Outlook

5.2.1 Rhamnolipid recombinant host improvement

Based on the maximum rhamnolipid titer produced from *P. putida* rhl-pca, the bioelectrochemical production of rhamnolipid was still far away from any industrial application. A strain improvement strategy can be applied to obtain a higher titer of the rhamnolipid production, e.g. by constructing a new rhamnolipid producer plasmid containing a synthetic promoter designed to enhance the rhamnolipid synthesis enzyme expression and precursor availability (Beuker et al., 2016) and also using constitutive promoter to omit the dependency of the plasmid inducer (Tiso et al., 2016). Another molecular approach is improving the copy number of genes in the genome-integrated strain to express more of the rhamnolipid enzymes. It could be achieved by applying the chromosomal integration of gene(s) with multiple copies (CIGC) method, using the flippase from the yeast 2- μ m plasmid (Gu et al., 2015). Hence, a better bioproduction strain chassis could be obtained to be combined with the phenazine plasmid.

5.2.2 BES reactor operation

Another approach proposed to be implemented for the optimization of bioelectrochemical production is the cultivation of *P. putida* rhl-pca in an electro-bioreactor. Basically, this is better integration of the electrochemical setup with classical, highly monitored bioprocess technology. It has been reported by Rosa *et al.*, who developed an upgrade kit (a bioreactor lid equipped with electrochemical control) integrated with the commercial fermenter system, which enables full process monitoring. In the case study of *Shewanella oneidensis* MR-1, they proved that this system could be applied to control, monitor, and scale microbial bioelectrochemical production of acetate and lactate, with a much better resolution of the experimental data provided (Rosa et al., 2017). Another study of this research group conducted by Gimkiewicz *et al.* has applied this system to show that *Gluconobacter oxydans* is not suitable to be employed in microbial

electrochemical technologies, due to the absence of an immediate link between the microbial metabolism and electric current generation (Gimkiewicz et al., 2016).

Moreover, a case study of *Clostridium kluyveri* with the synthetic electron mediator added using the same system by Koch *et al.*, showed that this type of bioreactor was applied to reveal that *C. kluyveri* is not able to directly interact with electrodes (Koch et al., 2017). These case studies showed the prospect of this advanced bioreactor system to be applied for bioelectrochemical production of valuable compounds from a wide range of electroactive bacterium species. Especially in the *P. putida* rhl-pca strain, the ability to endogenously produce phenazines as the electron mediator will be an advantage.

Furthermore, the bioelectrochemical production of rhamnolipid using this type of reactor will be interesting to be investigated, since this system is equipped with an integrated monitored and controlled system for bioproduction (pH, dissolved oxygen, foam). Therefore, the experimental variables for rhamnolipid production can be more in-depth studies, such as aeration level, inoculation, and pH. Collaboration contract negotiations and translation of the technology to our laboratory is almost completed, and bioproduction with the new phenazine and rhamnolipid producing strain in these electro-bioreactors will be conducted soon.

5.2.3 Integrated redox and flux balance analysis

Based on the finding of this study, the optimization of the bioelectrochemical production using phenazine as the electron shuttle in a passively aerated BES required a comprehensive understanding of the cellular electrons redox balance within *P. putida*. Especially, the molecular function of phenazines as an electron shuttle to carry electrons to the anode under passively aerated BES and the connection to an energy conservation process needs to be elucidated. This comprehensive physiological study can be integrated with flux balance analysis (based on pathway stoichiometry and product formation rates) (Lai et al., 2016) to discover an effective and efficient metabolic engineering strategy for biocatalysis of *P. putida* in an oxygen-limited BES.

References

- Abdel-Mawgoud, A.M., Lepine, F., Deziel, E. 2014. A stereospecific pathway diverts beta-oxidation intermediates to the biosynthesis of rhamnolipid biosurfactants. *Chem Biol*, **21**(1), 156-64.
- Averesch, N.J.H., Kromer, J.O. 2018. Metabolic engineering of the shikimate pathway for production of aromatics and derived compounds - present and future strain construction strategies. *Front Bioeng Biotechnol*, **6**, 32.
- Bahia, F.M., de Almeida, G.C., de Andrade, L.P., Campos, C.G., Queiroz, L.R., da Silva, R.L.V., Abdelnur, P.V., Correa, J.R., Bettiga, M., Parachin, N.S. 2018. Rhamnolipids production from sucrose by engineered *Saccharomyces cerevisiae*. *Sci Rep*, **8**(1), 2905.
- Bajracharya, S., Sharma, M., Mohanakrishna, G., Dominguez Benneton, X., Strik, D.P.B.T.B., Sarma, P.M., Pant, D. 2016. An overview on emerging bioelectrochemical systems (BESs): technology for sustainable electricity, waste remediation, resource recovery, chemical production and beyond. *Renew. Energ.*, **98**, 153-170.
- Ballerstedt, H., Volkers, R.J., Mars, A.E., Hallsworth, J.E., dos Santos, V.A., Puchalka, J., van Duuren, J., Eggink, G., Timmis, K.N., de Bont, J.A., Wery, J. 2007. Genomotyping of *Pseudomonas putida* strains using *P. putida* KT2440-based high-density DNA microarrays: implications for transcriptomics studies. *Appl Microbiol Biotechnol*, **75**(5), 1133-42.
- Behrens, B., Engelen, J., Tiso, T., Blank, L.M., Hayen, H. 2016. Characterization of rhamnolipids by liquid chromatography/mass spectrometry after solid-phase extraction. *Anal Bioanal Chem*, **408**(10), 2505-2514.
- Belda, E., van Heck, R.G., Jose Lopez-Sanchez, M., Cruveiller, S., Barbe, V., Fraser, C., Klenk, H.P., Petersen, J., Morgat, A., Nikel, P.I., Vallenet, D., Rouy, Z., Sekowska, A., Martins Dos Santos, V.A., de Lorenzo, V., Danchin, A., Medigue, C. 2016. The revisited genome of *Pseudomonas putida* KT2440 enlightens its value as a robust metabolic chassis. *Environ Microbiol*, **18**(10), 3403-3424.
- Benson, D.A., Karsch-Mizrachi, I., Lipman, D.J., Ostell, J., Wheeler, D.L. 2005. GenBank. *Nucleic Acids Res.*, **33**, D34-D38.
- Berger, C., Rosenbaum, M.A. 2017. Spontaneous quorum sensing mutation modulates electroactivity of *Pseudomonas aeruginosa* PA14. *Bioelectrochemistry*, **117**, 1-8.
- Beuker, J., Steier, A., Wittgens, A., Rosenau, F., Henkel, M., Hausmann, R. 2016. Integrated foam fractionation for heterologous rhamnolipid production with recombinant *Pseudomonas putida* in a bioreactor. *AMB Express*, **6**(1), 11.
- Blank, L.M., Ionidis, G., Ebert, B.E., Buhler, B., Schmid, A. 2008. Metabolic response of *Pseudomonas putida* during redox biocatalysis in the presence of a second octanol phase. *FEBS Journal*, **275**(20), 5173-90.
- Blankenfeldt, W., Parsons, J.F. 2014. The structural biology of phenazine biosynthesis. *Curr. Opin. Struct. Biol.*, **29**, 26-33.
- Bosire, E.M., Blank, L.M., Rosenbaum, M.A. 2016. Strain- and substrate-dependent redox mediator and electricity production by *Pseudomonas aeruginosa*. *Appl. Environ. Microbiol.*, **82**(16), 5026-38.

- Bosire, E.M., Rosenbaum, M.A. 2017. Electrochemical potential influences phenazine production, electron transfer and consequently electric current generation by *Pseudomonas aeruginosa*. *Front Microbiol*, **8**, 892.
- Cabrera-Valladares, N., Richardson, A.P., Olvera, C., Trevino, L.G., Deziel, E., Lepine, F., Soberon-Chavez, G. 2006. Monorhamnolipids and 3-(3-hydroxyalkanoyloxy)alkanoic acids (HAAs) production using *Escherichia coli* as a heterologous host. *Appl Microbiol Biotechnol*, **73**(1), 187-94.
- Caiazza, N.C., Shanks, R.M., O'Toole, G.A. 2005. Rhamnolipids modulate swarming motility patterns of *Pseudomonas aeruginosa*. *J Bacteriol*, **187**(21), 7351-61.
- Calero, P., Nikel, P.I. 2019. Chasing bacterial chassis for metabolic engineering: a perspective review from classical to non-traditional microorganisms. *Microb Biotechnol*, **12**(1), 98-124.
- Cha, M., Lee, N., Kim, M., Kim, M., Lee, S. 2008. Heterologous production of *Pseudomonas aeruginosa* EMS1 biosurfactant in *Pseudomonas putida*. *Bioresource Technology*, **99**(7), 2192-2199.
- Choi, K.H., Kumar, A., Schweizer, H.P. 2006. A 10-min method for preparation of highly electrocompetent *Pseudomonas aeruginosa* cells: application for DNA fragment transfer between chromosomes and plasmid transformation. *J. Microbiol. Methods*, **64**(3), 391-7.
- Chong, H., Li, Q. 2017. Microbial production of rhamnolipids: opportunities, challenges and strategies. *Microb Cell Fact*, **16**(1), 137.
- Cock, P.J., Antao, T., Chang, J.T., Chapman, B.A., Cox, C.J., Dalke, A., Friedberg, I., Hamelryck, T., Kauff, F., Wilczynski, B., de Hoon, M.J. 2009. Biopython: freely available Python tools for computational molecular biology and bioinformatics. *Bioinformatics*, **25**(11), 1422-3.
- Cui, Q., Lv, H., Qi, Z., Jiang, B., Xiao, B., Liu, L., Ge, Y., Hu, X. 2016. Cross-regulation between the *phz1* and *phz2* operons maintain a balanced level of phenazine biosynthesis in *Pseudomonas aeruginosa* PAO1. *PLoS One*, **11**(1), e0144447.
- Das, T., Kutty, S.K., Tavallaie, R., Ibugo, A.I., Panchompoo, J., Sehar, S., Aldous, L., Yeung, A.W., Thomas, S.R., Kumar, N., Gooding, J.J., Manefield, M. 2015. Phenazine virulence factor binding to extracellular DNA is important for *Pseudomonas aeruginosa* biofilm formation. *Sci Rep*, **5**, 8398.
- del Solar, G.H., Puyet, A., Espinosa, M. 1987. Initiation signals for the conversion of single stranded to double stranded DNA forms in the streptococcal plasmid pLS1. *Nucleic acids research*, **15**(14), 5561-5580.
- Diaz De Rienzo, M.A., Banat, I.M., Dolman, B., Winterburn, J., Martin, P.J. 2015. Sophorolipid biosurfactants: possible uses as antibacterial and antibiofilm agent. *N Biotechnol*, **32**(6), 720-6.
- Díaz De Rienzo, M.A., Kamalanathan, I.D., Martin, P.J. 2016. Comparative study of the production of rhamnolipid biosurfactants by *B. thailandensis* E264 and *P. aeruginosa* ATCC 9027 using foam fractionation. *Process Biochemistry*, **51**(7), 820-827.
- Dietrich, L.E., Price-Whelan, A., Petersen, A., Whiteley, M., Newman, D.K. 2006. The phenazine pyocyanin is a terminal signalling factor in the quorum sensing network of *Pseudomonas aeruginosa*. *Mol Microbiol*, **61**(5), 1308-21.

- Dusane, D.H., Zinjarde, S.S., Venugopalan, V.P., McLean, R.J., Weber, M.M., Rahman, P.K. 2010. Quorum sensing: implications on rhamnolipid biosurfactant production. *Biotechnol Genet Eng Rev*, **27**, 159-84.
- Escapa, I.F., Garcia, J.L., Buhler, B., Blank, L.M., Prieto, M.A. 2012. The polyhydroxyalkanoate metabolism controls carbon and energy spillage in *Pseudomonas putida*. *Environ Microbiol*, **14**(4), 1049-63.
- Eschbach, M., Schreiber, K., Trunk, K., Buer, J., Jahn, D., Schobert, M. 2004. Long-term anaerobic survival of the opportunistic pathogen *Pseudomonas aeruginosa* via pyruvate fermentation. *J Bacteriol*, **186**(14), 4596-604.
- Faivre, V., Rosilio, V. 2010. Interest of glycolipids in drug delivery: from physicochemical properties to drug targeting. *Expert Opin Drug Deliv*, **7**(9), 1031-48.
- Fernandez, M., Conde, S., Duque, E., Ramos, J.L. 2013. In vivo gene expression of *Pseudomonas putida* KT2440 in the rhizosphere of different plants. *Microb Biotechnol*, **6**(3), 307-13.
- Geys, R., De Graeve, M., Lodens, S., Van Malderen, J., Lemmens, C., De Smet, M., Mincke, S., Van Bogaert, I., Stevens, C., De Maeseneire, S., Roelants, S., Soetaert, W. 2018. Increasing uniformity of biosurfactant production in *Starmerella bombicola* via the expression of chimeric cytochrome P450s. *Colloids and Interfaces*, **2**(4), 42.
- Gibson, D.G., Young, L., Chuang, R.Y., Venter, J.C., Hutchison, C.A., 3rd, Smith, H.O. 2009. Enzymatic assembly of DNA molecules up to several hundred kilobases. *Nat. Methods*, **6**(5), 343-5.
- Gimkiewicz, C., Hunger, S., Harnisch, F. 2016. Evaluating the feasibility of microbial electrosynthesis based on *Gluconobacter oxydans*. *ChemElectroChem*, **3**(9), 1337-1346.
- Gingold, H., Tehler, D., Christoffersen, N.R., Nielsen, M.M., Asmar, F., Kooistra, S.M., Christophersen, N.S., Christensen, L.L., Borre, M., Sorensen, K.D., Andersen, L.D., Andersen, C.L., Hulleman, E., Wurdinger, T., Ralfkiaer, E., Helin, K., Gronbaek, K., Orntoft, T., Waszak, S.M., Dahan, O., Pedersen, J.S., Lund, A.H., Pilpel, Y. 2014. A dual program for translation regulation in cellular proliferation and differentiation. *Cell*, **158**(6), 1281-1292.
- Glasser, N.R., Kern, S.E., Newman, D.K. 2014. Phenazine redox cycling enhances anaerobic survival in *Pseudomonas aeruginosa* by facilitating generation of ATP and a proton-motive force. *Mol Microbiol*, **92**(2), 399-412.
- Gong, Z., Peng, Y., Wang, Q. 2015. Rhamnolipid production, characterization and fermentation scale-up by *Pseudomonas aeruginosa* with plant oils. *Biotechnol Lett*, **37**(10), 2033-8.
- Gu, P., Yang, F., Su, T., Wang, Q., Liang, Q., Qi, Q. 2015. A rapid and reliable strategy for chromosomal integration of gene(s) with multiple copies. *Sci Rep*, **5**, 9684.
- Harnisch, F., Aulenta, F., Schröder, U. 2011. Microbial fuel cells and bioelectrochemical systems: industrial and environmental biotechnologies based on extracellular electron transfer. in: *Comprehensive Biotechnology 2nd ed.*, (Ed.) M. Moo-Young, Elsevier B.V. (6.49, pp. 643-659).
- Hartmans, S., Smits, J.P., van der Werf, M.J., Volkering, F., de Bont, J.A.M. 1989. Metabolism of styrene oxide and 2-phenylethanol in the styrene-degrading *Xanthobacter* strain 124X. *Appl. Environ. Microbiol.*, **55**(11), 2850-2855.

- Hewald, S., Linne, U., Scherer, M., Marahiel, M.A., Kamper, J., Bolker, M. 2006. Identification of a gene cluster for biosynthesis of mannosylerythritol lipids in the basidiomycetous fungus *Ustilago maydis*. *Appl Environ Microbiol*, **72**(8), 5469-77.
- Hirata, Y., Ryu, M., Oda, Y., Igarashi, K., Nagatsuka, A., Furuta, T., Sugiura, M. 2009. Novel characteristics of sophorolipids, yeast glycolipid biosurfactants, as biodegradable low-foaming surfactants. *J Biosci Bioeng*, **108**(2), 142-6.
- Hu, J., Gao, G., Xia, S. 2015. Development of a mediator-type bioelectrochemical sensor based on polypyrrole immobilized ferricyanide and microorganisms for biochemical oxygen demand fast detection. *Int. J. Electrochem. Sci.*, **10** 9695 - 9705.
- Joshi-Navare, K., Prabhune, A. 2013. A biosurfactant-sophorolipid acts in synergy with antibiotics to enhance their efficiency. *Biomed Res Int*, **2013**, 512495.
- Kastenholz, L. 2017. Characterization of *Pseudomonas putida* phenazines-rhamnolipid producing strain. in: *Institute of Applied Microbiology (iAMB)*, Vol. Bachelor Thesis, RWTH Aachen University. Aachen.
- Kern, S.E., Newman, D.K. 2014. Measurement of phenazines in bacterial cultures. *Methods Mol. Biol.*, **1149**, 303-10.
- Koch, C., Kuchenbuch, A., Kracke, F., Bernhardt, P.V., Kromer, J., Harnisch, F. 2017. Predicting and experimental evaluating bio-electrochemical synthesis - A case study with *Clostridium kluyveri*. *Bioelectrochemistry*, **118**, 114-122.
- Kruth, S. 2017. Construction of a stable rhamnolipid producing *Pseudomonas putida* using genome integration techniques. in: *Institute of Applied Microbiology (iAMB)*, Vol. Master Thesis, RWTH Aachen University. Aachen.
- Kulakovskaya, E., Kulakovskaya, T. 2014. Structure and occurrence of yeast extracellular glycolipids. 1-13.
- Küpper, B., Mause, A., Halka, L., Imhoff, A., Nowacki, C., Wichmann, R. 2013. Fermentative Produktion von Monorhamnolipiden im Pilotmaßstab - Herausforderungen der Maßstabsvergrößerung. *Chem. Ing. Tech.*, **85**(6), 834-840.
- Lai, B., Yu, S., Bernhardt, P.V., Rabaey, K., Virdis, B., Kromer, J.O. 2016. Anoxic metabolism and biochemical production in *Pseudomonas putida* F1 driven by a bioelectrochemical system. *Biotechnol. Biofuels*, **9**, 39-51.
- Lang, K., Zierow, J., Buehler, K., Schmid, A. 2014. Metabolic engineering of *Pseudomonas* sp. strain VLB120 as platform biocatalyst for the production of isobutyric acid and other secondary metabolites. *Microbial cell factories*, **13**, 2-2.
- Liu, J., Qiao, Y., Lu, Z.S., Song, H., Li, C.M. 2012. Enhance electron transfer and performance of microbial fuel cells by perforating the cell membrane. *Electrochemistry Communications*, **15**(1), 50-53.
- Loeschcke, A., Thies, S. 2015. *Pseudomonas putida*-a versatile host for the production of natural products. *Appl. Microbiol. Biotechnol.*, **99**(15), 6197-214.
- Logan, B.E., Hamelers, B., Rozendal, R., Schroder, U., Keller, J., Freguia, S., Aelterman, P., Verstraete, W., Rabaey, K. 2006. Microbial fuel cells: methodology and technology. *Environ Sci Technol*, **40**(17), 5181-92.
- Lopez, P.H.H., Schnaar, R.L. 2006. Determination of glycolipid-protein interaction specificity. *Methods Enzymol*, **417**, 205-220.

- Lourith, N., Kanlayavattanakul, M. 2009. Natural surfactants used in cosmetics: glycolipids. *Int J Cosmet Sci*, **31**(4), 255-61.
- Martinez-Garcia, E., Nikel, P.I., Aparicio, T., de Lorenzo, V. 2014. *Pseudomonas* 2.0: genetic upgrading of *P. putida* KT2440 as an enhanced host for heterologous gene expression. *Microb Cell Fact*, **13**, 159.
- Mavrodi, D.V., Bonsall, R.F., Delaney, S.M., Soule, M.J., Phillips, G., Thomashow, L.S. 2001. Functional analysis of genes for biosynthesis of pyocyanin and phenazine-1-carboxamide from *Pseudomonas aeruginosa* PAO1. *J. Bacteriol.*, **183**(21), 6454-65.
- Mavrodi, D.V., Peever, T.L., Mavrodi, O.V., Parejko, J.A., Raaijmakers, J.M., Lemanceau, P., Mazurier, S., Heide, L., Blankenfeldt, W., Weller, D.M., Thomashow, L.S. 2010. Diversity and evolution of the phenazine biosynthesis pathway. *Appl Environ Microbiol*, **76**(3), 866-79.
- Mentel, M., Ahuja, E.G., Mavrodi, D.V., Breinbauer, R., Thomashow, L.S., Blankenfeldt, W. 2009. Of two make one: the biosynthesis of phenazines. *ChemBioChem*, **10**(14), 2295-304.
- Morita, T., Koike, H., Hagiwara, H., Ito, E., Machida, M., Sato, S., Habe, H., Kitamoto, D. 2014. Genome and transcriptome analysis of the basidiomycetous yeast *Pseudozyma antarctica* producing extracellular glycolipids, mannosylerythritol lipids. *PLoS One*, **9**(2), e86490.
- Muller, M.M., Hormann, B., Syltatk, C., Hausmann, R. 2010. *Pseudomonas aeruginosa* PAO1 as a model for rhamnolipid production in bioreactor systems. *Appl Microbiol Biotechnol*, **87**(1), 167-74.
- Nelson, K.E., Weinell, C., Paulsen, I.T., Dodson, R.J., Hilbert, H., Martins dos Santos, V.A., Fouts, D.E., Gill, S.R., Pop, M., Holmes, M., Brinkac, L., Beanan, M., DeBoy, R.T., Daugherty, S., Kolonay, J., Madupu, R., Nelson, W., White, O., Peterson, J., Khouri, H., Hance, I., Chris Lee, P., Holtzapple, E., Scanlan, D., Tran, K., Moazzez, A., Utterback, T., Rizzo, M., Lee, K., Kosack, D., Moestl, D., Wedler, H., Lauber, J., Stjepandic, D., Hoheisel, J., Straetz, M., Heim, S., Kiewitz, C., Eisen, J.A., Timmis, K.N., Dusterhoft, A., Tumbler, B., Fraser, C.M. 2002. Complete genome sequence and comparative analysis of the metabolically versatile *Pseudomonas putida* KT2440. *Environ Microbiol*, **4**(12), 799-808.
- Nickzad, A., Lepine, F., Deziel, E. 2015. Quorum sensing controls swarming motility of *Burkholderia glumae* through regulation of rhamnolipids. *PLoS One*, **10**(6), e0128509.
- Nikel, P.I., Chavarria, M., Fuhrer, T., Sauer, U., de Lorenzo, V. 2015. *Pseudomonas putida* KT2440 strain metabolizes glucose through a cycle formed by enzymes of the Entner-Doudoroff, Embden-Meyerhof-Parnas, and pentose phosphate pathways. *J. Biol. Chem.*, **290**(43), 25920-32.
- Nikel, P.I., de Lorenzo, V. 2018. *Pseudomonas putida* as a functional chassis for industrial biocatalysis: From native biochemistry to trans-metabolism. *Metab Eng*, **50**, 142-155.
- Nikel, P.I., Martinez-Garcia, E., de Lorenzo, V. 2014. Biotechnological domestication of pseudomonads using synthetic biology. *Nat Rev Microbiol*, **12**(5), 368-79.
- Ochsner, U.A., Fiechter, A., Reiser, J. 1994. Isolation, characterization, and expression in *Escherichia coli* of the *Pseudomonas aeruginosa* *rhlAB* genes encoding a rhamnosyltransferase involved in rhamnolipid biosurfactant synthesis. *Journal of Biological Chemistry*, **269**(31), 19787-95.

- Pant, D., Singh, A., Van Bogaert, G., Irving Olsen, S., Singh Nigam, P., Diels, L., Vanbroekhoven, K. 2012. Bioelectrochemical systems (BES) for sustainable energy production and product recovery from organic wastes and industrial wastewaters. *RSC Adv.*, **2**(4), 1248-1263.
- Parry, A.J., Parry, N. J., Peilow, C., and Stevenson, S., P. 2013. Combinations of rhamnolipids and enzymes for improved cleaning. *Patent no. EP 2596087 A1*.
- Parsons, J.F., Greenhagen, B.T., Shi, K., Calabrese, K., Robinson, H., Ladner, J.E. 2007. Structural and functional analysis of the pyocyanin biosynthetic protein PhzM from *Pseudomonas aeruginosa*. *Biochemistry*, **46**(7), 1821-8.
- Pechmann, S., Frydman, J. 2013. Evolutionary conservation of codon optimality reveals hidden signatures of cotranslational folding. *Nat. Struct. Mol. Biol.*, **20**(2), 237-43.
- Pettersen, E.F., Goddard, T.D., Huang, C.C., Couch, G.S., Greenblatt, D.M., Meng, E.C., Ferrin, T.E. 2004. UCSF Chimera--a visualization system for exploratory research and analysis. *J. Comput. Chem.*, **25**(13), 1605-12.
- Popov, A.L., Kim, J.R., Dinsdale, R.M., Esteves, S.R., Guwy, A.J., Premier, G.C. 2012. The effect of physico-chemically immobilized methylene blue and neutral red on the anode of microbial fuel cell. *Biotechnol. Bioproc. E.*, **17**(2), 361-370.
- Quax, T.E., Claassens, N.J., Soll, D., van der Oost, J. 2015. Codon bias as a means to fine-tune gene expression. *Mol. Cell* **59**(2), 149-61.
- Rahimnejad, M., Najafpour, G.D., Ghoreyshi, A.A., Shakeri, M., Zare, H. 2011. Methylene blue as electron promoters in microbial fuel cell. *Int. J. Hydrogen Energ.*, **36**(20), 13335-13341.
- Rau, U., Nguyen, L.A., Roeper, H., Koch, H., Lang, S. 2005. Downstream processing of mannosylerythritol lipids produced by *Pseudozyma aphidis*. *Eur. J. Lipid Sci. Technol.*, **107**(6), 373-380.
- Recinos, D.A., Sekedat, M.D., Hernandez, A., Cohen, T.S., Sakhtah, H., Prince, A.S., Price-Whelan, A., Dietrich, L.E. 2012. Redundant phenazine operons in *Pseudomonas aeruginosa* exhibit environment-dependent expression and differential roles in pathogenicity. *Proc. Natl. Acad. Sci. USA*, **109**(47), 19420-5.
- Reis, R.S., Pereira, A.G., Neves, B.C., Freire, D.M. 2011. Gene regulation of rhamnolipid production in *Pseudomonas aeruginosa*--a review. *Bioresour Technol*, **102**(11), 6377-84.
- Rendell, N.B., Taylor, G.W., Somerville, M., Todd, H., Wilson, R., Cole, P.J. 1990. Characterisation of *Pseudomonas* rhamnolipids. *Biochim Biophys Acta*, **1045**(2), 189-93.
- Rikalovic, M.G., Avramovic, N.S., Karadzic, I.M. 2017. Structure-function relationships of rhamnolipid and exopolysaccharide biosurfactants of *Pseudomonas aeruginosa* as therapeutic targets in cystic fibrosis lung infections.
- Rosa, L.F.M., Hunger, S., Gimkiewicz, C., Zehnsdorf, A., Harnisch, F. 2017. Paving the way for bioelectrotechnology: Integrating electrochemistry into bioreactors. *Eng. Life Sci.*, **17**(1), 77-85.
- Rosenbaum, M.A., Henrich, A.W. 2014. Engineering microbial electrocatalysis for chemical and fuel production. *Curr. Opin. Biotechnol.*, **29**, 93-8.
- RStudio_Team. 2015. RStudio: Integrated development for R. RStudio, Inc., <http://www.rstudio.com/>.
- Saika, A., Koike, H., Fukuoka, T., Yamamoto, S., Kishimoto, T., Morita, T. 2016. A gene cluster for biosynthesis of mannosylerythritol lipids consisted of 4-O-beta-D-mannopyranosyl-

- (2R,3S)-erythritol as the sugar moiety in a Basidiomycetous yeast *Pseudozyma tsukubaensis*. *PLoS One*, **11**(6), e0157858.
- Santos, D.K., Rufino, R.D., Luna, J.M., Santos, V.A., Sarubbo, L.A. 2016. Biosurfactants: multifunctional biomolecules of the 21st century. *Int J Mol Sci*, **17**(3), 401.
- Schmitz, S., Nies, S., Wierckx, N., Blank, L.M., Rosenbaum, M.A. 2015. Engineering mediator-based electroactivity in the obligate aerobic bacterium *Pseudomonas putida* KT2440. *Front. Microbiol.*, **6**(284), 1-13.
- Schmitz, S., Rosenbaum, M.A. 2018. Boosting mediated electron transfer in bioelectrochemical systems with tailored defined microbial cocultures. *Biotechnol Bioeng*, **115**(9), 2183-2193.
- Sekhon Randhawa, K.K., Rahman, P.K. 2014. Rhamnolipid biosurfactants-past, present, and future scenario of global market. *Front Microbiol*, **5**, 454.
- Sharp, P.M., Bailes, E., Grocock, R.J., Peden, J.F., Sockett, R.E. 2005. Variation in the strength of selected codon usage bias among bacteria. *Nucleic Acids Res.*, **33**(4), 1141-53.
- Sharp, P.M., Li, W.H. 1987. The Codon Adaptation Index--a measure of directional synonymous codon usage bias, and its potential applications. *Nucleic Acids Res.*, **15**(3), 1281-95.
- Shen, H.B., Yong, X.Y., Chen, Y.L., Liao, Z.H., Si, R.W., Zhou, J., Wang, S.Y., Yong, Y.C., OuYang, P.K., Zheng, T. 2014. Enhanced bioelectricity generation by improving pyocyanin production and membrane permeability through sophorolipid addition in *Pseudomonas aeruginosa*-inoculated microbial fuel cells. *Bioresour Technol*, **167**, 490-4.
- Siebenhaller, S., Grüniger, J., Sylđatk, C. 2018. Enzymatic synthesis of glycolipid surfactants. 293-313.
- Sievers, F., Higgins, D.G. 2018. Clustal Omega for making accurate alignments of many protein sequences. *Protein Sci.*, **27**(1), 135-145.
- Sievers, F., Wilm, A., Dineen, D., Gibson, T.J., Karplus, K., Li, W., Lopez, R., McWilliam, H., Remmert, M., Soding, J., Thompson, J.D., Higgins, D.G. 2011. Fast, scalable generation of high-quality protein multiple sequence alignments using Clustal Omega. *Mol. Syst. Biol.*, **7**, 539.
- Sivapathasekaran, C., Ramkrishna, S. 2017. Origin, properties, production and purification of microbial surfactants as molecules with immense commercial potential. *Tenside Surf. Det.*, **54**(2), 92-107.
- Sleutels, T.H., Darius, L., Hamelers, H.V., Buisman, C.J. 2011. Effect of operational parameters on Coulombic efficiency in bioelectrochemical systems. *Bioresour. Technol.*, **102**(24), 11172-6.
- Soberon-Chavez, G., Lepine, F., Deziel, E. 2005. Production of rhamnolipids by *Pseudomonas aeruginosa*. *Appl Microbiol Biotechnol*, **68**(6), 718-25.
- Solaiman, D.K., Liu, Y., Moreau, R.A., Zerkowski, J.A. 2014. Cloning, characterization, and heterologous expression of a novel glucosyltransferase gene from sophorolipid-producing *Candida bombicola*. *Gene*, **540**(1), 46-53.
- Spraggon, G., Kim, C., Nguyen-Huu, X., Yee, M.C., Yanofsky, C., Mills, S.E. 2001. The structures of anthranilate synthase of *Serratia marcescens* crystallized in the presence of (i) its substrates, chorismate and glutamine, and a product, glutamate, and (ii) its end-product inhibitor, L-tryptophan. *Proc. Natl. Acad. Sci. USA*, **98**(11), 6021-6.

- Steinbusch, K.J.J., Hamelers, H.V.M., Schaap, J.D., Kampman, C., Buisman, C.J.N. 2010. Bioelectrochemical ethanol production through mediated acetate reduction by mixed cultures. *Environ. Sci. Technol.*, **44**(1), 513-517.
- Sudarsan, S., Dethlefsen, S., Blank, L.M., Siemann-Herzberg, M., Schmid, A. 2014. The functional structure of central carbon metabolism in *Pseudomonas putida* KT2440. *Appl Environ Microbiol*, **80**(17), 5292-303.
- Sun, W., Alexander, T., Man, Z., Xiao, F., Cui, F., Qi, X. 2018. Enhancing 2-ketogluconate production of *Pseudomonas plecoglossicida* JUIM01 by maintaining the carbon catabolite repression of 2-ketogluconate metabolism. *Molecules*, **23**(10).
- Tashiro, Y., Desai, S.H., Atsumi, S. 2015. Two-dimensional isobutyl acetate production pathways to improve carbon yield. *Nat Commun*, **6**, 7488.
- Tiso, T., Sabelhaus, P., Behrens, B., Wittgens, A., Rosenau, F., Hayen, H., Blank, L.M. 2016. Creating metabolic demand as an engineering strategy in *Pseudomonas putida* - Rhamnolipid synthesis as an example. *Metab Eng Commun*, **3**, 234-244.
- Tiso, T., Zauter, R., Tulke, H., Leuchtle, B., Li, W.J., Behrens, B., Wittgens, A., Rosenau, F., Hayen, H., Blank, L.M. 2017. Designer rhamnolipids by reduction of congener diversity: production and characterization. *Microb Cell Fact*, **16**(1), 225.
- Vandenbergh, L.P.S., Karp, S.G., de Oliveira, P.Z., de Carvalho, J.C., Rodrigues, C., Soccol, C.R. 2018. Solid-state fermentation for the production of organic acids. in: *Current Developments in Biotechnology and Bioengineering*, Vol. Chapter 18, Elsevier, pp. 415-434.
- Venkataraman, A., Rosenbaum, M.A., Perkins, S.D., Werner, J.J., Angenent, L.T. 2011. Metabolite-based mutualism between *Pseudomonas aeruginosa* PA14 and *Enterobacter aerogenes* enhances current generation in bioelectrochemical systems. *Energy Environ. Sci.*, **4**(11), 4550.
- Wackett, L.P. 2003. *Pseudomonas putida*-a versatile biocatalyst. *Nat Biotechnol*, **21**(2), 136-8.
- Wang, Y., Newman, D.K. 2008. Redox reactions of phenazine antibiotics with ferric (hydr)oxides and molecular oxygen. *Environmental science & technology*, **42**(7), 2380-2386.
- Watanabe, K., Manefield, M., Lee, M., Kouzuma, A. 2009. Electron shuttles in biotechnology. *Curr Opin Biotechnol*, **20**(6), 633-41.
- Webb, B., Sali, A. 2014. Comparative protein structure modeling using MODELLER. *Curr. Protoc. Bioinformatics*, **47**, 5.6.1-32.
- Wen, Q., Kong, F., Ma, F., Ren, Y., Pan, Z. 2011. Improved performance of air-cathode microbial fuel cell through additional Tween 80. *Journal of Power Sources*, **196**(3), 899-904.
- Wen, Q., Kong, F., Ren, Y., Cao, D., Wang, G., Zheng, H. 2010. Improved performance of microbial fuel cell through addition of rhamnolipid. *Electrochemistry Communications*, **12**(12), 1710-1713.
- Wilhelm, S., Gdynia, A., Tielen, P., Rosenau, F., Jaeger, K.E. 2007. The autotransporter esterase EstA of *Pseudomonas aeruginosa* is required for rhamnolipid production, cell motility, and biofilm formation. *J Bacteriol*, **189**(18), 6695-703.
- Wittgens, A., Kovacic, F., Muller, M.M., Gerlitzki, M., Santiago-Schubel, B., Hofmann, D., Tiso, T., Blank, L.M., Henkel, M., Hausmann, R., Syltatk, C., Wilhelm, S., Rosenau, F. 2017. Novel insights into biosynthesis and uptake of rhamnolipids and their precursors. *Appl Microbiol Biotechnol*, **101**(7), 2865-2878.

- Wittgens, A., Santiago-Schuebel, B., Henkel, M., Tiso, T., Blank, L.M., Hausmann, R., Hofmann, D., Wilhelm, S., Jaeger, K.E., Rosenau, F. 2018. Heterologous production of long-chain rhamnolipids from *Burkholderia glumae* in *Pseudomonas putida*-a step forward to tailor-made rhamnolipids. *Appl Microbiol Biotechnol*, **102**(3), 1229-1239.
- Wittgens, A., Tiso, T., Arndt, T.T., Wenk, P., Hemmerich, J., Muller, C., Wichmann, R., Kupper, B., Zwick, M., Wilhelm, S., Hausmann, R., Syldatk, C., Rosenau, F., Blank, L.M. 2011. Growth independent rhamnolipid production from glucose using the non-pathogenic *Pseudomonas putida* KT2440. *Microb Cell Fact*, **10**, 80.

Appendix

A.1 Supplementary information Chapter 3.1

A Constructed Plasmids expressing phenazine genes used in Chapter 3.1

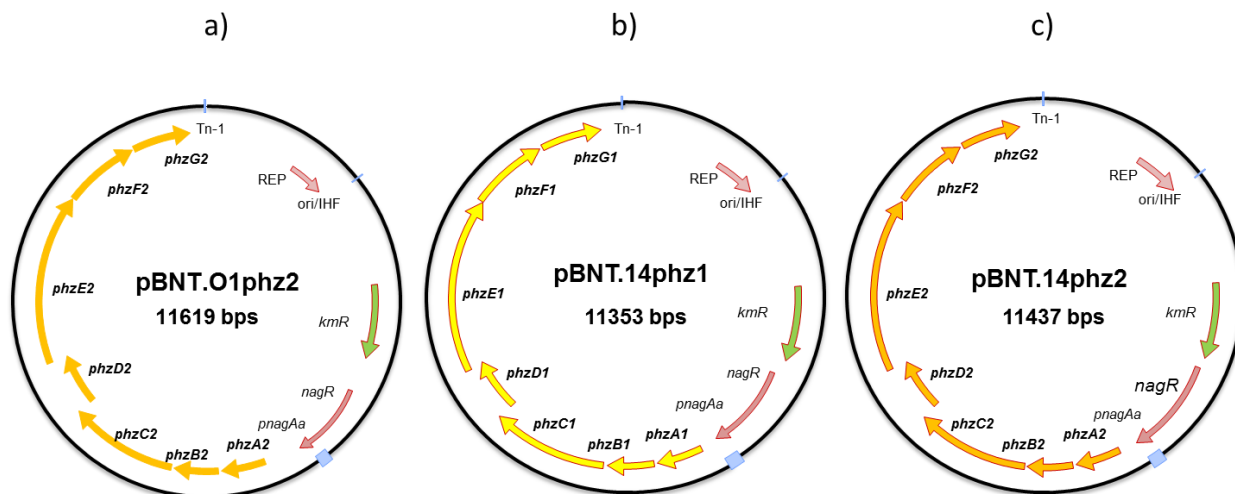


Figure S1: Vectors expressing phenazine genes used in chapter 3.1; (a) pBNT.O1phz2, expressing *phzA-G* operon 2 from *P. aeruginosa* PAO1 (PA1899-PA1905); (b) pBNT.14phz1, expressing *phzA-G* operon 1 from *P. aeruginosa* PA14 (PA14_09410-PA14_09480); (c) pBNT.14phz2, expressing *phzA-G* operon 2 from *P. aeruginosa* PA14 (PA14_39880-PA14_39970). The schemes represent all of the important elements, including the phenazine genes (*phzA-G*), the Kanamycin resistance cassette (*kmR*), the terminator (Tn-1), the origin of replication (*ori/IHF* for *Pseudomonas*), and the salicylate-induced promoter (*pnagAa/nagR*).

B *In silico* phenazine gene origin analysis

Data S1 - Protein alignments:

According to Clustal documentation (<http://www.clustal.org/omega/>), the meaning of the symbols in the output is the following (simplified):

- Asterisk: Conserved position
- Colon: Strongly similar properties (only for amino acids)
- Period: Weakly similar properties (only for amino acids)

The following UNIX command has been used with different inputs to perform all the alignments:

```
clustalo -i input_sequences.fasta -o output_alignment --outfmt clu  
--resno --force --guidetree-out output_tree
```


Alignment for PhzA:

CLUSTAL O(1.2.4) multiple sequence alignment

```
PAO1_1  MNGQRYRETPLDIERLRRNRATVERYMAMKGAERLQRHSLFVEDGCAGNWTTESGEPLV 60
PAO1_2  MREYQRLKGFDTNLELRRNRATVEHYMRMKAERLQRHSLFVEDGCAGNWTTESGEPLV 60
PA14_1  MNGQRYRETPLDIERLRRNRATVERYMAMKGAERLQRHSLFVEDGCAGNWTTESGEPLV 60
PA14_2  MREYQRLKGFDTNLELRRNRATVEHYMRMKAERLQRHSLFVEDGCAGNWTTESGEPLV 60
* : : * * * * *
PAO1_1  FRGHESLRLAEWLERCFPDWEWHNVRIFETEDPNHFWVECDGRGKALVPGYPQGYCENH 120
PAO1_2  FRGHESLRLAEWLERCFPDWEWHNVRIFETEDPNHFWVECDGRGKALVPGYPQGYCENH 120
PA14_1  FRGHESLRLAEWLERCFPDWEWRNVRIFETEDPNHFWVECDGRGKALVPGYPQGYCENH 120
PA14_2  FRGHESLRLAEWLERCFPDWEWHNVRIFETEDPNHLWVECDGRGKALVPGYPQGYCENH 120
* * * * *
PAO1_1  YHSFELENGRIKRNREFMNPQKLRALGIAPVQIKRDGIPT 162
PAO1_2  YHSFELENGRIKRNREFMNPQKLRALGIAPVQIKRDGIPT 162
PA14_1  YHSFELENGRIKRNREFMNPQKLRALGIAPVQIKRDGIPT 162
PA14_2  YHSFELENGRIKRNREFMNPQKLRALGIAPVQIKRDGIPT 162
* * * * *
```

Alignment for PhzB:

CLUSTAL O(1.2.4) multiple sequence alignment

```
PAO1_1  MPDTTNPIGFTDANELREKNRATVEKYMNTKGQDRLRRHELVEEDGCGGLWTTDTGSPIV 60
PAO1_2  MLDNAIPQGFEDAVELRRKNRET VVKYMNTKGQDRLRRHELVEEDGCGGLWTTDTGSPIV 60
PA14_1  MPDTTNPIGFTDANELREKNRATVEKYMNTKGQDRLRRHELVEEDGCGGLWTTDTGSPIV 60
PA14_2  MLDNAIPQGFEDAVELRRKNRET VVKYMNTKGQDRLRRHELVEEDGCGGLWTTDTGSPIV 60
* : * * * * *
PAO1_1  IRGDKLAEHAVWSLKCFPDWEWYNINIFGTDDPNHFWVECDGHGKILFPGYPEGYENH 120
PAO1_2  IRGDKLAEHAVWSLKCFPDWEWYNIKFETDDPNHFWVECDGHGKILFPGYPEGYENH 120
PA14_1  IRGDKLAEHAVWSLKCFPDWEWYNINIFGTDDPNHFWVECDGHGKILFPGYPEGYENH 120
PA14_2  IRGDKLAEHAVWSLKCFPDWEWYNIKFETDDPNHFWVECDGHGKILFPGYPEGYENH 120
* * * * *
PAO1_1  FLHSFELEDGKIKRNREFMNVFQQLRALSIPVPQIKREGIPT 162
PAO1_2  FLHSFELDDGKIKRNREFMNVFQQLRALSIPVPQIKREGIPT 162
PA14_1  FLHSFELEDGKIKRNREFMNVFQQLRALSIPVPEIKREGIPT 162
PA14_2  FLHSFELDDGKIKRNREFMNVFQQLRALSIPVPQIKREGIPT 162
* * * * *
```

Alignment for PhzC:

CLUSTAL O(1.2.4) multiple sequence alignment

```
PAO1_1  MDDLQRVRRCEALQQPEWGDPSRLRDVQAYLRGSPALIRAGDILALRATLARVARGEAL 60
PAO1_2  MDDLQRVRRCEALQQPEWGDPSRLRDVQAYLRGSPALIRAGDILALRATLARVARGEAL 60
PA14_1  MDDLQRVRRCEALQQPEWGDPSRLRDVQAYLRGSPALIRAGDILALRATLARVARGEAL 60
PA14_2  MDDLQRVRRCEALQQPEWGDPSRLRDVQAYLRGSPALIRAGDILALRATLARVARGEAL 60
* * * * *
```

PAO1_1	VVQC	GDAEDMDDHHAENVARKAAVLELLAGALRLAGRRPVIRVGRIAGQYAKPRSKPHE	120
PAO1_2	VVQC	GDAEDMDDHHAENVARKAAVLELLAGALRLAGRRPVIRVGRIAGQYAKPRSKPHE	120
PA14_1	VVQC	GDAEDMDDHHAENVARKAAVLELLAGALRLAGRRPVIRVGRIAGQYAKPRSKPHE	120
PA14_2	VVQC	GDAEDMDDHHAENVARKAAVLELLAGALRLAGRRPVIRVGRIAGQYAKPRSKPHE	120

PAO1_1	QVGE	QTLPVYRGDMVNGREAHAEQRRADPQRILKGAAARNIMRHLGWDAASGQEANASP	180
PAO1_2	QVGE	QTLPVYRGDMVNGREAHAEQRRADPQRILKGAAARNIMRHLGWDAASGQEANASP	180
PA14_1	QVGE	QTLPVYRGDMVNGREAHAEQRRADPQRILKGAAARNIMRHLGWDAASGQEANASP	180
PA14_2	QVGE	QTLPVYRGDMVNGREAHAEQRRADPQRILKGAAARNIMRHLGWDAASGQEANASP	180

PAO1_1	VWTS	HEMLLLDYELSMLREDEQRRVYLGSTHWPWIGERTRQVDGAHVALLAEVLNPVACK	240
PAO1_2	VWTS	HEMLLLDYELSMLREDEQRRVYLGSTHWPWIGERTRQVDGAHVALLAEVLNPVACK	240
PA14_1	VWTS	HEMLLLDYELSMLREDEQRRVYLGSTHWPWIGERTRQVDGAHVALLAEVLNPVACK	240
PA14_2	VWTS	HEMLLLDYELSMLREDEQRRVYLGSTHWPWIGERTRQVDGAHVALLAEVLNPVACK	240

PAO1_1	VGPE	IGRDQLLALCERLDPREPGRLTIARMGAQKVGGERLPLVEAVRAAGHPVIWLS	300
PAO1_2	VGPE	IGRDQLLALCERLDPREPGRLTIARMGAQKVGGERLPLVEAVRAAGHPVIWLS	300
PA14_1	VGPE	IGRDQLLALCERLDPREPGRLTIARMGAQKVGGERLPLVEAVRAAGHPVIWLS	300
PA14_2	VGPE	IGRDQLLALCERLDPREPGRLTIARMGAQKVGGERLPLVEAVRAAGHPVIWLS	300

PAO1_1	PMHG	NTIVAPCGNKTRLVRSIAEEVAAFRLAVSGSGGVAAGLHLETPDDVTECVADSSG	360
PAO1_2	PMHG	NTIVAPCGNKTRLVRSIAEEVAAFRLAVSGSGGVAAGLHLETPDDVTECVADSSG	360
PA14_1	PMHG	NTIVAPCGNKTRLVRSIAEEVAAFRLAVSGSGGVAAGLHLETPDDVTECVADSSG	360
PA14_2	PMHG	NTIVAPCGNKTRLVRSIAEEVAAFRLAVSGSGGVAAGLHLETPDDVTECVADSSG	360

PAO1_1	LHQV	SRHYTSLCDPRLNPWQALSAVMAWSGAEIAPSATFPLETVA	405
PAO1_2	LHQV	SRHYTSLCDPRLNPWQALSAVMAWSGAEIAPSATFPLETVA	405
PA14_1	LHQV	GRHYTSLCDPRLNPWQALSAVMAWAGAEATPSATFPLETVA	405
PA14_2	LHQV	SRHYTSLCDPRLNPWQALSAVMAWAGAEIAPSATFPLETVA	405
****.*****.*****.*****			

Alignment for PhzD:

CLUSTAL O(1.2.4) multiple sequence alignment

PAO1_1	MSGI	PEITAYPLPTAQQLPANLARWSLEPRRAVLLVHDMQRYFLRPLPESLRAGLVANAA	60
PAO1_2	MSGI	PEITAYPLPTAQQLPANLARWSLEPRRAVLLVHDMQRYFLRPLPESLRAGLVANAA	60
PA14_1	MSGI	PEITAYPLPTAQQLPANLARWSLEPRRAVLLVHDMQRYFLRPLPESLRAGLVANAA	60
PA14_2	MSGI	PEITAYPLPTAQQLPANLARWSLKPRAVLLVHDMQRYFLRPLPESLRAGLVANAA	60

PAO1_1	RLRR	WCVEQGVQIAYTAQPGSMTEEQRLLKDFWGPGRASPADREVVEELAPGPDDWLL	120
PAO1_2	RLRR	WCVEQGVQIAYTAQPGSMTEEQRLLKDFWGPGRASPADREVVEELAPGPDDWLL	120
PA14_1	RLRR	WCVEQGVQIAYTAQPGSMTEEQRLLKDFWGPGRASPADREVVEELAPGPDDWLL	120
PA14_2	RLRR	WCVEQGVQIAYTAQPGSMTEEQRLLKDFWGPGRASPADREVVEELAPGPDDWLL	120

PAO1_1	TKWR	YSAFFHSDLLQRMRAAGRDQLVLCGVYAHVGVLISTVDAYSNDIQPFLVADAIADF	180
PAO1_2	TKWR	YSAFFHSDLLQRMRAAGRDQLVLCGVYAHVGVLISTVDAYSNDIQPFLVADAIADF	180
PA14_1	TKWR	YSAFFHSDLLQRMRAAGRDQLVLCGVYAHVGVLISTVDAYSNDIQPFLVADAIADF	180
PA14_2	TKWR	YSAFFHSDLLQRMRAAGRDQLVLCGVYAHVGVLISTVDAYSNDIQPFLVADAIADF	180

PAO1_1 SEAHHRMALEYAASRCAMVVTTDEVLE 207
 PAO1_2 SEAHHRMALEYAASRCAMVVTTDEVLE 207
 PA14_1 SEAHHRMALEYAASRCAMVVTTDEVLE 207
 PA14_2 SEAHHRMALEYAASRCAMVVTTDEVLE 207

Alignment for PhzE:

CLUSTAL O(1.2.4) multiple sequence alignment

PAO1_1 MNALPTSLQRLLEPAPFALLYRPESNGPGLLDVIRGEALELHGLADLPLDEPGPLPR 60
 PAO1_2 MNALPTSLQRLLEPAPFALLYRPESNGPGLLDVIRGEALELHGLADLPLDEPGPLPR 60
 PA14_1 MNALPTSLQRLLEPAPFALLYRPESNGPGLLDVIRGETLELHGLADLPLDEPGPLPR 60
 PA14_2 MNALPTSLQRLLEPAPFALLYRPESNGPGLLDVIRGETLELHGLADLPLDEPGPLPR 60

PAO1_1 HDLLALIPYRQIAERGFEALDDGTPLLALKVLEQELPLEQALALLPNQALELSEEGFDL 120
 PAO1_2 HDLLALIPYRQIAERGFEALDDGTPLLALKVLEQELPLEQALALLPNQALELSEEGFDL 120
 PA14_1 HDLLALIPYRQIAERGFEALDDGTPLLALKVLEQELPLEQALALLPNQALELSEEFDL 120
 PA14_2 HDLLALIPYRQIAERGFEALDDGTPLLALKVLEQELPLEQALALLPNQALELSEEFDL 120

PAO1_1 DDEAYAEVVGRVIADEIGRGEANFVIKRRFQARIDGYATASALSFFRQLLREKGAYWT 180
 PAO1_2 DDEAYAEVVGRVIADEIGRGEANFVIKRRFQARIDGYATASALSFFRQLLREKGAYWT 180
 PA14_1 DDEAYAEVVGRVIADEIGRGEANFVIKRRFQARIDGYATASALSFFRQLLREKGAYWT 180
 PA14_2 DDEAYAEVVGRVIADEIGRGEANFVIKRRFQARIDGYATASALSFFRQLLREKGAYWT 180

PAO1_1 FIVHTGERTLVGASPERHISVRDGLAVMNPISGTYRYPAGPNLAEVMEFLDNRKEADEL 240
 PAO1_2 FIVHTGERTLVGASPERHISVRDGLAVMNPISGTYRYPAGPNLAEVMEFLDNRKEADEL 240
 PA14_1 FIVHTGERTLVGASPERHISVRDGLAVMNPISGTYRYPAGPNLAEVMEFLDNRKEADEL 240
 PA14_2 FIVHTGERTLVGASPERHISVRDGLAVMNPISGTYRYPAGPNLAEVMEFFDNRKEADEL 240

PAO1_1 YMVVDEELKMARICEDGGRVLGPYLKEMAHLAHEFYFIEGQTSRDVREVLRETLFAPTV 300
 PAO1_2 YMVVDEELKMARICEDGGRVLGPYLKEMAHLAHEFYFIEGQTSRDVREVLRETLFAPTV 300
 PA14_1 YMVVDEELKMARICEDGGRVLGPYLKEMAHLAHEFYFIEGQTSRDVREVLRETLFAPTV 300
 PA14_2 YMVVDEELKMARICEDGGRVLGPYIKEMAHLAHEFYFIEGQTSRDVREVLRETLFAPTV 300

PAO1_1 TGSPLESACRVIRRYEPQGRGYSGVAALIGGDGQGGRGLDSAILIRTAIEIGDGRRLRIG 360
 PAO1_2 TGSPLESACRVIRRYEPQGRGYSGVAALIGGDGQGGRGLDSAILIRTAIEIGDGRRLRIG 360
 PA14_1 TGSPLESACRVIRRYEPQGRGYSGVAALIGGDGQGGRGLDSAILIRTAIEIESDGRRLRIG 360
 PA14_2 TGSPLESACRVIRRYEPQGRGYSGVAALIGGDGQGGRGLDSAILIRTAIEIESDGRRLRIG 360

PAO1_1 VGSTIVRHSDDLGEAAESRAKASGLIAALKSQAPQRLGSHPHVVAALASRNAPIADFWLR 420
 PAO1_2 VGSTIVRHSDDLGEAAESRAKASGLIAALKSQAPQRLGSHPHVVAALASRNAPIADFWLR 420
 PA14_1 VGSTIVRHSDDLGEAAESRAKASGLIAALKSQAPQRLGSHPHVVAALASRNAPIADFWLR 420
 PA14_2 VGSTIVRHSDDLGEAAESRAKASGLIAALKSQAPQRLGSHPHVVAALASRNAPIADFWLR 420

PAO1_1 GASERQQLQADLSGREVLIVDAEDFTFSMIKQLKSLGLTVTVRFGFQEPYSFDGYDLVIM 480
 PAO1_2 GASERQQLQADLSGREVLIVDAEDFTFSMIKQLKSLGLTVTVRFGFQEPYSFDGYDLVIM 480
 PA14_1 GASERQQLQADLSGREVLIVDAEDFTFSMIKQLKSLGLTVTVRFGFQEPYSFDGYDLVIM 480
 PA14_2 GASERQQLQADLSGREVLIVDAEDFTFSMIKQLKSLGLTVTVRFGFQEPYSFDGYDLVIM 480

PAO1_1 GPGPGNPTEIGQPKIGHLHLAIRSLLSERRPFLAVCLSHQVLSLCLGLDLQRRQEPNQG 540
 PAO1_2 GPGPGNPTEIGQPKIGHLHLAIRSLLSERRPFLAVCLSHQVLSLCLGLDLQRRQEPNQG 540
 PA14_1 GPGPGNPTEIGQPKIGHLHLAIRSLLSERRPFLAVCLSHQVLSLCLGLDLQRRQEPNQG 540
 PA14_2 GPGPGNPTEIGQPKIGHLHLAIRSLLSERRPFLAVCLSHQVLSLCLGLDLQRRQEPNQG 540

PAO1_1 QKQIDLFGAAERVGFYNTFAARALQDRIEIVGPIEISRDRETGEVHALRGPRFASM 600
 PAO1_2 QKQIDLFGAAERVGFYNTFAARALQDRIEIVGPIEISRDRETGEVHALRGPRFASM 600
 PA14_1 QKQIDLFGAAERVGFYNTFAARALQDRIEIVGPIEISRDRETGEVHALRGPRFASM 600
 PA14_2 QKQIDLFGAAERVGFYNTFAARALQDRIEIVGPIEISRDRETGEVHALRGPRFASM 600

PAO1_1 HPESVLTREGPRIADLLRHALVERR 627
 PAO1_2 HPESVLTREGPRIADLLRHALVERR 627
 PA14_1 HPESVLTREGPRIADLLRHALVERR 627
 PA14_2 HPESVLTREGPRIADLLRHALVERR 627

Alignment for PhzF:

CLUSTAL O(1.2.4) multiple sequence alignment

PAO1_1 MHRYVVIDAFASEPLQGNPVAVFFDCDDLSGERMQRMAREMNLSESTFVLRPQQDGDARI 60
 PAO1_2 MHRYVVIDAFASEPLQGNPVAVFFDCDDLSGERMQRMAREMNLSESTFVLRPQQDGDARI 60
 PA14_1 MHRYVVIDAFASEPLQGNPVAVFFDCDDLSGERMQRMAREMNLSESTFVLRPQQDGDARI 60
 PA14_2 MHRYVVIDAFASEPLQGNPVAVFFDCDDLSGERMQRMAREMNLSESTFVLRPQQDGDARI 60

PAO1_1 RIFTPVNELPFAGHPLLGTALGAETDKDRLEFLETRMGTVPFALERQDGKVVACSMQQP 120
 PAO1_2 RIFTPVNELPFAGHPLLGTALGAETDKDRLEFLETRMGTVPFALERQDGKVVACSMQQP 120
 PA14_1 RIFTPVNELPFAGHPLLGTALGAETDKDRLEFLETRMGTVPFALERQDGKVVACSMQQP 120
 PA14_2 RIFTPVNELPFAGHPLLGTALGAETDKDRLEFLETRMGTVPFALERQDGKVVACSMQQP 120

PAO1_1 IPTWEHFSRPAELLAALGLKGSTFPIEVYRNGPRHVFVGLSVAALSALHPDHRALCDFP 180
 PAO1_2 IPTWEHFSRPAELLAALGLKGSTFPIEVYRNGPRHVFVGLSVAALSALHPDHRALCDFP 180
 PA14_1 IPTWEHFSRPAELLAALGLKGSTFPIEVYRNGPRHVFVGLSVAALSALHPDHRALCDFP 180
 PA14_2 IPTWEHFSRPAELLAALGLKGSTFPIEVYRNGPRHVFVGLSVAALSALHPDHRALCDFP 180

PAO1_1 DLAVNCFAGAGRHWRSRMFSPAYGVVEDAATGSAAGPLAIHLARHRQIPYGQQIEILQGV 240
 PAO1_2 DLAVNCFAGAGRHWRSRMFSPAYGVVEDAATGSAAGPLAIHLARHRQIPYGQQIEILQGV 240
 PA14_1 DLAVNCFAGAGRHWRSRMFSPAYGVVEDAATGSAAGPLAIHLARHRQIPYGQQIEILQGV 240
 PA14_2 DLAVNCFAGAGRHWRSRMFSPAYGVVEDAATGSAAGPLAIHLARHRQIPYGQQIEILQGV 240

PAO1_1 EIGRPSRMYARAEGAGERSAVEVSGNGAAFAEGRAYL 278
 PAO1_2 EIGRPSRMYARAEGAGERSAVEVSGNGAAFAEGRAYL 278
 PA14_1 EIGRPSRMYARAEGAGERSAVEVSGNGAAFAEGRAYL 278
 PA14_2 EIGRPSRMYARAEGAGERSAVEVSGNGAAFAEGRAYL 278

Alignment for PhzG:

CLUSTAL O(1.2.4) multiple sequence alignment

```
PAO1_1  -MGVNNANISESLTGTIEAPFPEFEAPPANPMEVLRNWLERARRYGVREPRALALATVDGQ    59
PAO1_2  MMGVNNANISESLTGTIEAPFPEFEAPPANPMEVLRNWLERARRYGVREPRALALATVDGQ    60
PA14_1  MMGVNNANISESLTGTIEAPFPEFEAPPANPMEVLRNWLERARRYGVREPRALALATVDGQ    60
PA14_2  MMGVNNANISESLTGTIEAPFPEFEAPPANPMEVLRNWLERARRYGVREPRALALATVDGQ    60
*****

PAO1_1  GRPSTRIVVIAELGERGVVFATHADSQKGRELAQNPWASGVLYWRESSQIILNGRAERL    119
PAO1_2  GRPSTRIVVIAELGERGVVFATHADSQKGRELAQNPWASGVLYWRESSQIILNGRAERL    120
PA14_1  GRPSTRIVVIAELGERGVVFATHADSQKGRELAQNPWASGVLYWRESSQIILNGRAERL    120
PA14_2  GRPSTRIVVIAELGERGVVFATHADSQKGRELAQNPWASGVLYWRESSQIILNGRAERL    120
*****

PAO1_1  PDERADAQWLSRPYQTHPMSIASRQSETLADIHALRAEARRLAETDGPLRPPGYCLFEL    179
PAO1_2  PDERADAQWLSRPYQTHPMSIASRQSETLADIHALRAEARRLAETDGPLRPPGYCLFEL    180
PA14_1  PDERADAQWLSRPYQTHPMSIASRQSETLADIHALRAEARRLAETDGPLRPPGYCLFEL    180
PA14_2  PDERADAQWLSRPYQTHPMSIASRQSETLADIHALRAAARRLAETDGPLRPPGYCLFEL    180
*****

PAO1_1  CLESVEFWGNGTERLHERLRYDRDEGGWKHRYLQP          214
PAO1_2  CLESVEFWGNGTERLHERLRYDRDEGGWKHRYLQP          215
PA14_1  CLESVEFWGNGTERLHERLRYDRDEGGWKHRYLQP 215
PA14_2  CLESVEFWGNGTERLHERLRYDRDEGGWKHRYLQP 215
*****
```

Data S2 - Other regulatory elements:

Other intergenic regions presenting RBS have been detected but with no differences among them.

This region is located between phzE and phzF.

```
PAO1_1  gccaggagagccc
PAO1_2  gccaggagagccc
PA14_1  gccaggagagccc
PA14_2  gccaggagagccc
*****
```

This region is located between phzF and phzG.

```
PAO1_1  acgggcagaacggaggaacgcc
PAO1_2  acgggcagaacggaggaacgcc
PA14_1  acgggcagaacggaggaacgcc
PA14_2  acgggcagaacggaggaacgcc
*****
```

Table S1: Codon Adaptation Index data (Caiazza et al.) for all genes belonging to the four clusters of interest. This index is a measurement to predict the level of expression of a gene taking into account the codon usage, being 1 the best expressed and 0 the worst expressed.

	phzA	phzB	phzC	phzD	phzE	phzF	phzG
PAO1_1	0.56597	0.56428	0.75984	0.80336	0.80311	0.78943	0.81193
PAO1_2	0.57295	0.70126	0.75669	0.80336	0.80311	0.78943	0.81275
PA14_1	0.57851	0.55609	0.76213	0.83363	0.80116	0.79080	0.79645
PA14_2	0.58449	0.68544	0.75925	0.83363	0.80643	0.79080	0.79181

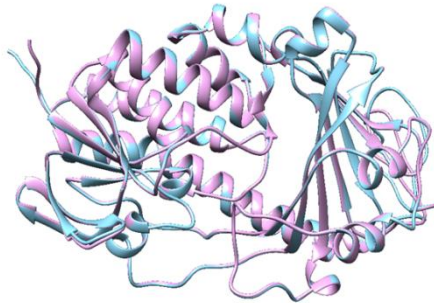


Figure S2: Structural alignment PhzS. PA14-PhzS is used as the reference for the alignment (blue). RMSD for PAO1-PhzS (purple): 0.178 Å.

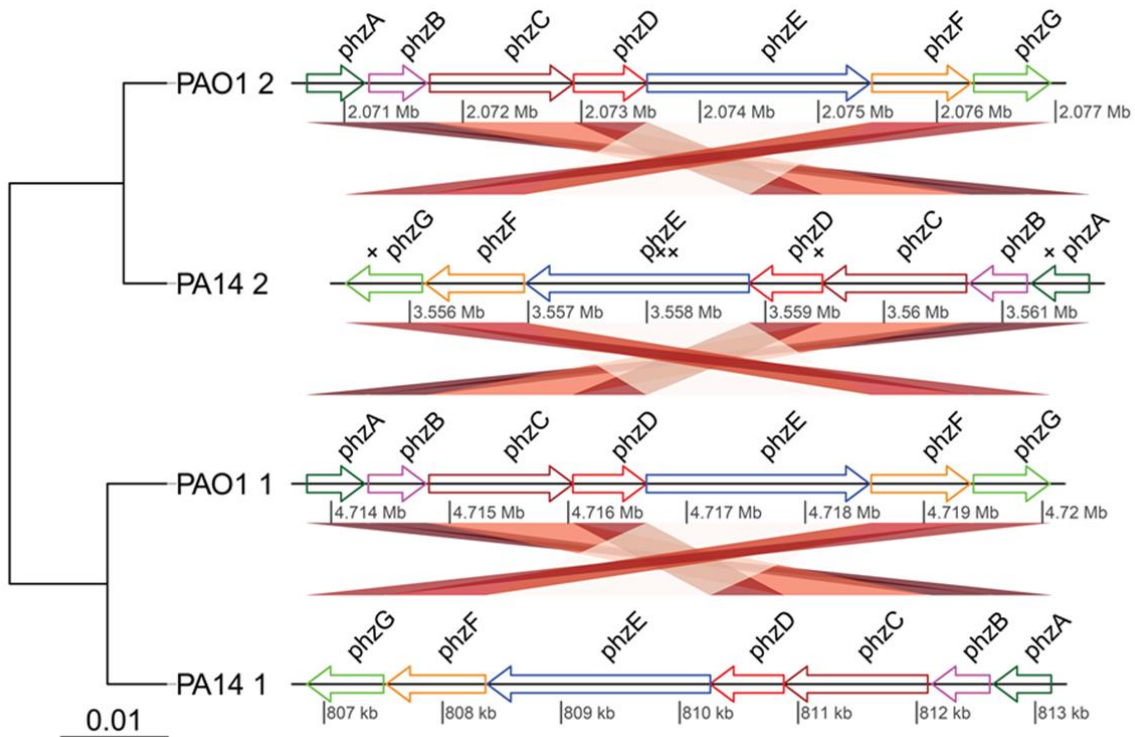


Figure S3: Phylogenetic tree and genomic plot of the phenazine production clusters. Links between homology genes are represented with red shading where the intensity of the colour is decreasing with the length of the gene. Unique amino acid changes are marked with an x in the best phenazine-producing cluster (PA14.2).

C Structural analysis of phenazine synthesis proteins:

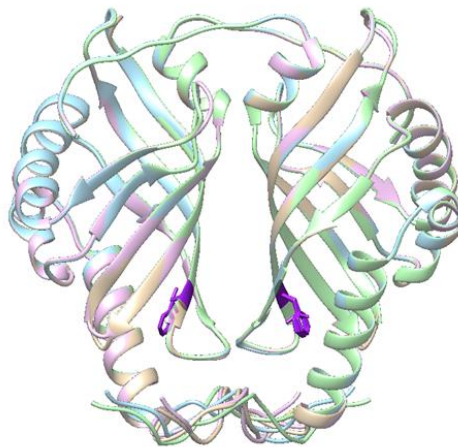


Figure S4: Structural alignment PhzA. PA14-PhzA2 is used as the reference for the alignment (blue). RMSD for PA14-PhzA1 (pink): 0.177 Å. RMSD for PAO1-PhzA1 (light purple): 0.141 Å. RMSD for PAO1-PhzA2 (green): 0.249 Å. Unique amino acid changes regarding PA14-PhzA2 (p.L97F) are marked in purple.

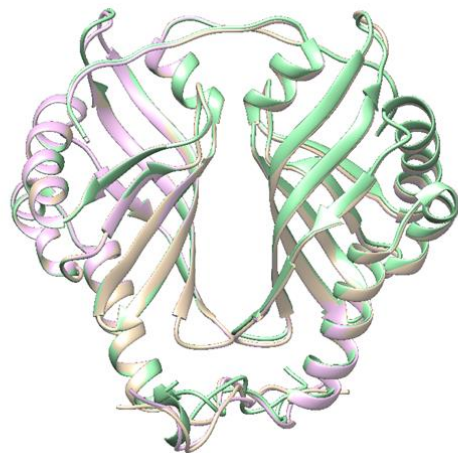


Figure S5: Structural alignment PhzB. PA14-PhzB2 is used as the reference for the alignment (green). RMSD for PA14-PhzB1 (pink): 0.277 Å. RMSD for PAO1-PhzB1 (light purple): 0.348 Å. PAO1-PhzB2 is identical to PA14-PhzB2.

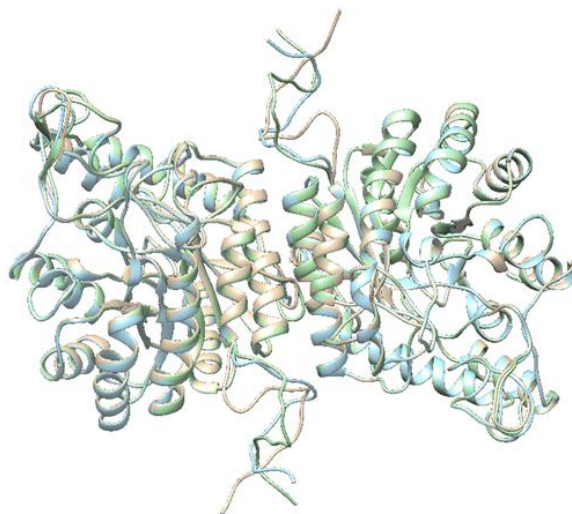


Figure S6: Structural alignment PhzC. PA14-PhzC2 is used as the reference for the alignment (blue). RMSD for PA14-PhzC1 (pink): 0.185 Å. RMSD for PAO1-PhzC1 (green): 0.209 Å. PAO1-PhzC2 is identical to PAO1-PhzC1.

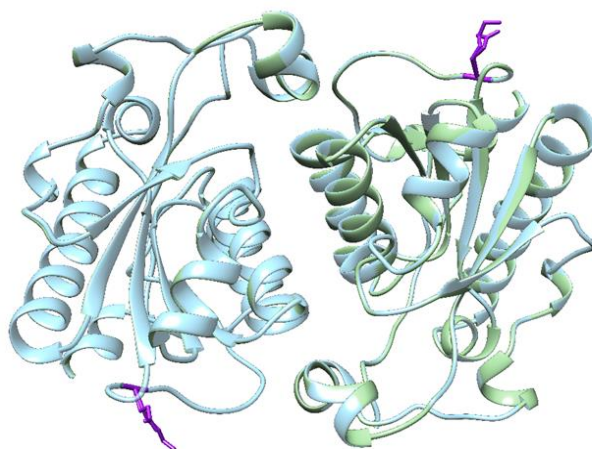


Figure S7: Structural alignment PhzD. PA14-PhzD2 is used as the reference for the alignment (blue). RMSD for PA14-PhzD1 (green): 0.059 Å. PAO1-PhzD1 and PAO1-PhzD2 are identical to PA14-PhzD1. Unique amino acid changes regarding PA14-PhzD2 (p.K28E) are marked in purple.

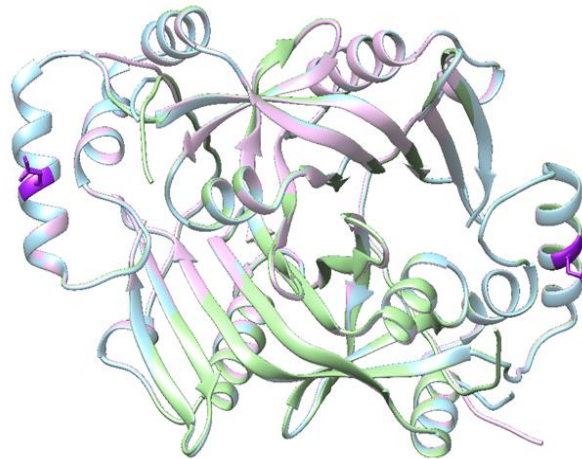


Figure S8: Structural alignment PhzG. PA14-PhzG2 is used as the reference for the alignment (blue). RMSD for PA14-PhzG1 (green): 0.231 Å. RMSD for PAO1-PhzG1 (light purple): 0.159 Å. PAO1-PhzG2 is identical to PA14-PhzG1. Unique amino acid changes regarding PA14-PhzG2 (p.A158E) are marked in purple.

A.2 Supplementary information Chapter 3.2

A Constructed Plasmids expressing phenazine and rhamnolipid genes used in Chapter 3.2

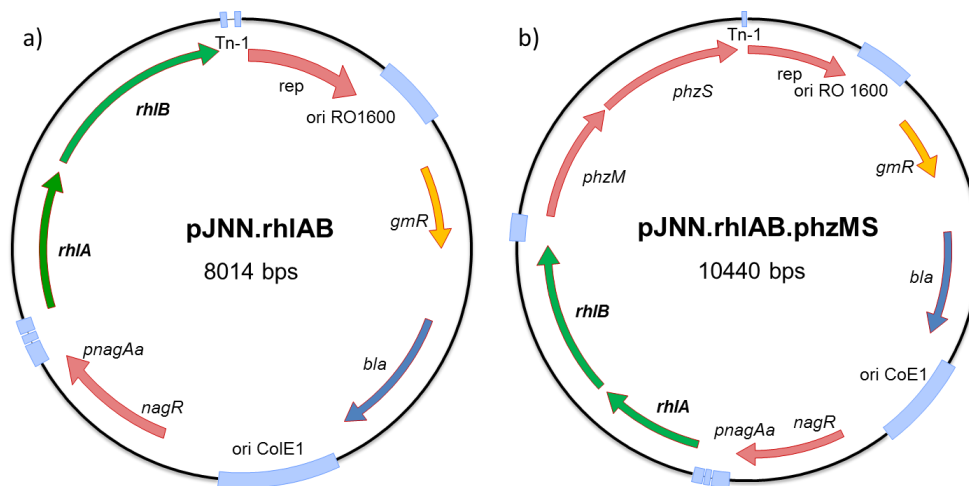


Figure S9: Vectors expressing mono-rhamnolipid and phenazine genes used in chapter 3.2; (a) pJNN.rhIAB, expressing *rhIA* and *rhIB* from *P. aeruginosa* PAO1; (b) pJNN.rhIAB.phzMS, expressing *rhIA*, *rhIB*, *phzM*, and *phzS* from *P. aeruginosa* PAO1; The schemes represent all of the important elements, including the phenazine genes (*phzA-G*), the Kanamycin resistance cassette (*kmR*) for *Pseudomonas*, the ampicillin resistance cassette for *E.coli* (*bla*), the terminator (Tn-1), the origin of replication (ori RO1600 for *Pseudomonas* and ori ColE1 for *E.coli*), and the salicylate-induced promoter (*pnagAa/nagR*).

B BES experiments

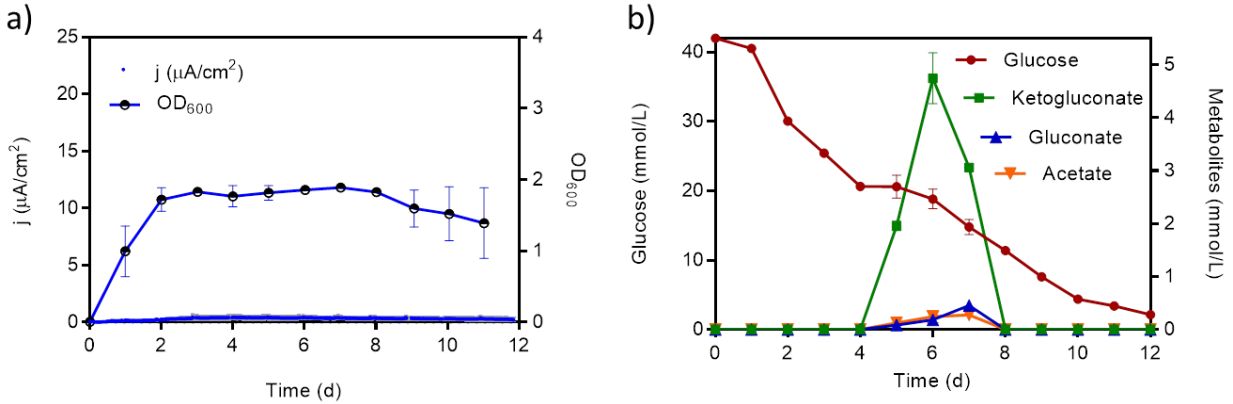


Figure S10: Bioreactor performance of *P. putida rhl* strain without electrode. AA at a flow rate of 30 ml/minute for 48 hours, then continued with passive headspace aeration. The reactors data are means from biological triplicates.

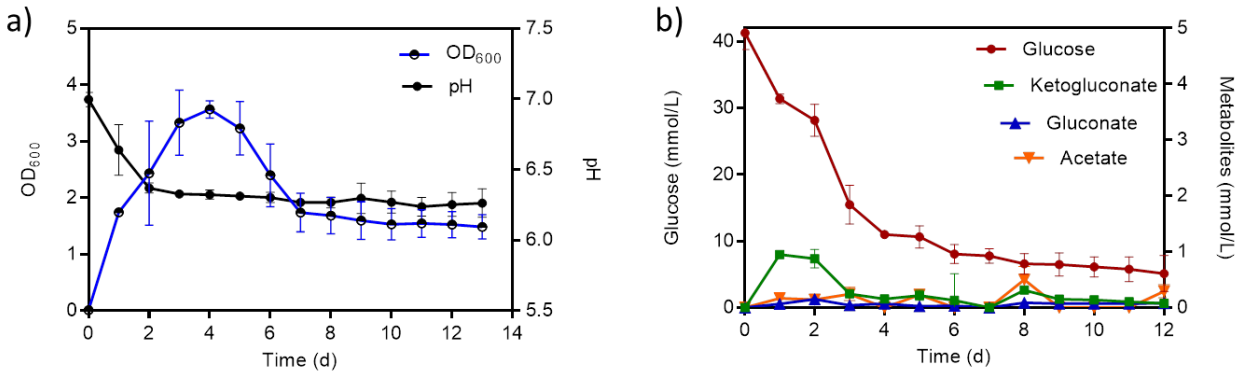


Figure S11: BES performance of *P. putida rhl* at an applied potential of 0.2 V vs. RE. BES set up under active aeration, AA, at a flow rate of 30 ml/minute for 48 hours, then continued with passive headspace aeration. The BES data are means from biological triplicates.

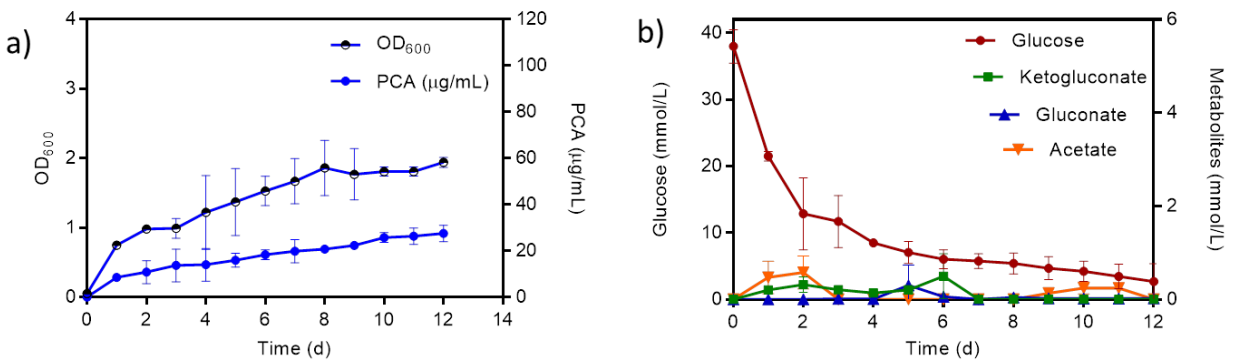


Figure S12: Bioreactor performance of *P. putida rhl-pca* strain without electrode. AA at a flow rate of 30 ml/minute for 48 hours, then continued with passive headspace aeration. The reactors data are means from biological triplicates.

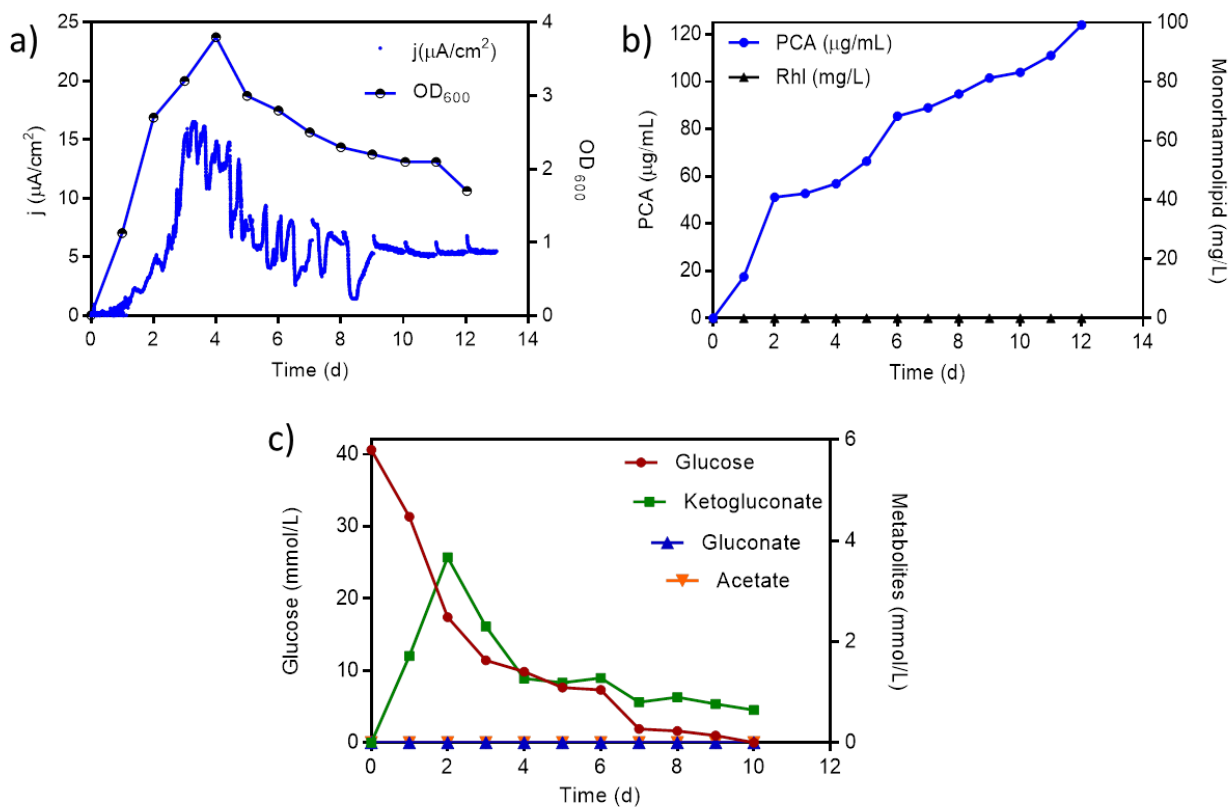


Figure S13: BES performance of *P. putida rhl-pca* (plasmid sustainability test) at an applied potential of 0.2 V vs. RE. BES set up under active aeration plus, AA+, at a flow rate of 50 ml/minute continuously until the end of the experiment. The BES data was from single reactor.

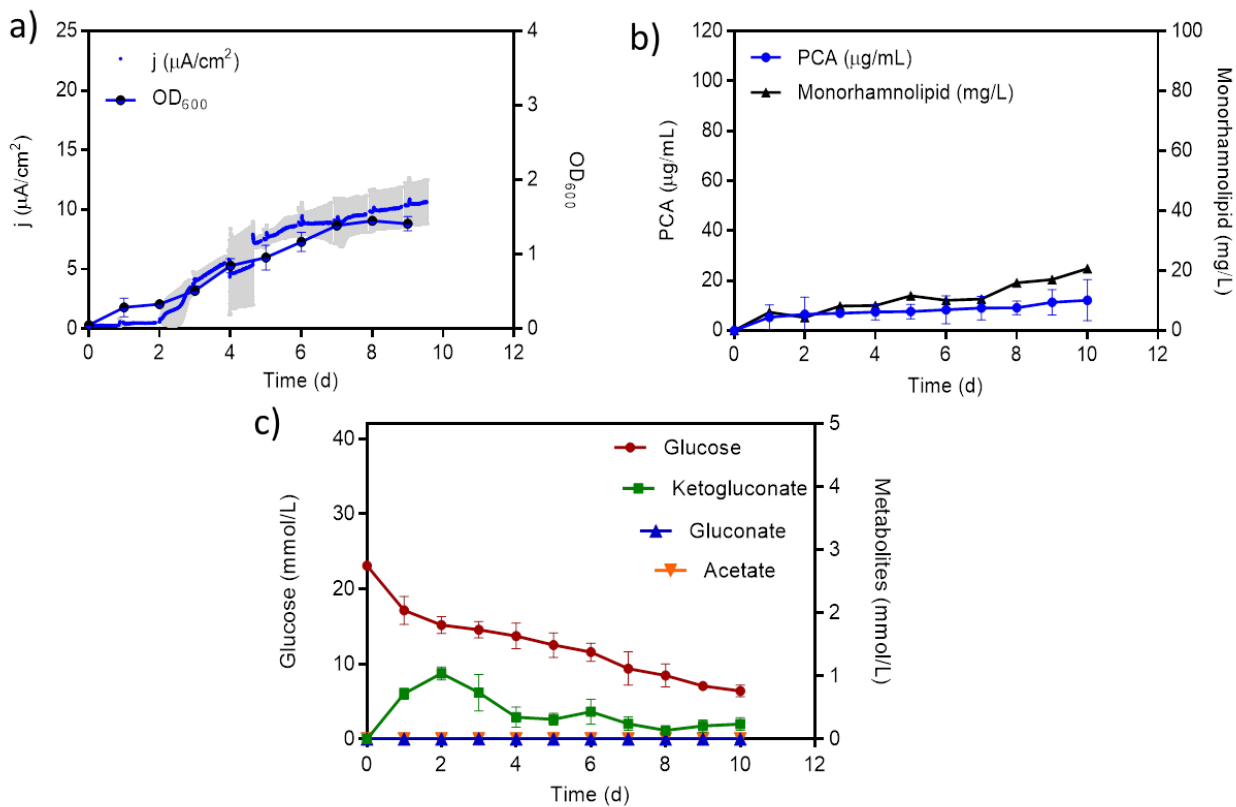


Figure S14: Second BES performance of *P. putida rhl-pca* at an applied potential of 0.2 V vs. RE. (a-c) BES set up under passive aeration (replication experiment). The BES data are means from biological triplicate. The data showed in the same range to first experiment for all of parameters.

Curriculum vitae

Personal Information

Name: Theresia Desy Askitosari
Born: Surakarta, January 27th, 1985
Nationality: Indonesian

Education

09/2015-present PhD
RWTH Aachen University, Germany
Institute of Applied Microbiology

9/2009-10/2011 Master of Biotechnology
Gadjah Mada University, Indonesia
Biotechnology Graduate School

08/2002-11/2006 Bachelor of Science
Gadjah Mada University, Indonesia
Faculty of Biology

06/1999-06/2002 SMU Negeri 3 Surakarta (High school)

Work experience

09/2015-present PhD thesis at the Institute of Applied Microbiology, RWTH Aachen University
Topic: Engineering *Pseudomonas putida* KT2440 for Efficient Bioelectrochemical Production of Glycolipids
Supervisor: Univ.-Prof. Dr.-rer. nat. Miriam Agler-Rosenbaum
Univ.-Prof. Dr.-Ing. Lars M. Blank

07/2012-present Researcher and Lecturer at Faculty of Biotechnology, University of Surabaya, Surabaya
Subject: Basic Microbiology, Soil Microbiology

03/2013-09/2013 Research Training Fellowship - NAM S&T Award at Indian Institute of Science Research and Education – Kolkata, India
Topic: Molecular Detection of Bacterial Symbionts Associated with Entomopathogenic Nematodes from the Agricultural Soils of Indonesia - Implications in Pest Management"
Supervisor: Associate Prof. Punyasloke Bhadury

- 08/2009-06/2012 Practical course assistant at Faculty of Biotechnology, Atmajaya University, Yogyakarta, Indonesia
Subject: Biochemistry and Molecular Biology
- 09/2010-08/2011 Master thesis at Biotechnology Graduate School, Gadjah Mada University, Yogyakarta, Indonesia
Topic: Allele Frequency Distributions of the Drug Metabolizer Genes *CYP2C9*2*, *CYP2C9*3*, and *CYP2C19*17* in the Buginese Ethnic Population of Indonesia
Supervisor: Prof. Dr. Zullies Ikawati, Apt.,
 dr. Agus Surono, Ph.D., M.Sc., Sp.THT-KL
- 01/2007-06/2009 Research & Development staff at Muara Manggalindo, Ltd., Jakarta, Indonesia. Integrated processing frozen seafood company.
- 06/2005-05/2006 Bachelor thesis at Faculty of Biology, Gadjah Mada University, Yogyakarta, Indonesia
Topic: Pathogenicity Test of Entomopathogenic Nematodes on Lettuce Crop Pest *Crocidolomia binotalis* L.
Supervisor: Dr. Hari Purwanto, M.P.

Publications

Accepted abstract: "Boosting heterologous phenazine production in *Pseudomonas putida* KT2440 through the exploration of the natural sequence space" in *Frontiers in Microbiology*, section Microbiological Chemistry and Geomicrobiology.

Authors: Theresia D. Askitosari, Santiago T. Boto, Lars M. Blank, Miriam A. Rosenbaum

Accepted abstract: "Biosurfactants and synthetic surfactants in bioelectrochemical systems: a mini-review" in *Frontiers in Microbiology*, section Microbiological Chemistry and Geomicrobiology.

Authors: Grzegorz Pasternak, Theresia D. Askitosari, Miriam A. Rosenbaum

Purwanto, Maria Goretti Marianti and Gunawan, Renardi and Artadana, Ida Bagus Made and Goeltom, Mangihot Tua and Askitosari, Theresia Desy (2018) Isolation and Identification of *Bacillus thuringiensis* from *Aedes aegypti* Larvae as Potential Source of Endotoxin to Control Dengue Vectors. *Pertanika Journal of Tropical Agricultural Science (JTAS)*, **41 (3)**. 1423 -1435. ISSN 2231-8542

Askitosari, Theresia Desy and Purwanto, Maria Goretti Marianti and Sabrina, Kezia Eunike (2015) Sweet Potato and Cassava as Alternative Substrates for Growing Spawn of Shiitake (*Lentinula edodes* B.) and Lingzhi (*Ganoderma lucidum* K.). *Journal of Science & Technology*, **17 (2)**. 22-28. ISSN 1685-7941

Ikawati, Zullies and Askitosari, Theresia Desy and Hakim, Lukman and Tucci, Joseph and Mitchell, John (2015) Allele Frequency Distributions of the Drug Metabolizer Genes *CYP2C9*2*, *CYP2C9*3*, and *CYP2C19*17* in the Buginese Population of Indonesia. *Journal of Current Pharmacogenomics and Personalized Medicine*, **12 (4)**. 236-293. ISSN 1875-6913

Askitosari, Theresia Desy and Bhadury, Punyasloke (2013) Molecular Detection of Bacterial Symbionts associated with Entomopathogenic Nematodes (EPN) from the Agricultural Soils of Indonesia - Implications in Pest Management. *NAM S&T Newsletter*, **23 (3)**. ISSN 0971-4200

Oral Presentations

Theresia D. Askitosari and Miriam A. Rosenbaum (November 26th-27th, 2017)
Comparison studies of genetic foundation for heterologous production of phenazine in *Pseudomonas putida* KT2440, DBU workshop (Workshop der Plattforminitiative Mikrobielle Bioelektrotechnologie), Frankfurt, Germany.

Theresia D. Askitosari and Miriam A. Rosenbaum (September 12th-14th, 2018)
Comparative study of genetic foundation for heterologous production phenazine in *Pseudomonas putida* KT2440, 4th European Meeting of the International Society of Microbial Electrochemistry and Technology (EU-ISMET), Newcastle upon Tyne, UK.

Poster Presentations

Theresia D. Askitosari and Miriam A. Rosenbaum (September 26th-28th, 2016)
Characterization of engineered *Pseudomonas putida* for rhamnolipid production in bioelectrochemical system, 3rd European Meeting of the International Society of Microbial Electrochemistry and Technology (EU-ISMET), Rome, Italy.

Theresia D. Askitosari, Till Tiso, Lars M. Blank, Miriam A. Rosenbaum (October 3-6, 2017)
Combining the electroactivity of phenazines-producing *Pseudomonas putida* with rhamnolipid production in a bioelectrochemical system, 6th General Meeting of the International Society for Microbial Electrochemistry and Technology (ISMET6), Lisbon, Portugal.